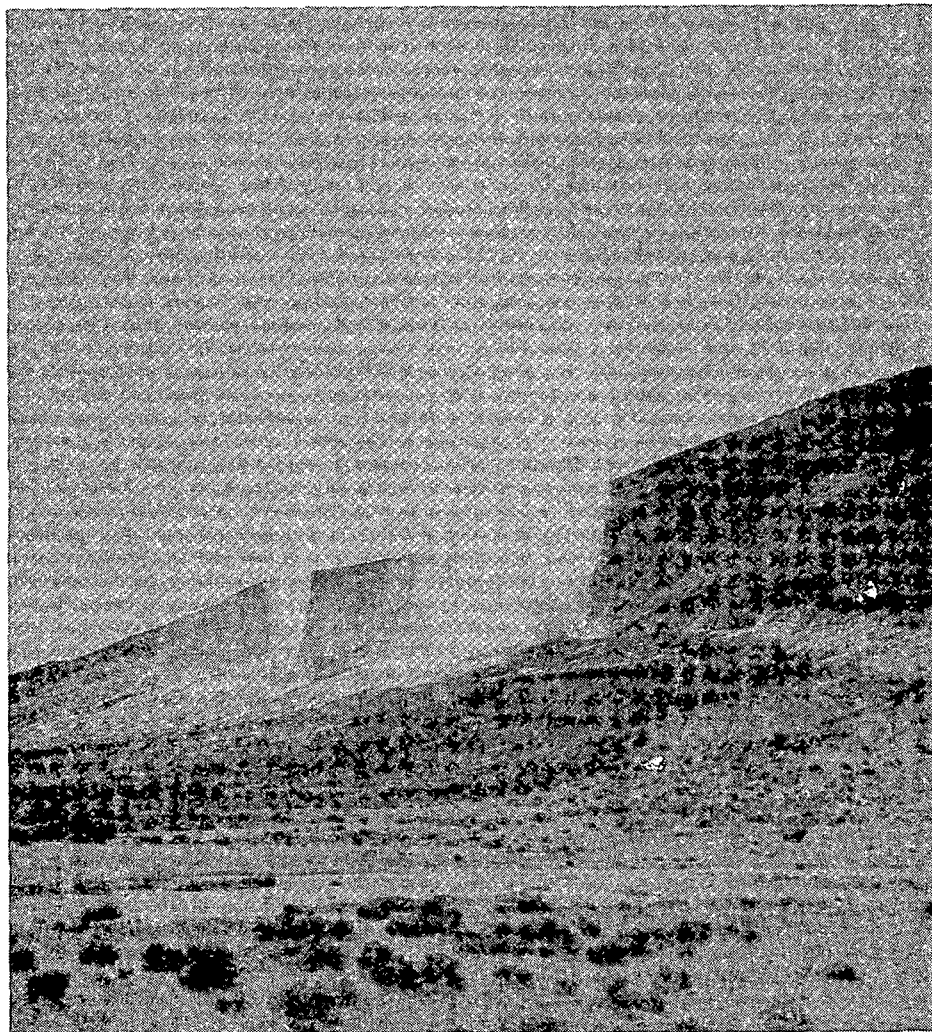


AREA
NV
Lander
Beowawe
Zoback

6107303

STANFORD UNIVERSITY PUBLICATIONS • GEOLOGICAL SCIENCES • VOLUME XVI

A GEOLOGIC AND GEOPHYSICAL INVESTIGATION OF THE BEOWAWE GEOTHERMAL AREA, NORTH-CENTRAL NEVADA



MARY LOU C. ZOBACK

UNIVERSITY OF UTAH
RESEARCH INSTITUTE
EARTH SCIENCE LAB.

GEOLOGIC AND GEOPHYSICAL INVESTIGATION OF
THE BEOWAWE GEOTHERMAL AREA,
NORTH-CENTRAL NEVADA

MARY LOU C. ZOBACK

Department of Geophysics
Stanford University
School of Earth Sciences

STANFORD UNIVERSITY PUBLICATIONS
Geological Sciences, Volume 16

SCHOOL OF EARTH SCIENCES
Stanford University, Stanford, California

1979

© 1979 by the Board of Trustees of the
Leland Stanford Junior University

Printed in the United States of America

CONTENTS

Abstract -----	1
----------------	---

INTRODUCTION

Physical Setting -----	3
Previous Work -----	5
Purpose -----	5
Acknowledgements -----	6

GEOLOGY

Geologic Setting -----	7
Description of Rock Units -----	9
Ordovician Valmy Formation -----	9
Late Oligocene-Early Miocene tuffaceous sediments -----	11
Mid-Miocene basaltic andesite -----	12
Late Miocene (?) tuff -----	14
Late Miocene (?) gravels -----	16
Late Miocene (?) basalt -----	16
Quaternary-Tertiary (?) calcedony-carbonate vein -----	16
Quaternary landslide deposits -----	17
Quaternary siliceous sinter -----	17
Quaternary alluvium -----	19
Hydrothermal Activity and Ore Deposits -----	20
Past geothermal activity -----	20
Ore deposits -----	21
Modern geothermal system -----	22
Drill Hole Data -----	25
Structure -----	28
Folds -----	28
Faults -----	28
Regional Structural Synthesis -----	34
Geologic History -----	35

GEOPHYSICAL INVESTIGATIONS

Geophysical Setting -----	37
Bipole-Dipole Resistivity -----	41

Self Potential -----	45
Seismic Noise -----	53
Gravity Data -----	56
Magnetic Investigations -----	61
Geophysical Summary -----	67

CONCLUSIONS AND RECOMMENDATIONS

Nature of the Geothermal System and Possible Reservoirs -----	69
Economic Considerations -----	73
Recommendations for Further Work -----	74
References -----	76

ILLUSTRATIONS

TABLES

1. Chemical compositions of basaltic andesite -----	15
2. Paleomagnetic data: Beowawe volcanic rocks -----	64

PLATES

I. Geologic map and cross-section of the Beowawe geothermal area. -----	<i>In pocket</i>
II. Generalized colored geologic map. -----	<i>In pocket</i>

FIGURES

1. Index map -----	4
2. Regional geologic map -----	8
3. Geomorphic expression of tuffaceous seiments unit -----	11
4. Interbedded siliceious tuff in tuffaceous sediments unit ---	13
5. Cross-bedding in gravel in tuffaceous sediments unit -----	13
6. Sinter terrace, view from valley -----	18
7. Layered structure in sinter -----	18
8. Generalized geologic logs of deep geothermal wells -----	26
9. Structure map -----	29
10. Interpreted structural setting of deep wells -----	31

11.	Battle Mountain heat flow high -----	38
12.	Aeromagnetic map of north-central Nevada -----	39
13.	Bipole-dipole resistivity --valley transmitter -----	42
14.	Bipole-dipole resistivity--range transmitter -----	43
15.	Location of self potential survey lines -----	46
16.	Self potential test profile -----	48
17.	Contour map of self potential data -----	49
18.	Self potential data on cross valley line -----	51
19.	Self potential cross valley profile -----	48
20.	Seismic noise values in Whirlwind Valley -----	54
21.	Bouguer gravity values in Whirlwind Valley -----	57
22.	Interpreted valley structure with computed gravity model ---	58
23.	Gravity profile parallel to range front -----	60
24.	Aeromagnetic map of Mal Pais ridge area -----	62
25.	Paleomagnetic sampling sites -----	63
26.	Natural remanent magnetization directions after partial demagnetization -----	65
27.	Summary of modern geothermal convection system -----	70

ABSTRACT

Results of a detailed geologic and geophysical investigation of a natural, hot-water geothermal system located near the town of Beowawe, north-central Nevada are reported. Geologic mapping revealed an alluvial deposit of gravels and tuffaceous sediments at the base of the Cenozoic section; this alluvial deposit is overlain by a series of mid-Miocene basaltic andesite flows which cap the modern range. The Cenozoic section was deposited unconformably on Paleozoic siliceous rocks of the upper plate of the Roberts Mountain thrust. Paleozoic carbonate rocks comprise the autochthonous basement at depth.

The basaltic andesite varies in thickness from roughly 100 m on the northeast end of the range to more than 1 km in the vicinity of the hot springs and to the west. This variation in thickness is attributed to a NNW-trending graben developed in mid-Miocene time into which the flows accumulated and eventually overflowed. The main uplift and gentle, southeast tilting of the modern range was subsequently accomplished along a ENE-trending Basin and Range normal fault; however, movement has apparently continued on the NNW faults resulting in a nearly orthogonal, cross-faulting trend. This cross-faulting trend is associated with mild topographic expression; activity along it is most likely responsible for large landsliding (area roughly 3.5 km²) along the Mal Pais ridge near a major intersection of the two trends.

Current geothermal activity is limited to the southwestern end of the range where a 65 m high siliceous sinter terrace has built up along the main bounding fault. By estimating the volume of silica deposited and assuming pre-exploitation silica concentrations and flow rate for the entire life of the system, the age of the modern system was calculated to be around 200,000 years with an uncertainty of about 50%. Using an estimate of the discharge of the natural system and assuming a base temperature of 215°C (from geochemical data and shallow drilling results) a convective heat flux of 91 HFU was calculated.

The localization of the modern geothermal system along the range-front fault attests to the important role that normal faulting plays in the movement of thermal waters to the surface. A shallow, near-surface magma body is unlikely as a heat source because of the nature and age of the most recent volcanism (basaltic rocks probably 6-10 m.y. in age); however, the heat source for this system and numerous others in the area is no doubt related to the Battle Mountain high, a broad region of extremely high heat-flow values in north-central Nevada (Sass et al., 1971). Deep circulation of meteoric water along normal faults would encounter hot rock at the observed reservoir temperatures (210°-215°) at depths of only 6-7 km in this high heat-flow region.

Geophysical investigations were undertaken to establish signatures for the known geothermal area and to examine other faulting for geothermal activity lacking surface manifestations. Surveys within the active hot springs and geyser area revealed a bipole-dipole resistivity low, a broad

positive self-potential anomaly (+80 mv) with many superimposed short wavelength fluctuations, and a relatively high seismic noise level. Most susceptible to lateral variations in resistivity, the bipole-dipole survey outlined a low associated with the present active area; however, gave no information as to the depth extent of the anomaly. The self-potential anomaly emerges well above the noise level and is thought to reveal upwelling of water primarily along a subsidiary range front fault within the active hot springs area. The anomaly pattern is probably complicated by a complex pattern of flow--both lateral and vertical--near the surface. A seismic noise survey was plagued by the strong dependence of measured amplitudes on recorder site geology.

The valley in the vicinity of the main NNW-trending cross faulting was investigated for possible subsurface geothermal activity. A small, N-S resistivity low as well as a localized noise anomaly was detected in this region. The favored interpretation of the resistivity and seismic noise data, consistent with the self-potential data, is that the anomalies are related to a possible eastward extension of a sub-parallel, subsidiary, ENE-trending range front fault. The anomalies might then be correlated with fluid movement along this fault. Because both hot and cold springs are aligned along this subsidiary fault it is unknown whether the moving fluid is thermal or ordinary meteoric water.

The geothermal system at Beowawe is apparently characterized by permeable zones and storage at several different levels: a deep zone of circulation presumably located within carbonate rocks of the lower plate of the Roberts Mountains thrust (based on geochemical data), a possible intermediate level fracture zone (approximately 1 km depth) created by complex fault intersections and tapped by both the main and the subsidiary range front fault, and a shallow (about 200 m depth) reservoir presumably within the basaltic andesite section in the uplifted, range block. Meteoric water is probably heated conductively by rocks at roughly 7 km depth within a highly permeable (possibly cavernous) region in the autochthonous carbonate sequence. Intersection of the main range front fault with this deep permeable zone provides a channel for rapid upward migration of the geothermal water. Structural controls have apparently resulted in significant northeastward lateral diversion (at least 2.5 km) of water rising along the main range front fault at some level above 2.9 km depth.

INTRODUCTION

Recent interest in geothermal power has spurred studies of natural geothermal areas throughout the world, including the western United States, a center of relatively recent vulcanism and tectonism. Hot spring systems are abundant within the Basin and Range physiographic province and at least one of these, in the Beowawe area of north-central Nevada, is associated with natural geyser activity.

Once a site of many beautiful small geysers, the Beowawe spring terrace was disturbed by excavation and drilling by commercial power interests in the early 1960's and nearly all natural geyser activity was destroyed. Only three small geysers, numerous fumaroles, and a few hot springs are the natural remnants of this commercial activity. Two uncapped geothermal wells vent steam continuously into the atmosphere playing to heights of 15-25 m. These wells have received the misnomer of the "Beowawe Geysers".

Physical Setting

The town of Beowawe is located on State Highway 21, 8 km south of Interstate 80, the main throughfare through northern Nevada. The hot springs are 13 km southwest of Beowawe and can be reached by a well-maintained gravel road located about 2.4 km south of town, off Highway 21.

The geothermal activity is limited to a small area on the southwest margin of Whirlwind Valley (see Figure 1). A flat, elongated, northeast trending valley, Whirlwind Valley separates the two spurs that project off the northernmost end of the Shoshone Range, the Mal Pais and the Argenta Rim. These spurs, capped with mid-Miocene basaltic andesite flows, have been uplifted along normal faults and tilted to the southeast. The "Beowawe Geysers" and related geothermal activity are located along the range front fault bounding the Mal Pais ridge.

The land in this region is relatively arid, typical of the Basin and Range Province. Gilluly and Gates (1965) reported that the mean annual precipitation at Beowawe is 16.25 cm. The predominant type of vegetation both in the ranges and the valley is sage brush; however, parts of the valley floor are covered by salt grass. Portions of the valley floor are marshy, suggesting that at least locally the water table is near the surface.

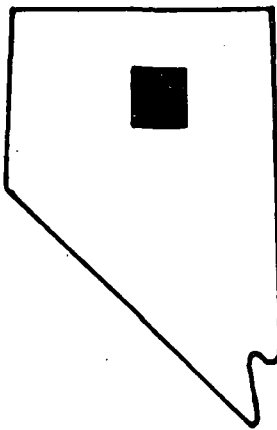
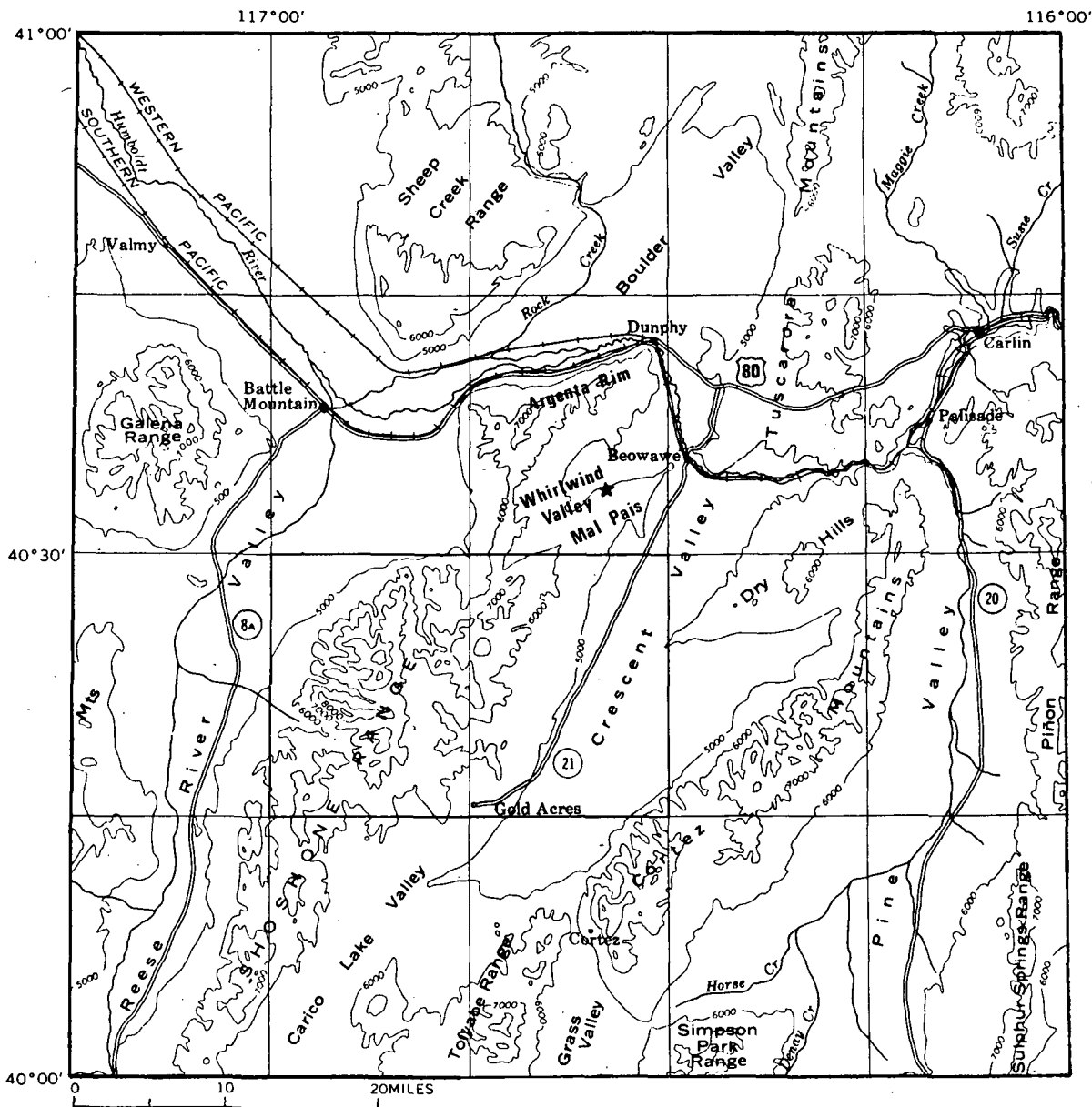


Figure 1. Index map, star gives location of the Beowawe geysers and hot springs area.

Previous Work

The earliest known geologic reconnaissance in the region was conducted in 1877 by members of the Fortieth Parallel Survey and reported by Hague and Emmons (1877). They described the volcanic rocks capping the northern Shoshone Range, the Argenta Rim and the Mal Pais, but made no mention of the thermal activity, indicating that they probably did not closely investigate the Mal Pais. The thermal activity was first described in a popular article by Albert S. Evans (1869) during construction of the Central Pacific Railroad.

In 1932, T. B. Nolan and G. H. Anderson visited the Beowawe Geyser area and gave an excellent, detailed report (1934) of the geothermal activity which included several chemical analysis of the water. This report is valuable for a complete description of the natural thermal activity before the area was exploited.

A county map of Eureka County (Roberts et al., 1967) included part of the Mal Pais, listing unpublished reconnaissance data as the source. Stewart et al. (1977) mapped the southwest portion of the Mal Pais to be included in their map of Lander County. Parts of their map are included on the present author's map (Plate 1) to clarify relationships with the adjoining areas.

In the course of drilling exploration holes commercial power interests heavily worked the sinter terrace in the early 1960's and destroyed the natural geyser activity there. In 1968, Rinehart (1968) studied three small remaining geysers on the valley floor west of the terrace and attempted to establish seismic signatures for them. Hose and Taylor (1974) mapped the sinter terrace in detail showing all the various forms of geothermal activity located there.

Purpose

Field work was conducted by the author in July of 1974 to gain more information about the known geothermal area and to investigate the possibility of additional reservoirs lacking surface manifestations. The geology was mapped in an effort to gain information about the reservoir unit stratigraphically, and to interpret the relatively recent structural history which apparently controls the present day activity.

Seismic noise and self potential surveys, which have both been used to detect movement of thermal waters in geothermal regions, were conducted in Whirlwind Valley. The known resource area was investigated as well as the surrounding region, focusing on favorable areas as indicated by fault patterns and by results of deep resistivity surveys conducted by Lawrence Berkeley Laboratory.

Acknowledgements

I am very much indebted to a great number of people whose cooperation made this study possible. Harold Wallenberg of Lawrence Berkeley Laboratories and Harry Beyer of the geothermal group at University of California, Berkeley willingly provided background information on the area including the results of their bipole-dipole resistivity study. NASA's Earth Resources Data Facility provided color aerial photographs. William Mero, of Chevron Resources Company furnished drill hole information. Frank Olmstead, of the U.S. Geological Survey, provided information on the shallow heat flow holes in Whirlwind Valley. Discussions with James Koenig on early geothermal development of the region were very useful.

Warm thanks go to the the Matt Day family of Beowawe, Nevada for providing living accommodations for the duration of the field work, and also to David Boore, Helen Dawson, Chuck Mueller and Mark Zoback for field assistance. Special thanks also to George Thompson and Don White for their inspiration and incentive.

GEOLOGY

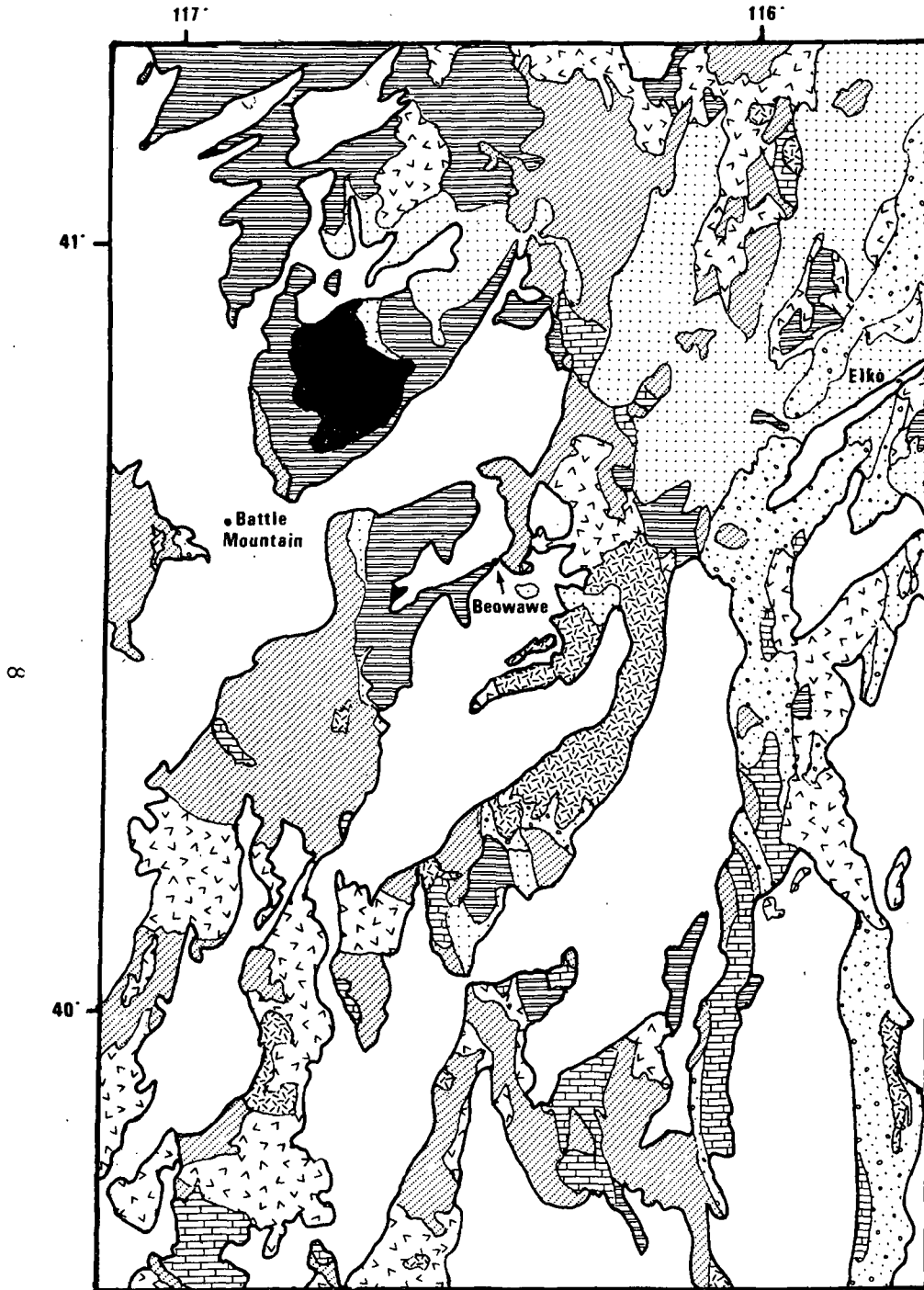
Geologic Setting

In this region of north-central Nevada sedimentary and igneous rocks of Paleozoic, Mesozoic, and Tertiary age are exposed in the ranges. The intermontaine valleys are filled with Quaternary alluvium and playa deposits. Figure 2 is a regional geologic map, the general features of which are discussed below.

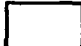





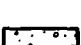
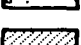
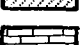
During the Antler Orogeny in mid-Paleozoic times, siliceous "eugeosynclinal" rocks were thrust eastward over a carbonate "miogeosynclinal" assemblage that had been deposited in the eastern half of Nevada. This thrust relationship, called the Roberts Mountains Thrust (named for excellent exposures in the Roberts Mountains area 90 km to the south) is recognizable despite subsequent uplift, erosion, and orogeny. Rocks of the eastern carbonate assemblage are predominantly limestone and dolomite, in contrast to the western assemblage which includes chert, siliceous clastics and some greenstone. In this region of north-central Nevada mainly rocks of the upper plate of the Roberts Mountains Thrust (the siliceous western assemblage) are exposed; however, the carbonate rocks are found at depth and in windows through the upper plate. During the late Paleozoic clastics were shed from the emerged areas of the Antler orogenic belt to flanking seas, creating an overlap assemblage. Directly to the southeast, in the Frenchie Creek quadrangle, this sedimentation may have continued uninterrupted into the early Mesozoic.

Evidence in the Frenchie Creek quadrangle to the southeast also suggests that igneous activity in the area may have begun as early as Permian time (Muffler, 1964) and has continued throughout the region sporadically up to 10 m.y. ago (Stewart et al., 1977). Mesozoic and Early Tertiary volcanic and intrusive rocks are nearly all silicic, generally rhyolite to quartz latite and granodiorite to adamellite in composition (Muffler, 1964; Gilluly and Gates, 1965). However, in the Late Miocene (about 15-16 m.y. ago) a distinct new phase of igneous activity, marked by extensive basaltic andesite flows and minor rhyolite began. A similar overall compositional shift from predominately silicic to bimodal basalt-rhyolite magmatism is recorded in igneous activity throughout the Basin and Range province between 19 and 15 m.y. ago (see McKee, 1971, for example).

The basaltic andesite capping the ranges in this area (see Figure 2) as well as diabase dikes exposed in the Cortez Mountains and Roberts Mountains to the southeast (Gilluly and Gates, 1965; Gilluly and Masursky, 1965; Muffler, 1965; Murphy et al., 1978) are thought to represent this compositional shift. The diabase dike swarms in the Cortez and Roberts Mountains are generally believed to be feeders for the basaltic andesite flows in those ranges. Compositions and age relations are consistent, although the dikes have not been found either to cut or to unite with any of the flows. It has also been suggested that these dikes, which strike roughly north-northwest are related to a marked aeromagnetic and



LEGEND

-  Quaternary alluvial and playa deposits
-  Late Miocene (?) basalt
-  Mid-Miocene volcanic rocks, predominantly basaltic andesite to the south and rhyolite to the north
-  Miocene tuffaceous sedimentary rock
-  Lower Tertiary volcanic rock
-  Mesozoic to Tertiary intrusive rock, also includes Mesozoic sedimentary and volcanic rock
-  Upper Paleozoic overlap assemblage
-  Lower Paleozoic siliceous and volcanic assemblage
-  Lower Paleozoic carbonate assemblage

SCALE

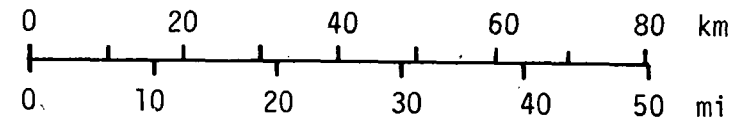


Figure 2. Regional geologic map adapted from the Geologic Map of Nevada (Stewart and Carlson, 1974).

structural lineation of the same strike that cuts through north-central Nevada and extends into Oregon (Robinson, 1970; Stewart et al., 1975; Zoback and Thompson, 1978).

In this region of northern Nevada siliceous igneous activity occurred in conjunction with this pulse of intermediate-basic vulcanism as is evidenced by rhyolite plugs and flow domes that cut the basaltic andesite. Examples of these somewhat younger rhyolitic rocks (ages between 13.5-14.5 m.y., McKee and Silberman, 1970) can be found in the Sheep Creek Range to the northwest and the Cortez Range to the south. The final pulse of volcanic activity in the area however, is an alkaline olivine basalt exposed in the Sheep Creek Range and dated as 10.0 m.y. old (McKee and Silberman, 1970).

Erosion and formation of alluvial deposits occurred between individual igneous episodes throughout the area. The alluvial deposits are, in general, composed of locally derived gravels and are rich in pyroclastic material. Where the base of the basaltic andesite section capping the ranges is exposed, it is generally seen lying over such a tuffaceous sedimentary gravel section which unconformably overlies cherts and quartzites of the Ordovician Valmy Formation.

Evidence discussed elsewhere suggests that the initiation of Basin and Range extensional tectonics in this area may have been synchronous with the basaltic andesite episode (see Zoback and Thompson, 1978). Since that time normal faulting and associated east to southeast tilting created the present day ranges and valleys. Older alluvial deposits fill the valleys and continuing activity on the range front faults has resulted in a well-developed fan system along the escarpments. A major set of cross faults cut the trend of the main range front faults at nearly right angles.

A well developed sinter terrace (nearly 65 m high) has formed along the Mal Pais escarpment and sinter deposits extend about 600 m out on the valley floor. The present day geothermal activity is located in this area, but evidence of hydrothermal activity all along the fault suggests shifting centers of activity.

Description of Rock Units

Plate 1 is a geologic map of the Beowawe region. Cenozoic deposits once covered the entire mapping area. Normal faulting, responsible for the uplift of the range, has exposed the only pre-Tertiary rock, the allochthonous Ordovician Valmy Formation. The aggregate thickness of Tertiary rocks now exposed on the Mal Pais Range varies from a minimum of about 90 m to more than 340 m. The maximum thickness of Quaternary alluvial deposits in Whirlwind Valley is estimated from gravity data and structural projections at approximately 305-425 m. Only a minimum thickness of approximately 90 m can be given for the Valmy Formation because the base is not exposed.

Ordovician Valmy Formation. By far the oldest rock unit exposed in the mapping area, the Valmy Formation can be seen to underlie the range northeast of White Canyon. Part of the upper section of the siliceous western assemblage of the Roberts Mountains Thrust, the Valmy in this area

generally forms bold, resistant outcrops and is characterized by a bright red-weathering soil. This sequence of quartzite, chert, siltstone, calc-dony, and siliceous conglomerate was tentatively assigned to the Valmy Formation by Roberts et al. (1967) as a result of reconnaissance work in the area.

The predominant rock type of the Valmy exposed in the area is a grey to bright red-weathering siliceous siltstone which in places grades to quartzite. On a fresh surface the rock is generally pale grey and often shows a red-purple lining of small fractures. This coloring is probably due to oxidation of iron by water along small cracks. Thin section examination of the siltstone reveals that it is formed largely of quartz, with minor detrital feldspars and micas with a slight foliation detectable. The remarkably uniform-sized quartz grains in the quartzite exhibit a mosaic texture due to overgrowth. The grains are roughly .2 cm in diameter and are readily visible by hand lens inspection, but the rock is a true quartzite and breaks across the grains.

No stratigraphic section could be established for the Valmy in the present area. Because of internal mechanical deformation and hydrothermal alteration, it is difficult to correlate exposures from outcrop to outcrop. Red Hill, in the extreme northeast corner of the area, exposes the greatest thickness of the Valmy. There the grey siltstone and a chert conglomerate are interbedded; beds are on the order of 3 to 4.5 m. thick. Minor shale is also found in the section there. Further to the southwest, at the Red Devil mines, a siliceous pebble conglomerate interbedded with quartzite and minor shale is exposed. The prominent ledges along the range front are, for the most part, grey siltstone and quartzite, chert, and some very minor siliceous pebble conglomerate.

The chert conglomerate consists of generally poorly sorted, subangular to subrounded chert clasts varying in size from 0.6 to 3.8 cm in diameter. The matrix is siliceous and grey to grey-brown in color and the chert grains are often green, grey, and brown. Although both have a grey matrix, the chert conglomerate is easily distinguished from the pebble conglomerate mentioned above. In the latter the siliceous pebbles are generally well sorted and are white, grey, and black in color. The rounded to well rounded pebbles generally vary in size from 0.6 to 1.25 cm. Both the chert and the pebble conglomerates show varying degrees of silicification; however, in all cases the relict conglomerate structure is still easily recognized.

Minor shale sections are present also within the Valmy and are generally pale grey in color. In the Red Devil mines area the shale has been converted to porcellanite as a result of silicification, probably related to hydrothermal alteration.

The Valmy Formation was first described in its type location by Roberts (1951) in the Antler Peak Quadrangle, 50 km to the west. In the Shoshone Range to the southwest Gilluly and Gates (1965) found great thicknesses of the Valmy exposed at the surface and also in the same structural setting as seen in the present mapping area, overlain by a tuffaceous sedimentary section and capped with the basaltic andesite.

Late Oligocene-Early Miocene (?) tuffaceous sediments. A Late Tertiary tuffaceous gravel section rests unconformably on the Ordovician Valmy Formation. In places this gravel section may be as thick as 75 m. Excellent exposures of the moderately sorted gravel interbedded with silicic (?) tuff beds can be seen in the gravel pits in section 6. Along the range front only one exposure of this unit is preserved. At the toe of the easternmost landslide on a steep face a tuff bed about 1.5 m thick is exposed with an apparent dip of 28° westward. Close inspection reveals parts of a gravel section above and below it. The bed cannot be traced for more than 60 m before it begins to merge with landslide debris. This fact, along with the steep dip of such a well-bedded unit suggests that this particular exposure is a single block slumped during landsliding.

Because the gravel section slumps readily, the unit is poorly exposed, and contacts between it and overlying and underlying rocks must be mapped on the basis of float. However, a characteristic geomorphologic feature along the steep faulted front of the range helps to define this poorly consolidated unit. Looking along strike of the range front, the topographic profile is commonly steep near the base of the range, then it flattens out, and finally steepens again near the top (see Figure 3). This break in slope is due to preferential weathering of the unconsolidated unit. Also characteristic of this unit is a light tan, clay-rich soil that is fluffy when dry, and plastic when wet. The soil probably contains a great deal of bentonite derived from weathering of feldspars and glass in the silicic tuff interbedded in the unit.

Well-rounded to sub-angular pebbles and cobbles in the gravel sections of this unit contain a large variety of rock types, including: grey, green, brown, and black chert; grey, brown, and black quartzite; grey sandstone; and silicic volcanics and conglomerates. The green chert gravel is useful to distinguish the unit from float from the Valmy since no green chert was found in the Valmy in this area. Very well rounded pebbles may have been reworked from older stream deposits. Source rock for the abundant chert, sandstone, and quartzite was probably largely the siliceous western assemblage of Paleozoic rocks thrust into the area in Late Paleozoic time. Mesozoic silicic volcanic

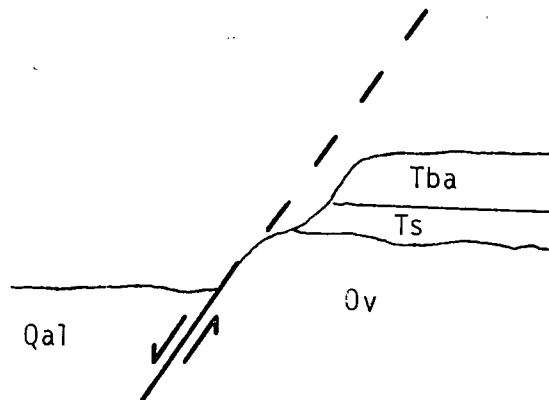


Figure 3: Bench-like expression of the tuffaceous sediments underlying the basaltic andesite capping the range.

rocks in the Frenchie Creek quadrangle to the southeast (the Pony Tail Group of Muffler, 1964) may be the source of the silicic volcanic cobbles. In general, the lithologies of the gravel are easily distinguishable from float of the various rock types found in the Valmy in the present mapping area.

Tuff beds from 0.3 - 1 m thick are found interlayered within the gravel section (see Figure 4). Contacts with the gravel are generally gradational; the matrix of the gravel sections appears to be a mixture of sand and pyroclastic material. The tuff is pale grey in color, fine-grained and generally well bedded. In mapping stratigraphically equivalent tuffaceous sedimentary units in the Shoshone Range to the southwest, Gilluly and Gates (1965) also mention interbedded rhyolitic tuff.

Very coarse bedding in the gravel, crossbedding in the tuff and gravel (see Figure 5) and occasional lenses of sand indicate stream deposition. The entire unit may represent a large alluvial complex that overlapped the Valmy.

It is significant to note the rather widespread extent of this unit (or stratigraphically similar units) throughout the region. In the Shoshone Range to the southwest and in the Cortez Mountains to the south, wherever the base of the basaltic andesite is exposed, it is found to overlie the tuffaceous sediments. Thus, pre-lava topography was no doubt characterized by broad alluvial regions accounting for the apparently equivalent exposures that now cap four separate ranges.

Mid-Miocene basaltic andesite. Flows of intermediate to basic lava cap the Mal Pais forming a prominent cuesta. The flows extend for almost 16 km to the southwest and also cap the Argenta Rim to the north across Whirlwind Valley. Apparently once a coherent unit, these flows have been broken by normal faults and tilted to the southeast 5° - 8° , forming relatively smooth dip slopes on the back (south) side of the ranges. In the Mal Pais region the rocks generally strike about $N70^{\circ}E$. K-Ar dating of the basaltic andesite section in the Crescent Valley quadrangle to the southwest yielded an age of 16.7 m.y. (McKee and Silberman, 1970).

Southwest of the geyser area is a great thickness (more than 1100 feet, 335 m) of the basaltic andesite sequence is exposed, uplifted along an extension of the Corral Creek fault (as mapped in the Crescent Valley quadrangle to the southwest by Gilluly and Gates, 1965). In the vicinity of the Beowawe Geysers the fault changes strike and is broken by several NW-trending cross faults (see the geologic map, Plate 1). The basaltic andesite section thins markedly (to about 100 m) just northeast of White Canyon, and continues to thin gradually (to ~60 m) to the vicinity of Red Devil mines where it ends abruptly, probably as a result of erosion.

Individual flows in the Beowawe vary in thickness from less than 1.5 m to apparently greater than 15 m. The flows are often jointed; however, true polygonal columns characteristic of basalt are



Figure 4. Siliceous tuff interbedded with gravel within the late Oligocene-early Miocene (?) tuffaceous sediments unit. Hammer for scale.

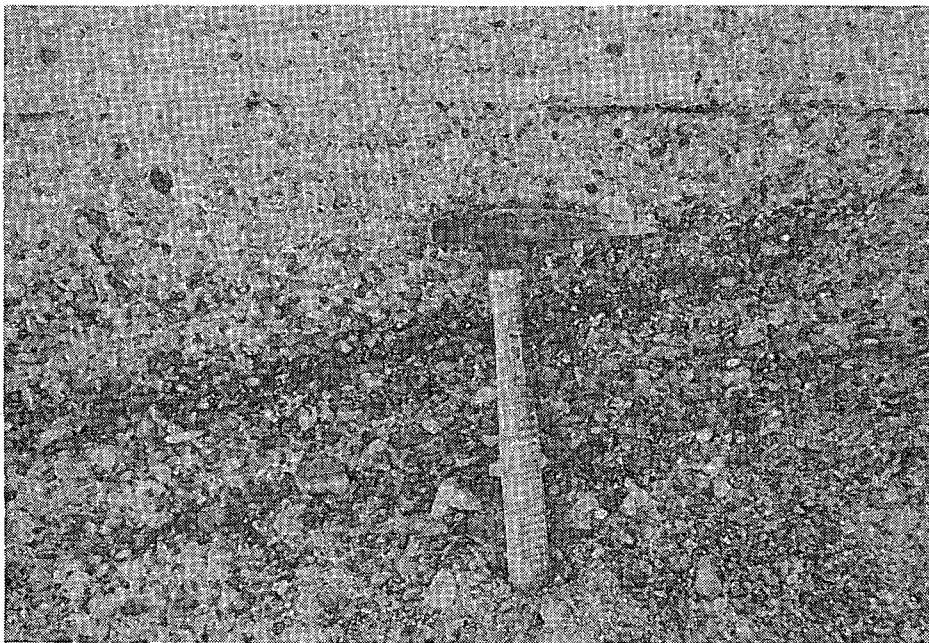


Figure 5. Cross-bedding in gravel within the late Oligocene-early Miocene (?) tuffaceous sediments unit. Hammer for scale.

absent. Platy joints (roughly .6 to 1.5 m apart) along foliations defined by flow banding of plagioclase phenocrysts mark some flows. The non-platy flows range from massive to very vesicular (with vesicles up to 3.8 cm long).

The basaltic andesite is generally dark grey to black on a fresh surface and weathers a reddish brown. Phenocrysts of plagioclase (up to 2 mm long), pyroxene, and rarely, olivine, can be recognized by hand lens inspection, as well as (in pyroclastic material) occasional clear to pale amber glass particles now partially devitrified. Under the microscope the ground mass is seen to be composed of euhedral laths of plagioclase of microlite size, pyroxene, olivine, and numerous opaques (possibly magnetite; both Gilluly and Gates, 1965 and Gilluly and Masursky, 1965, report abundant magnetite in the flows). Much of the plagioclase is gradationally zoned and, in general, the ground-mass appears more sodic than the phenocrysts. Gilluly and Gates (1965) identified the plagioclase as labradorite and reported zoning from An₆₅ in the interior to An₅₅ near the edge of the crystals. They also observed some interstitial glass (much of which was slightly devitrified) and rarely, interstitial quartz.

The volcanic sequence has been referred to both as andesitic basalt and basaltic andesite by various workers in the surrounding areas. The published chemical analyses done on the basaltic andesite are given in Table I. The samples were collected in the Shoshone Range and Cortez Mountains to the south. As the chemical analyses indicate, the rock, in bulk composition, is neither a true basalt nor a true andesite but is probably closer to an average quartz basalt. Because the quartz of the norm is almost wholly occult, Gilluly and Masursky retained the designation of basaltic andesite as had been used in the Northern Shoshone Range by Gilluly and Gates (1965).

An interesting part of the basaltic andesite section can be seen on the northeastern face of White Canyon. Included there is a tuff breccia consisting of irregularly shaped, leached, light-colored blocks in a dark red aphanitic matrix. One possible origin for such a rock may be mudflow action during volcanism (K. Krauskopf, 1975, personal communication). Overlying this zone is a region of abundant spherical lapilli (from 1 mm to 1.5 cm in diameter) and bombs formed of aggregate lapilli (up to 7.5 cm in diameter). These have apparently eroded out of the basaltic andesite in which they can be observed to form nearly level layers within a rather massive basalt not unlike conglomeratic gravel layers within a sandstone. The layers were probably laid down during a "rain" of such ejecta, then later covered by a basaltic andesite flow. The lapilli weather dark brown, but on a fresh surface the material is grey-brown and contains abundant glassy fragments. This interlayered lapilli and massive flows unit section was only found exposed along the northeastern edge of White Canyon. It suggests the possibility of a volcanic vent close by; however, there is no modern geomorphic expression of such a structure.

Late Miocene (?) tuff. At the head of White Canyon a section of well-bedded silicic tuff (roughly 200 ft, 65m, thick) folded in a gentle syncline overlies the basaltic andesite. Hand lens inspection of the

TABLE 1
Chemical Compositions

	1	2	3	4	5	6
	Cortez Mtn. Flow	Shoshone Range Flow	Sheep Creek Range Flow	Roberts Mtn. Flow	Roberts Mtn. dikes	Average Continental tholeiite
SiO ₂	55.01	55.89	59.1	55.3-62.5	52.8-58.3	50.7
Al ₂ O ₃	15.01	14.70	17.3	15.3-16.1	13.3-14.6	14.4
Fe ₂ O ₃	3.22	2.90	4.0	}10 - 11	}10 - 11	3.2
FeO	6.31	7.37	1.7			9.8
MgO	4.14	3.98	2.2		2.1-5.5	6.2
CaO	8.09	7.39	3.4			9.4
Na ₂ O	3.02	3.11	4.8			2.6
K ₂ O	1.52	1.84	3.6	> 1.0	1.2-3.0	1.0
H ₂ O ⁺	0.68	0.34	1.6			--
H ₂ O ⁻	0.76	0.48	1.0			--
TiO ₂	1.30	1.36	0.83	≈ 1.0	1.3-1.6	2.0
P ₂ O ₅	0.37	0.46	0.43			--
MnO	0.15	0.16	0.12			0.2
CO ₂	0.03	0.02	0.05			--

1. Gilluly and Masursky, 1965
2. Gilluly and Masursky, 1965
3. Stewart et al., 1977

4. E.H. McKee, pers. communication
5. E.H. McKee, pers. communication
6. Hyndman, 1972

white to pale grey unit reveals that it is composed predominantly of volcanic ash and minor sands. The composition and stratification indicate deposition in water.

Late Miocene (?) gravels. Onlapping the andesite and apparently truncating the late Miocene (?) tuff beds, a section of gravels has been mapped. Possibly an ancient pediment deposit related to the cross faulting trend, the unit consists solely of basaltic andesite debris (as opposed to the variety of rock types found in the younger alluvium) and a pale sandy soil. In one region, in the southwest corner of section 16, extremely well-rounded cobbles of basaltic andesite (up to 10 cm in diameter) can be found. The degree of roundness of these cobbles indicates a large distance from their source and suggests that this deposit formed long before the present breakup of the ranges. These gravels may be much more widespread; however, because of their general similarity to younger alluvium they were not distinguished elsewhere on the range.

Late Miocene (?) basalt. Gently dipping flows of basaltic rock are exposed in Whirlwind Valley west of the Geysers. These flows dip $\sim 3^\circ - 4^\circ$ eastward (into the axis of the valley) and appear to lie upon the dip slope of the basaltic andesite capping Argenta Rim although the contact was not observed. A minimum thickness of 30 m (consisting of two flows) is exposed. Drill hole data from Chevron Resource Company (discussed in a later section) indicates a total thickness of approximately 110 m of these younger flows in Ginn #1-13, 1 km to the east of the outcrop in the valley (see plate 1 or Figure 9 for location).

The exposed flows consist of a massive lower unit with a vesicular upper portion. Phenocrysts of plagioclase and olivine are visible with a hand lens in most specimens. Superficially the dark-grey rock appears quite similar to the basaltic andesite. Paleomagnetic work on the flows (also discussed later) indicates that the valley flows have distinct natural remanent magnetization (NRM) directions and Koenigsberger ratios (remnant magnetic intensity/induced magnetic intensity) relative to the basaltic andesite capping the ranges.

Tentatively these flows are correlated with similar basaltic flows capping the Sheep Creek Range to the north which have been dated at 10.0 ± 0.3 m.y. (McKee and Silberman, 1970). The gentle dip of the flows and their apparent localization in Whirlwind Valley indicate that they were extruded after modern structural activity in the region had begun. A K-Ar date on these flows would be useful in detailing the timing of deformation in this region.

Quaternary-Tertiary (?) chalcedony-carbonate vein. A massive white to pale grey silicic-carbonate vein cutting through the basaltic andesite is exposed at the opening of White Canyon. Steeply dipping (about 70° S), the vein strikes N80W and is 40-45 m wide in the thickest region. It can be traced nearly 250 m along strike but then appears to fade into the volcanic sequence on the west end (where it is probably truncated by the main range front fault), while on the eastern end it bifurcates again and again into many small veins (some less than one foot in width).

Although the vein is composed predominately of chalcedony, minor carbonate can be found on freshly broken surfaces of the vein rock. Preferentially leached, carbonate is now rather rare in the weathered rock; however, polygonal molds on exposed surfaces of chalcedony suggest eroded carbonate. Internal structure of the vein is generally massive although there is a parting parallel to the contacts with the volcanic rocks. In addition, some parts of the vein contain a chalcedony breccia recemented with silica, suggesting fault movement (?) during formation of the vein. In places the contacts with the basaltic andesite are clear cut and well defined; elsewhere, however, extreme silicification of the volcanic rocks has obscured these contacts.

The composition and structure of this vein suggests that it may represent part of an ancient geothermal system where hot water moved through a fracture zone in the basaltic andesite and gradually "self-sealed" by deposition of silica and minor carbonate. The carbonate was probably deposited as a result of minor pH fluctuations in the geothermal system (D.E. White, personal communication, 1975).

Quaternary landslide deposits. Landsliding probably associated with NNW-trending cross faulting has broken the steep range front and developed hummocky topography that extends out into Whirlwind Valley. Two different types of landslide deposits can be distinguished. Debris deposits are associated with typical landslide features of a rounded toe and a semi-circular break-away zone at the head which left near-vertical cliffs of basaltic andesite 90 to 125 m high at the top of the range. The debris includes parts of the Valmy Formation, some of the gravel from the tuffaceous sedimentary section, and large coherent blocks of lava in round mounds. These "typical" debris deposits are located on the east and west end of the region of landsliding. Between the two typical landslide areas, a second style of landslide deposits exist. In this area there is no one well defined break-away zone, but rather there are many small cliffs 6 to 9 m high. These small cliffs appear to represent separate blocks of the lava that were broken away and down-dropped in a step-like fashion.

Quaternary siliceous sinter. Formed by continuing accretion of opal from silica-rich thermal waters moving along the main range front fault, the sinter terrace is now over a mile long and about 60 m high (see Figure 6). Present thermal activity on the terrace is limited to a central half mile zone, but old, layered sinter can be seen both on the northeast and southwest end of the terrace. Old porous sinter can also be seen on the slope above the present terrace. Nolan and Anderson (1934) reported that the layering in this sinter appeared tilted, which would suggest renewed movement along the range front fault. The author observed this layering and alternatively suggests that the apparent dip may be depositional, the deposits forming from geysers which in the past were much larger.

The siliceous sinter composing the terrace varies a great deal in both appearance and texture. For the most part, the material forming the terrace is a loosely cemented aggregate of light grey to white opal fragments. Local layering may be defined by color or textural variations in

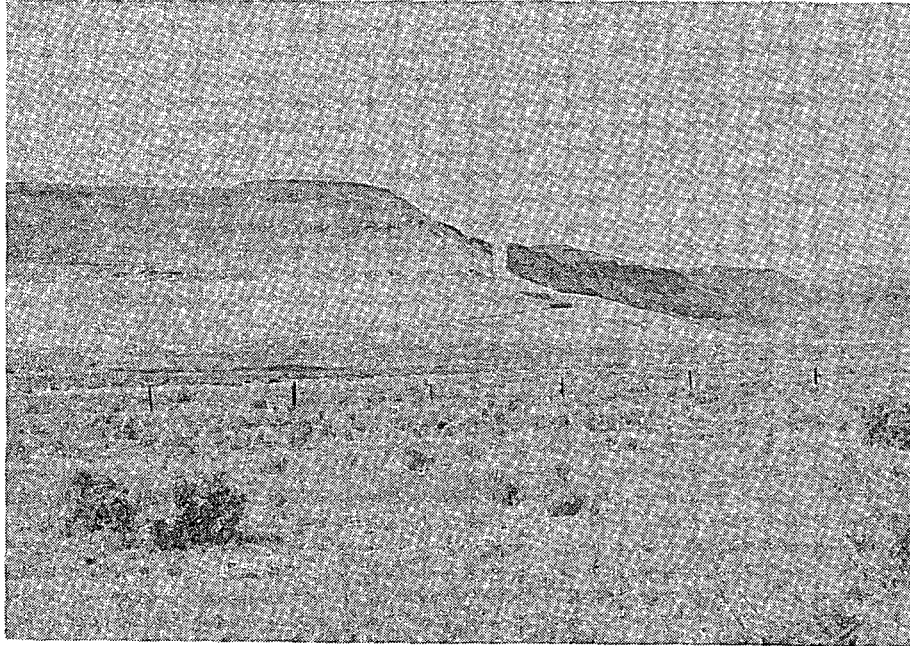


Figure 6. Sinter terrace, looking southwest from across Whirlwind Valley.



Figure 7. Well-developed layered structure in an exposure of old sinter near the base of the terrace. Hammer for scale.

the sinter (see Figure 7). Smooth surfaces (often found in the older, well-layered sinter on the southwestern end of the terrace) are commonly formed of a white dense opal occasionally with a suggestion of iridescence. Nolan and Anderson (1934) report that locally in the sinter sporadic quartz grains and aggregates of clay minerals are found, together with small quantities of carbonates and sulphates of sodium and calcium. Also, they report that the older sinter on the ridge above the present terrace is very similar to that now being formed except for a greater abundance of clay minerals, and a common staining by iron oxides.

Quaternary alluvium. Included in this unit are the surficial deposits which comprise the bulk of the valley fill, alluvial fan deposits along the steep face of the range front, and modern stream and arroyo deposits presently being deposited. The alluvial sand is pale tan in color and contains fragments of locally derived material. In places a desert pavement of volcanic rocks cemented with caliche has developed. In the center of the valley the older alluvial surface has been dissected by modern streams to a depth of at most 3 m.

Hydrothermal Activity and Ore Deposits

Past geothermal activity. In addition to the modern manifestations of geothermal activity at Beowawe, there is abundant evidence of past hydrothermal and geothermal activity all along the Mal Pais Ridge. The most striking remnant of this activity is the chalcedony-carbonate vein, described previously, located at the mouth of White Canyon. The numerous bifurcations of the vein, sharp contacts (in places) with the volcanic rock, and layering parallel to these contacts can be easily explained if the vein does, in fact, represent a feeder to a self-sealed geothermal system that once moved through a fracture zone in the basaltic andesite. Recurring movement along this fracture zone may be responsible for the brecciation and re-cementation of chalcedony observed in places within the vein.

As mentioned previously, field evidence suggests that, in part, the vein formed by co-precipitation of chalcedony and carbonate. Such an occurrence is not unusual in geothermal systems and is probably in response to minor fluctuations in the pH of the hydrothermal water (D. E. White, 1975, personal communication). Fragments of botryoidal opal common in the float of the basaltic andesite all along the range, are most abundant in the vicinity of the vein. There also, one can find opal-filled vesicles in the volcanic rock in addition to opal geodes as large as 8 cm. However, more direct surficial expressions of this early geothermal activity (particularly sinter-type deposits) have been destroyed by erosion, if they in fact ever existed. White (1970) points out that many high-temperature, silica-depositing geothermal systems do not form sinter if flow to the surface is slow. In this case heat is lost by conduction and the SiO_2 is precipitated prior to discharge. Thus, the chalcedony-carbonate vein probably represents part of the "plumbing" of such a sluggish geothermal system.

In places along the periphery of the vein the basaltic andesite has been intensely altered and is largely silicified. The degree of alteration diminishes rapidly away from the vein to a relatively unaltered state within about a meter. One is tempted to extrapolate the trace of the roughly east-west trending vein; just west of White Canyon the vein was apparently truncated by the main range front fault while to the east of the canyon the vein bifurcates many times and appears to die out near the contact between the Valmy quartzite and the basaltic andesite. This near-vertical contact has been interpreted as a NNW-trending fault which may have exerted some control on localizing the system.

Another notable example of hydrothermal alteration along the range is found near the base of the volcanic section on the western scarp of the main landslide where the basaltic andesite lies unconformably on a chert conglomerate in the Valmy. The rock has been replaced almost entirely by silica and forms one large rather resistant outcrop that varies in color from tan and grey to pinkish-purple. In some instances the silica replacement has been complete and a sub-connected framework of grey to grey-brown chalcedony can be seen. The rock is considered altered volcanic rock because the original rock appears to have been made up of a variety of minerals that resulted in varying degrees of alteration and leaching as opposed to the rather homogeneous

siliceous quartzites and cherts of the Valmy. This rather localized region of intense alteration lies approximately along the trace of one of the main cross faults and is no doubt related to the movement of hydrothermal fluids along that fault.

A third example of apparent fault-related hydrothermal activity is a carbonate (largely travertine) breccia deposit located along a splay of the main range front fault in section 12, Eureka County. The abundant carbonate suggests a relatively low temperature geothermal system moving along the fault. Subsurface temperatures commonly 100°C or less have been linked to carbonate deposition, whereas silica deposition indicates subsurface temperatures in excess of 180°C (White, 1970).

Acid alteration (from oxidation of H₂S) in the vicinity of barite prospects in section 12 is also probably related to past hydrothermal activity in the Mal Pais area. The cinnabar mined in the Red Devil claims (discussed in the next section) is thought to be related to hydrothermal activity. It is difficult to date any of this activity; however, the formation of the chalcedony-carbonate vein and the carbonate breccia zone are obviously events that postdate the basaltic andesite eruptions.

Ore deposits. The only commercial ore deposit in the Mal Pais Ridge area is located near the northeast end of the range, the Red Devil workings. This group of claims was set up in 1924 by R. S. Harris and C. M. Wilkinson who were in search of quicksilver (Roberts et al., 1967). The mine was worked on and off for about 20 years and produced about 150 flasks of mercury. Cinnabar, the only ore mineral found, occurs in the silicified pebble conglomerate, quartzite, and shale of the Valmy Formation, particularly where the rock had been highly brecciated along faults and subsequently silicified. The pebble structure is still clearly recognizable, although the quartzite and shale have been completely altered to porcellanite. The cinnabar forms veinlets, lines cavities and coats breccia fragments (Roberts et al., 1967).

This cinnabar deposit probably formed as a result of hydrothermal activity; the only age control is post-Paleozoic. It is the largest known cinnabar deposit in Eureka County, a region of highly productive metallic ore deposits of other kinds. The connection between mercury deposits and geothermal activity is now well established (White, 1967). The Sulphur Bank region in the vicinity of "The Geysers" in Sonoma County in northern California is a notable example of a major hot-spring quicksilver association.

Also of economic interest in the area is a non-metallic mineral, barite, that is quite common and widespread in north-central Nevada. The prospects in section 12, Eureka County (geologic map, Plate I) explored a minor deposit of bedded barite within the Valmy Formation. To the southwest, in the Crescent Valley and Mount Lewis quadrangles, abundant deposits of bedded barite occur interbedded with chert and limestone of the Devonian Slaven Chert Formation. Extensive studies of the economic geology of this region by Ketner (1965) indicate that the barite is not related to the copper-lead-zinc ore deposits in the area and is apparently primarily controlled by bedding rather than faults. The barite in the present area may be a replacement product of chert

in the Valmy, formed as a diagenetic replacement of sea-bottom sediments by barium sulfate from sea water, as Ketner (1965) proposed for the bedded barite within the Slaven chert. Ketner found no positive evidence that such barite deposits were related to hydrothermal activity.

Modern geothermal system. Hot springs are abundant throughout the Basin and Range province; however, Beowawe is nearly unique (along with Steamboat Springs, Nevada) as an area of natural geyser activity. Chemical analyses of the thermal waters indicate that the geothermal system is a hot-water system, rather than a vapor-dominated one (White, 1974, p. 88). The average surface temperature of the present hot springs is about 96°C (this value is roughly the same as reported for the undisturbed system by Nolan and Anderson, 1934); however, drilling in the hot springs area encountered temperatures of approximately 210-215°C at depths of only 150-200 m (Koenig, 1970). Slightly higher temperatures were measured at a depth of 2.92 km along the main range front fault (William Mero, Chevron Resource Co., personal communication) and agree moderately well with geochemically predicted reservoir temperatures between 226-240°C (Renner et al., 1975).

Surficial geothermal activity in the Beowawe region is now limited to a sinter terrace formed along the scarp of the main range front fault and a small portion of the valley floor at the base of this terrace. Over 65 m high and more than 1.6 km in length (Figure 6), the sinter terrace appears to have been slowly built up by the deposition of silica (predominantly opal) from the thermal waters. The location of the terrace suggests that the range front fault provides a major channelway for hot water traveling to the surface. In addition to the obvious structural controls that have acted to localize the geothermal activity, the system apparently also responds to variations in the amount of ground water available as is evidenced by the more energetic activity during the winter months (Nolan and Anderson, 1934).

The top of the terrace is covered with numerous vents, fumaroles, and bubbling springs as well as small intermittent geysers and, presently, two uncapped wells that continuously vent steam and hot water to the atmosphere. These blowing wells create a tremendous roar and play to heights of more than 30 m; in winter they produce a snow-like coating of ice on the terrace, which is locally covered by soft gray-white silica several centimeters thick. After extensive drilling of the area in the early 1960's (discussed in the next section) nearly all natural geyser activity was destroyed leaving only the two or three intermittent geysers. Detailed descriptions of the various surface expressions of the geothermal system both before and after drilling activity have been given by several workers (see Hose and Taylor, 1974; Rinehart, 1968; Nolan and Anderson, 1934; and Evans, 1869).

If a slow, steady accretion process is assumed responsible for the buildup of the sinter terrace, the age of the modern geothermal system can be determined from the volume of silica deposited and the rate of accumulation. The concentration of silica in the modern thermal waters before exploitation was reported to be around 425 ppm by Nolan and Anderson (1934). Because the solubility of silica increases with increasing temperature (assuming other variables remain approximately the same), this modern value

of 425 ppm would represent a lower limit if the system is considered to have been losing heat. (It is possible that heat loss is not important during the life-span of the system, either because of the nature of the heat source or because of the short time interval).

The volume of sinter forming the terrace and veneer on the valley floor near the base of the terrace can be roughly estimated at around 1.80×10^{13} cm^3 . If a porosity of 50% is assumed (certainly not off by more than a factor of 1.5), then the total volume of silica deposited is 8.8×10^{12} cm^3 which corresponds to 1.76×10^{10} kg using a density of 2.0 g/cm^3 for opal. Assuming a constant concentration of 425 ppm SiO_2 in the thermal waters, the amount of these waters reaching the surface would be in excess of 4.14×10^{13} kg or 4.3×10^{13} l (1.14×10^{13} gal). The final step in estimating the age of the system requires a value for the flow rate. Using a constant rate of around 400 l/min (about 90 gal/min)--estimated for the natural system without the uncapped wells (Renner et al., 1975)--an approximate age of 210,000 years is determined. This rough calculation agrees well with estimates of the ages of modern geothermal systems at Yellowstone ($\sim 150,000$ years, D. E. White, 1973, written communication) and Waireki, New Zealand ($\sim 500,000$ years, Studt and Thompson, 1969).

The rate of discharge of the thermal water and its temperature can also be used to calculate the total convective heat discharge by springflow of the system using the formula:

$$\left(\begin{array}{l} \text{heat discharge} \\ \text{by springflow} \end{array} \right) = \left(\begin{array}{l} \text{total volumetric} \\ \text{discharge} \end{array} \right) \left(\begin{array}{l} \text{density} \\ \text{heat} \end{array} \right) \left(\begin{array}{l} \text{specific} \\ \text{excess temp.} \\ \text{above mean annual} \end{array} \right)$$

The average surface temperature of the springs is 96°C ; hence, the excess temperature (spring temperature - mean annual temperature) is 87°C ($96^\circ\text{C} - 9^\circ\text{C}$). The estimated surface discharge of the natural system, as given above, is 400 l/min (Renner et al., 1975). For this order of magnitude calculation a density of 1.0 g/cm^3 and a heat capacity of $1.0 \text{ cal/gm } ^\circ\text{C}$ was used for the hot water. Substituting these values into the equation above, the heat discharge calculated is 0.58×10^6 cal/sec.

To compare this value with the regional conductive heat flux, the heat flow, 0.58×10^6 cal/sec, must be divided by the area over which the heat is reaching the surface. Using 1.5 km^2 , the approximate area of the sinter terrace and present-day hot spring activity, the convective heat flux due to springflow is calculated at 39 HFU ($\mu\text{cal/cm}^2\text{sec}$). This value is 10-15 times the measured regional conductive heat flux of 2.5 - 3.0 HFU (Sass et al., 1971). This convective heat flux for the system is a minimum value, based only on hot spring discharge. It does not include various other modes of heat discharge in thermal areas such as (1) lateral movement of warm ground water beyond the margin of the area; (2) steam discharge from geysers, vents, or fumaroles, as well as heated air escaping from the soil surface; (3) evaporation from hot-water surfaces; (4) radiation to the atmosphere from warm soil and water surfaces; (5) conduction through near-surface materials..

In a similar manner as described above, White (1968, p. 99) was able to estimate a somewhat more accurate convective heat flow of 11.6×10^6 cal/sec for Steamboat Springs, Nevada, using the base temperature of the system because there the total discharge is well known from Cl and B concentration studies in a nearby creek. The Steamboat Springs system has an area of 5 km^2 thus the total convective heat flux is 236 HFU.

Drill Hole Data

Commercial exploration of the Beowawe geothermal area began in 1959. Between that date and 1964 Magma Power Company and associated companies drilled 12 wells within the active hot springs and geysers area, several of which were capable of producing geothermal fluids. (For a complete list of wells drilled and locations see Garside, 1974.) Koenig (1970) reported that the maximum temperature was 214°C and production came from very shallow depths (between 150-200 m). One well was capable of producing over 50,000 pounds per hour of steam, and 1,400,000 pounds of hot water at a temperature of 172°C (342°F) and a well ^{head} pressure of 116 psi; however, problems of scale forming in the pipes and cold water inflow probably rendered this and the other wells non-commercial (Koenig, 1970).

Because of renewed interest in geothermal prospects, exploration began again in the area in 1974. In January of that year Standard Oil of California and American Thermal Resources began jointly drilling a well in Whirlwind Valley, west of the Geysers in the southeast corner of section 13 (Ginn #1-13, henceforth referred to as the Ginn well; see Figure 9 for location). Drilling ended in 1975 at a depth of 9563' due to a complete loss of circulation. Magma Power Company returned to the area in 1975 to drill a 6000' well, Batz #1, (henceforth referred to as the Batz well) at the base of the sinter terrace, in the northeastern part of section 17 (see Figure 9). To date, neither well is producing.

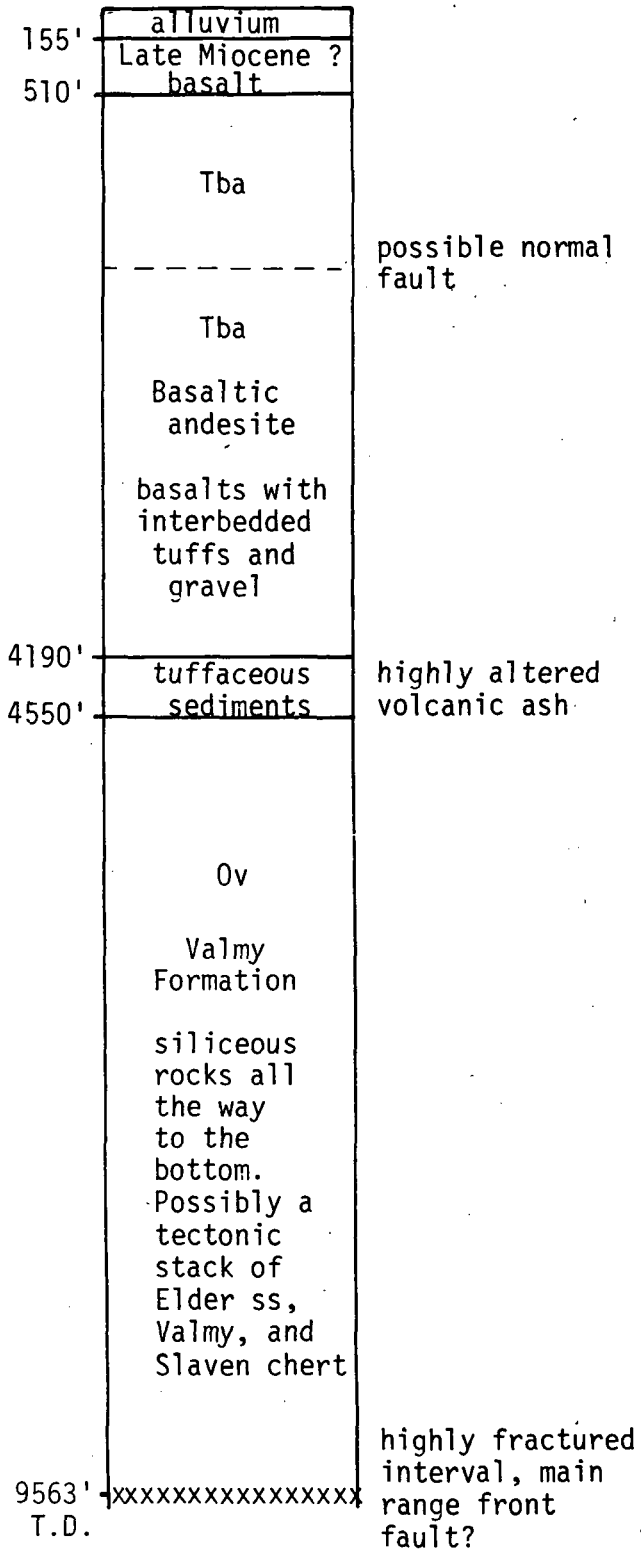
A generalized geologic log of the Ginn well provided by Chevron Resource Company (William Mero, personal communication) and an unofficial summary of the log for the Batz well are given in Figure 8. Both wells penetrated the mid-Tertiary volcanic and tuffaceous sediment cover and bottomed out in the siliceous upper plate assemblage of the Roberts Mountains thrust (possibly a tectonic stack of Ordovician, Silurian, and Devonian quartzites, cherts, and siliceous shales).

The Ginn well is believed to have bottomed out at the range front fault at a depth of 9563 feet (2.92 km). The well is located approximately 1.35 km from the surface trace of the range front fault implying a dip of 65° for that fault. The Batz well was drilled at the base of the sinter terrace into the uplifted block with an inclination of roughly 5° from vertical. Temperature data indicate that a major fault was intersected at a depth of approximately 480' (146 m); this fault was probably the main range front fault with very high measured temperatures reflecting hot water traveling along it to feed the springs directly above on the sinter terrace. The shallow depth at which this fault was encountered requires a near-surface dip of only 40° for the fault if the fault is assumed to crop out at the back of the sinter terrace; on the other hand the scarp may have been eroded back on a now-buried pediment surface. Such a low dip however is steeper than the exposed, eroded scarp (slope ≈30°). In this shallow interval (basin surface to about 500 feet) the scarp may be in part erosional resulting in a low apparent dip. Eventually, with depth, this main fault must steepen to yield a dip of about 65° between the surface and 3 km as indicated by the Ginn well.

Chevron--ATR Well

Ginn #1-13, 1974

surface elevation 4940'



Magma Power Co. Well

Batz #1, 1975

surface elevation 4840'

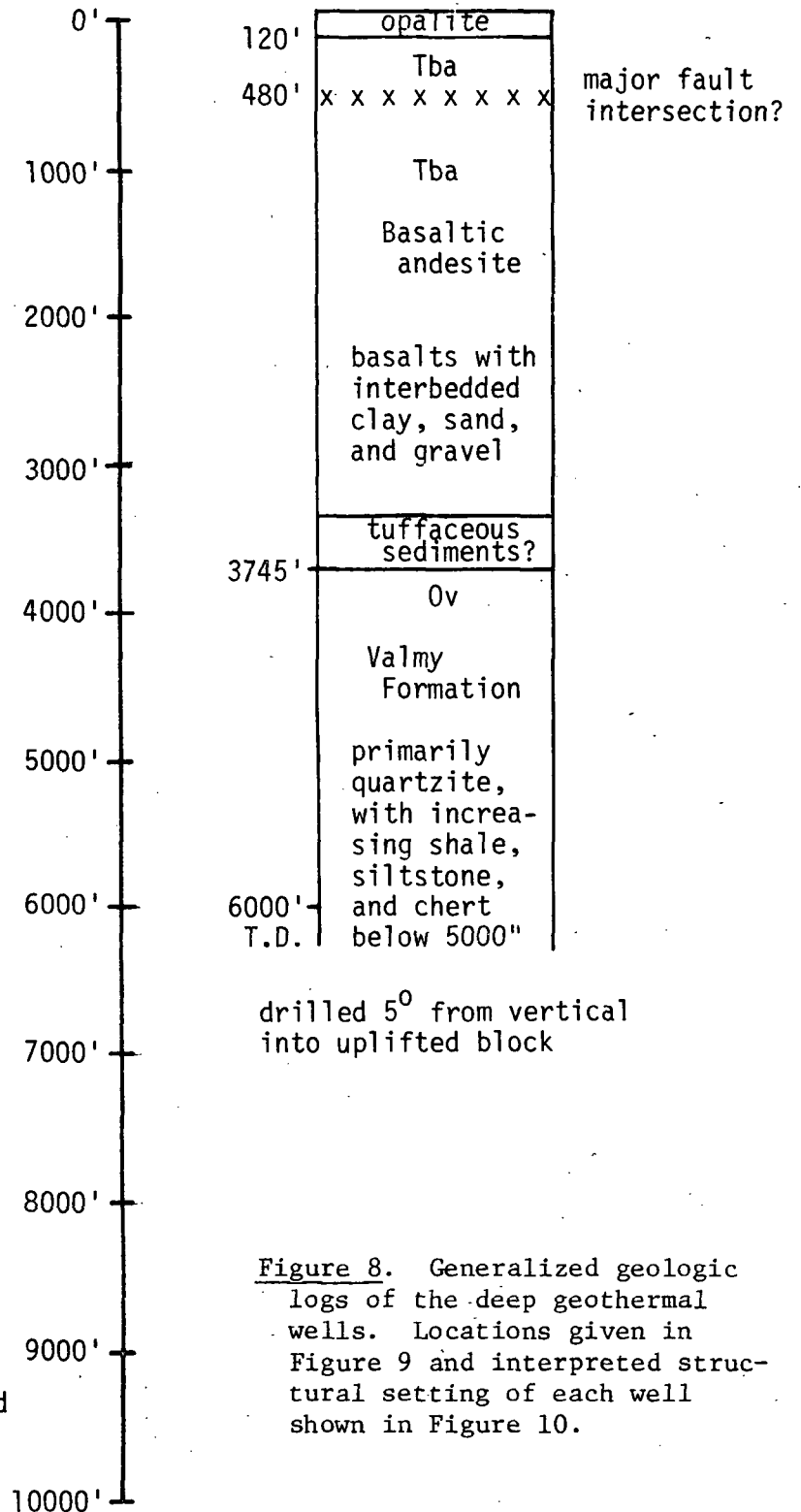


Figure 8. Generalized geologic logs of the deep geothermal wells. Locations given in Figure 9 and interpreted structural setting of each well shown in Figure 10.

In addition to the direct structural data, the drilling results have revealed two facts with important structural implications (1) the great thickness of basaltic andesite in the southwest end of the range, and (2) the presence of a section (~100 m thick) of young basalt (Late Tertiary?) in the valley. After tectonic corrections the drilling data suggest a maximum thickness of basaltic andesite of 1265 m in the vicinity of the Batz well and a maximum thickness of 1330 m near the Ginn well. This thick section of basaltic andesite is notable particularly with regards to the thin volcanic section (~100 m) lying on the Tertiary tuffaceous sediments which in turn overlie the Ordovician Valmy formation exposed less than 1.5 km to the east in the range. This fact along with the general NNW-alignment of exposures of the underlying tuffaceous sediments in the Mal Pais and the Argenta Rim to the north and the localized lateral extent of the basaltic andesite flows regionally (see Figure 2) suggest structural control through NNW-trending feeders and/or faulting as will be discussed in the next section.

The 110 m of Quaternary-Tertiary(?) basalt encountered at the top of the Ginn well no doubt correlates with the section of young basalt flows (minimum thickness, 30 m) exposed on the west end of Whirlwind Valley (see geologic map). The thicker section encountered in the Ginn well and the apparent localization of these flows in the valley indicate that the modern structural deformation of the region had begun by the time they had been extruded. However, the lack of a significant basin fill section (no mention in geologic log) between the young basalt and basaltic andesite in the Ginn well, suggests that the valley must have been youthful.

Structure

Folds. No major folding is exposed in the Mal Pais area. During pre-Tertiary thrusting and orogeny, the Ordovician Valmy Formation undoubtedly underwent intense deformation; however, in the present area exposures are relatively poor and no direct evidence of internal structure in the Valmy was detected. A gentle syncline of late Cenozoic age is exposed on the dip slope side of the range, at the head of White Canyon. This locality was the site of deposition of a roughly 50 m thick lens of well-bedded, tuffaceous, water-laid sediments overlying the basaltic andesite. Tilting of the range has resulted in a gentle plunge of the syncline to the south. Both the tuff beds and the underlying flows have been gently downwarped; dips of as much as 20° in the sediments are too steep to be depositional and suggest gentle subsidence of the basin, possibly during deposition of the tuffaceous material. The downwarping could be due to collapse of a depleted, near-surface magma chamber. Warm, still ductile lava could have deformed and created the downwarped structure which allowed the tuffaceous material to accumulate.

Faults. Extensional tectonics characterized by Basin and Range normal faulting have produced the dominant structural features of the Mal Pais Ridge area. Figure 9 reveals the complex interactions and bends of these faults. Two major trends of normal faulting can be recognized: a N 50-70° E trend responsible for the main uplift of the range, and a nearly orthogonal NNW-trend responsible for the spurs on the south side of the Mal Pais and the Argenta Rim to the north. In addition, there are two minor sets of faults: a NW-striking set possibly related to the bend in the main range front fault in the vicinity of the geysers which appears important in localization of the modern geothermal system; and fracturing in an E-W direction represented by the chalcedony-carbonate vein at the mouth of White Canyon which was apparently truncated by the N 50-70° E trend of faulting.

Main uplift of the range was accomplished by faulting along a N 50-70° E trend. Southwest of the geysers a second, parallel fault bounds two knobs of basaltic andesite down-dropped with respect to the range. Volcanic stratigraphy in the knob directly west of the hot springs area can be matched to the stratigraphy at the top of the main escarpment. The extension of this parallel and more northerly (basinward) fault to the east is concealed by alluvial and sinter deposits; however, the cold springs in section 8 (Eureka County) appear aligned along the presumed trace. This basinward fault is hereafter referred to as the subsidiary range front fault. Antithetic faulting along a NE trend on the SE side of the knob in section 18 (Lander County) has created a small graben. A splay of the main range front fault in sections 11, 12, and 1 (Eureka County) has locally down-dropped the basaltic andesite to the level of the Ordovician Valmy formation.

The tilting of the Mal Pais Ridge block to the south (and southeast) by 5-7° formed a gentle dip slope that extends under Crescent Valley in the same way that the Argenta Rim flows extend under Whirlwind Valley. The dip slope southwest of the Geysers is broken locally by faults with relatively small displacements (less than 60 m) which are subparallel to the adjacent portions

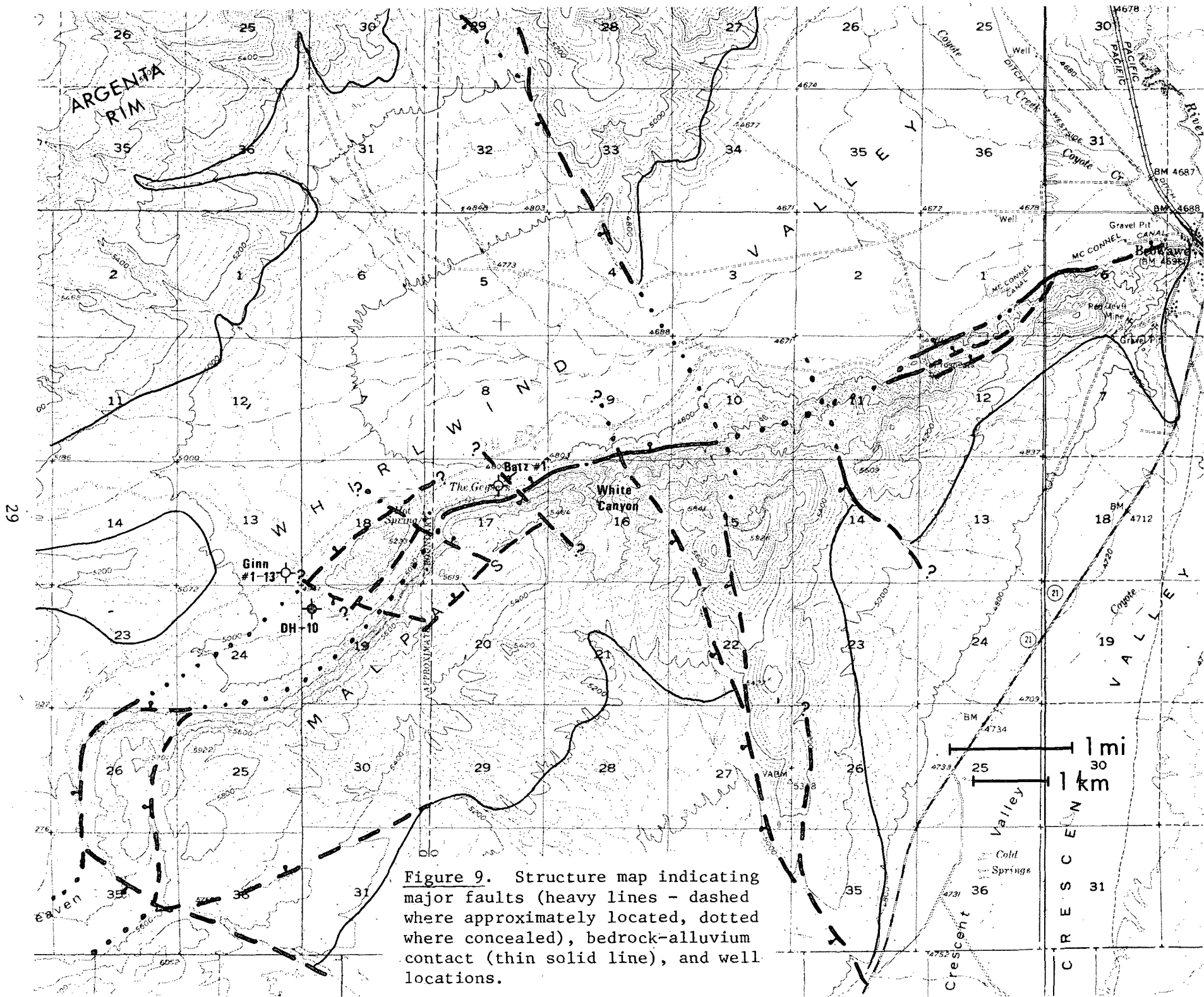


Figure 9. Structure map indicating major faults (heavy lines - dashed where approximately located, dotted where concealed), bedrock-alluvium contact (thin solid line), and well locations.

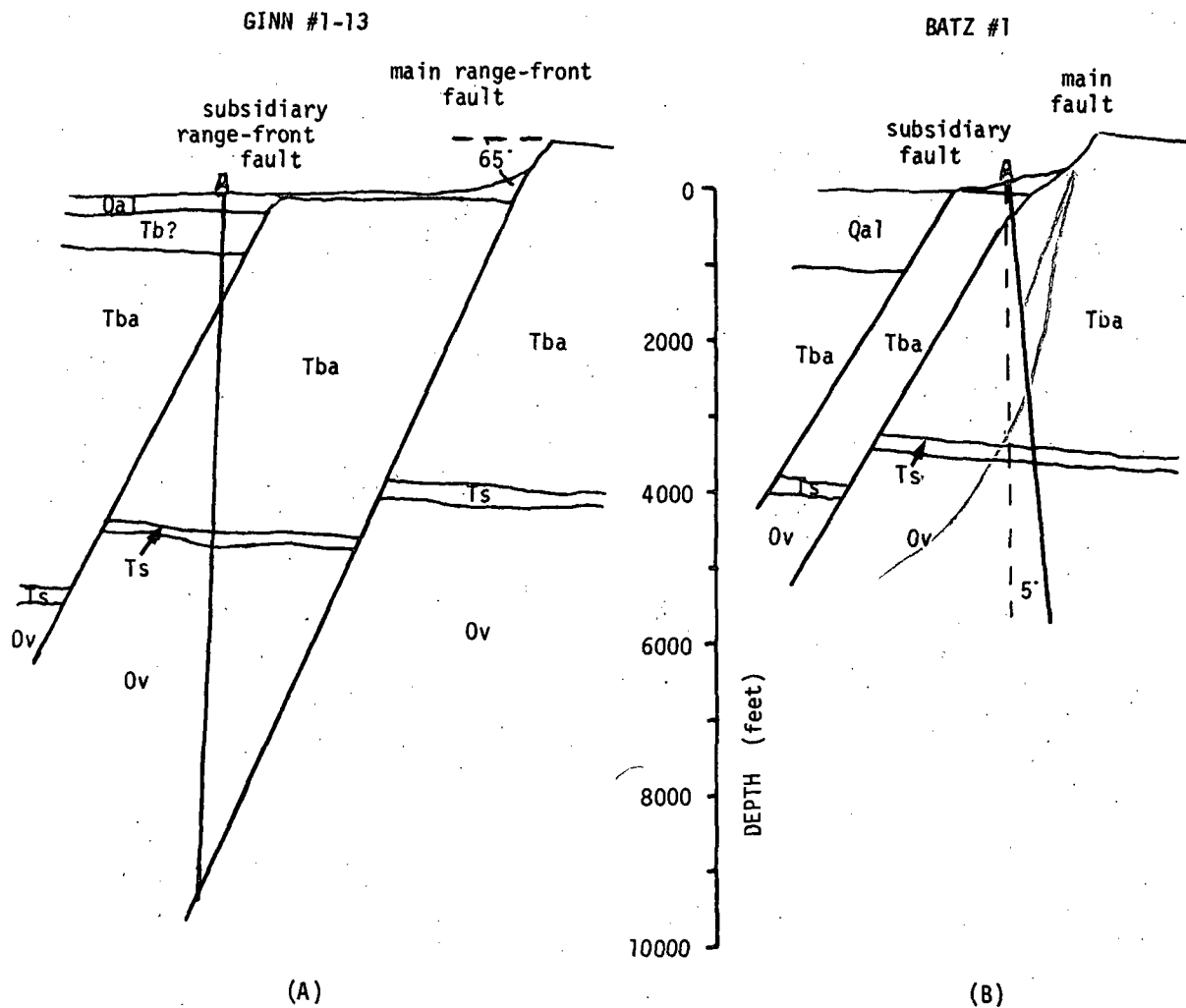
of the range front fault and probably part of the same extensional episode. The sense of offset on the dip slope faults is the same as on the range front faults, south side up.

Total vertical offset along the faults bounding the range can be estimated geometrically by assuming the lava surface once formed a continuous sheet and projecting the dip slope of the basaltic andesite capping Argenta Rim under the alluvium of Whirlwind Valley. This method predicts a maximum net vertical offset of 1700-2150 feet (520-650 m) along the Mal Pais front. This vertical displacement is taken up in part by the subsidiary, basinward, parallel fault southwest of the geysers and also by possible additional extensions of this fault and other faults buried under the alluvium.

Fault dips as well as offsets can be estimated from the drill hole data discussed in the previous section. Figure 10 gives the interpreted structural setting of each of the two deep wells from the drilling information combined with the surface geology. From the Ginn well, the dip of the main range front fault (inferred to be the highly permeable zone intersected as the bottom of the hole) is about 65° . The location of the subsidiary, basinward fault shown in Figure 10a, is based largely upon surface geology, as discussed previously; it may correspond to the possible normal fault detected at 1650 feet (Figure 8). Offset on the main range front fault is best obtained by a comparison of the level of the top of the basaltic andesite on the Mal Pais Ridge and on the subsidiary block. Control for the depth to the top of the basaltic andesite on the subsidiary block in the vicinity of the Ginn well is provided by a shallow heat-flow hole which indicates only a thin veneer (5.8 M) of alluvium (Hole DH-10 location given in Figure 9, Frank Olmsted, USGS Water Resources, written communication, 1975). The net offset between this subsidiary block and the top of the volcanic sequence on the Mal Pais is about 750 feet (230 m). Offset on the subsidiary fault, obtained by matching the tops of the basaltic andesite section on the subsidiary block and in the Ginn well is about 500 feet (150 m), indicating a total vertical offset of 1250 feet (380 m).

As shown in Figure 10b and discussed in the Drill Hole Data section, the Batz well is inferred to have intersected the main range front fault at a depth of 480 feet (146 m). This requires a low apparent near-surface dip for the fault of only 40° . As discussed previously, this low dip is thought to be due possibly to an eroded scarp (hidden under the sinter terrace). Very high temperatures measured along this presumed fault suggest that it is the main range front fault with hot water traveling along it to feed the hot springs directly above on the sinter terrace.

Offset on the main range front fault in this region is roughly 740 feet (225 m), obtained from the depth to the basaltic andesite on the subsidiary block (about 120 feet or 37 m in the Batz well) relative to the height of the escarpment in this region. This is in good agreement with the 750 foot (229 m) offset in the vicinity of the Ginn well. Because the Batz well was drilled near the base of the main escarpment on the subsidiary block (unlike the Ginn well which was drilled basinward of both faults, see Figure 9) there is no well information on offset of the subsidiary fault in this region.



Horizontal Scale = Vertical Scale

LEGEND

- Qa1-Quaternary alluvium
- Tb?-Late Miocene (?) basalt
- Tba-Mid-Miocene basaltic andesite
- Ts -Miocene tuffaceous sediments
- Ov -Ordovician Valmy formation

Figure 10. Interpreted structural setting of deep geothermal wells: (A) Ginn #1-13, (B) Batz #1. Summary of accompanying geologic logs given in Figure 8.

Important control on the timing of the ENE-trending faulting is provided by the young basalt flows exposed in the western end of Whirlwind Valley and presumed to have been encountered in the Ginn well. Their apparent localization in Whirlwind Valley indicates that the valley must have been formed by the time they were erupted. Lack of a substantial basin fill section in the geologic well log between them and the underlying basaltic andesite suggests that the valley was youthful. A K-Ar date on these flows would be extremely useful in establishing the approximate age of the ENE-trending faulting.

The second major trend of normal faulting strikes NNW, cutting the ENE trend nearly orthogonally (these faults are also referred to in the text as "cross faults"). As can be seen in Figure 9, this faulting is arranged in a left-stepping en echelon pattern and is responsible for the formation of the spur-like features on the dip slope of the Argenta Rim and the Mal Pais. The major landsliding along the Mal Pais escarpment was probably localized by this faulting.

Total vertical offsets along the NNW fault responsible for the main spur on the dip slope side of the Mal Pais probably do not exceed 120 m. The easternmost landsliding as well as exposure of the tuffaceous sedimentary section under the basaltic andesite near the top of the range in section 14 may be due to an additional NNW-trending fault with a net vertical offset of between 60 and 80 m. The sense of displacement on all these NNW faults appears to be west side down.

Early movement along this NNW trend is thought to have created the exposures of the Valmy and the Tertiary tuffaceous sediments on the eastern ends of both the Argenta Rim and the Mal Pais and to have formed a major graben into which the basaltic andesite accumulated. Realistically, creation of the graben and its filling with basaltic andesite probably occurred contemporaneously consistent with the rather uniform thickness of the underlying Tertiary tuffaceous sediments (~100 m) encountered in both the wells and exposed under the thin volcanic section in the range. However, the thickness of the volcanic section changes from roughly 100 m to 1.26 km (4145 feet) in the less than 1.5 km distance between the Batz well and with the postulated major NNW fault east of White Canyon that juxtaposes Ordovician Valmy and the basaltic andesite. An estimate of the cumulative offset along this NNW fault, 4048 feet (1234 m), is obtained by comparing the level of the Valmy formation in the main range block on either side of the NNW fault. This offset may have occurred entirely on the one fault or possibly in part on additional subparallel NNW faults which are now concealed by the volcanic pile in the 1.5 km region between the contact with the Valmy and the well. The overlapping of flows across the presumed fault trace indicates that the major movement was completed by the end of the volcanic episode.

A third set of faults, striking NW to WNW, are found in the active hot springs area. These faults apparently play an important role in restricting the near-surface circulation of the geothermal fluids. All the modern geothermal activity is localized in a WNW-trending graben created by these faults which cuts the main range front fault (see Figure 9). The fault immediately southwest of the geysers area marks the termination of all

present geothermal activity and evidence of past activity. Net vertical displacement on this fault is about 40-45 m with the eastern side down. A second NW-trending fault forming the east edge of the graben bounds the active thermal area and separates region of cold water upwelling (cold springs in section 8) from active areas of thermal upwelling to the southwest. Displacement on this fault probably does not exceed 40 m; sense of displacement is west side down. An additional WNW trending fault bounds the horst block to the west of the geysers; displacement on this fault is roughly 50 m. All these NW to WNW trending faults appear related to the bend in the range front fault and may have initiated along planes of weakness inherited from the NNW trend of faulting.

In summary, the following scenario of late Tertiary deformation emerges for the Mal Pais ridge area. (Earlier deformation possibly recorded in the limited exposures of the Ordovician Valmy formation was not investigated.) The oldest trend of faulting is the NNW direction. Faulting along this trend is apparently associated with abrupt changes in the thickness of the basaltic andesite section which suggests initiation of movement preceding or possibly contemporaneous with the volcanic episode (between 15 and 16.5 m.y.B.P. based on regional dating, Stewart et al., 1975). The young landsliding along the front of the range (assumed to be Quaternary or late Pliocene in age based on morphology and vegetation) was apparently localized by faulting along this NNW trend suggesting continuing activity to the present. East-west fracturing, of which the chalcedony carbonate vein is the only example, was truncated by the N 50-70 E (ENE) faulting responsible for the main uplift of the range. Gently tilted basalt flows (2-4°) restricted to the valley are undated but would provide an important constraint on the timing of this ENE-trending faulting. The NW-trending faults in the geysers area in the vicinity of a major bend in the main fault zone have localized the modern geothermal activity. These NW faults offset the main range front fault suggesting a relatively young age. No evidence of very recent movement (e.g., offsets in the alluvium) was found along any of the trends in the area.

The regional significance of the patterns and timing of faulting described above are discussed in the next section.

Regional Structural Synthesis

Regional relationships can be brought to bear on the timing and style of structural deformation in the Mal Pais ridge area. A 3-5 km wide, NNW-trending zone of diabase dike intrusion which extends through the crust marks a 250 km long mid-Miocene rift which transected north-central Nevada (Zoback and Thompson, 1978; a more complete discussion of the rift is given in the Geophysical Setting). Locally the dike swarm fed graben-filling basaltic flows (including the Beowawe flows). This Nevada rift along with contemporaneous rifting and basaltic volcanism on the Columbia Plateau have been used to infer a WSW-ESE mid-Miocene extension direction.

Abundant geologic and geophysical data throughout the northern Basin and Range suggest a uniform pattern of horizontal displacements despite the geometric complexity of the fault blocks. The inferred modern extension direction is WNW-ESE (see Thompson and Burke, 1973; and Zoback, 1978, for detailed references). The postulated 45° clockwise change in extension direction is constrained to have occurred between 15 and 6 m.y.B.P. in a region 50 km to the north of the Beowawe area (Zoback and Thompson, 1978). In the modern stress regime NNE-trending faults (oriented orthogonal to the extension direction) exhibit pure dip-slip movement whereas obliquely oriented faults exhibit a combination of lateral and dip-slip movement; i.e., NNW- to NW-trending faults exhibit right-lateral components of slip while NE- to ENE-trending faults exhibit left-lateral components of slip.

This regionally observed pattern of displacements can be used to predict slip on faults in the Mal Pais ridge area. The generally NE- to ENE-trending range front faults should have components of left-lateral slip. The left-stepping, en-echelon nature of the NNW-trending cross faulting responsible for the spurs off both the Mal Pais and the Argenta Rim is suggestive of a component of right-lateral shear across this faulting. Small right-lateral offsets on the NW-trending faults which bound the active system may have played an important role in localization of the modern activity.

Geologic History

In early Paleozoic time the Mal Pais Ridge area was the site of marine carbonate deposition within the broad geosyncline that covered Nevada. Eugeosynclinal conditions existed several tens of miles to the west. During the Antler orogeny in late Devonian and Mississippian time, the siliceous western assemblage was thrust eastward over the carbonate rocks along the Roberts Mountains Thrust. The Ordovician Valmy Formation in the present area is part of the western siliceous assemblage, but because exposures of the formation are so limited nothing more than its involvement in the Antler orogeny (which presumably brought it to its present location) can be determined. Paleozoic carbonate rocks of the eastern assemblage at depth are thought to comprise the autochthonous basement in this region.

The Antler orogeny is the last event recorded in the rocks in the Mal Pais Ridge until Tertiary time. However, during this local hiatus deposition and igneous activity occurred in surrounding areas. Deposition of a section of tuffaceous sedimentary rocks (gravels with inter-layered ash beds) unconformably on the Ordovician Valmy Formation marked the end of the local hiatus in the Mal Pais Ridge area.

Modern exposures of this tuffaceous sedimentary section and equivalent units are extensive (see Figure 2) and suggest widespread alluvial plain deposition of varying thickness on the irregular topography of the siliceous Paleozoic rocks in this region of north-central Nevada. Lying conformably(?) on top of these sediments are numerous flows of basaltic andesite. Potassium-argon dating of these flows yielded ages between about 15.0 and 16.5 m.y. (Stewart et al., 1975) so that underlying tuffaceous sediments are probably Miocene in age. Similar stratigraphic relationships are found in the Shoshone and Cortez Mountains (some 40 km to the south) as is shown in Figure 2.

Chemically compatible with the basaltic andesite flows, diabase dikes in the Cortez and Roberts Mountains area (see Figure 2) strike NNW and are inferred to be feeders for the basaltic andesite flows. Dating of these dikes in the Roberts Mountains area yielded ages between 15 and 16 m.y. (E. H. McKee, personal communication, 1978) consistent with the feeder dike interpretation. The limited east-west lateral extent of the flows (see Figure 2) suggests localizing control, either through linear feeder vents and/or structural control. Data in the present area, discussed in an earlier section, indicate that faulting along the NNW trend (possibly related to the dike emplacement) created a graben along that trend which is responsible for the accumulation of a thick pile of volcanic rocks. Both where exposed in the range and in drill holes in Whirlwind Valley, the tuffaceous rocks (presumably Miocene in age) underlie the flow rocks. Faulting responsible for downdropping of the Valmy to the level indicated in the drill holes must have occurred in the early stages of volcanism or only slightly preceding it to maintain the rather uniform thickness (from exposures and drill hole data) of unconsolidated tuffaceous sediments. Similar relationships of the basaltic andesite filling a NNW-trending graben are exposed in the Cortez Mountains and the Simpson Park Range 40 km and 60 km to the south (Gilluly and Masursky, 1965; Masursky, 1978, personal communication).

The next event recorded in the area is the gentle downwarping on the dip slope of the range in section 16 which allowed roughly 60 m of water-laid silicic tuff to accumulate. The dips now recorded in the tuffs are too steep for depositional surfaces and suggest subsidence. Rhyolite flows and domes, which are possible sources for this siliceous tuff, can be found both to the north and south of the Mal Pais Ridge area. Where dated, these domes and flows are only slightly younger (~1 m.y.) than the basaltic andesite they cut and overlie. This tuff deposit was truncated by the late Tertiary(?) gravels, possibly a pediment deposit related to the NNW faulting trend. The extremely well-rounded basaltic andesite cobbles must have formed in through-going drainage before the present breakup of the ranges.

At some time after the deposition and cooling of the basaltic andesite, fracturing along an east-west trend allowed silica-rich fluids to migrate upwards. This early geothermal system was apparently quite sluggish and eventually self-sealed itself by precipitation of silica and minor carbonate creating the chalcedony-carbonate vein at the mouth of White Canyon. Post-volcanic hydrothermal activity is also recorded in the intense alteration of volcanic rocks in the vicinity of the vein and by abundant botryoidal fragments and vesicle linings of opal. The cinnabar deposits on the east end of the range in section 6 (Eureka County) resemble deposits associated with geothermal activity and may be related to this pulse of activity.

Faulting along a N 50-70° E trend and gentle tilting (~5-7°) of the uplifted blocks to the southeast created the present major ranges in the region. Eruption of the late Miocene(?) basalt exposed in the western end of Whirlwind Valley probably followed soon after the initiation of this faulting as suggested by the lack of a significant basin fill section between these flows and the underlying mid-Miocene basaltic andesite. The older NNW-trend of normal faulting probably remained active until fairly recent times. In late Pliocene-Quaternary(?) time (based on geomorphic appearance) wet clay-rich tuffaceous sediments underlying the basaltic andesite provided a base for landsliding possibly initiated by seismic activity on the main NNW cross fault.

Faulting along a NW to WNW trend in the vicinity of a major bend in the range created a graben in which the modern activity has been localized. Major upwelling of thermal waters along the main range front fault within this graben probably began about 200,000 years ago. The sinter terrace was built up along the fault escarpment by deposition from these silica-rich fluids. Great thicknesses of older sinter outside of the limits of the present activity suggests shifting centers of activity along this 1.5 km stretch of range front.

GEOPHYSICAL INVESTIGATIONS

The Beowawe-Mal Pais Ridge area has been the site of numerous geophysical investigations by private companies. Reported here is work conducted by the author largely in the summer of 1974 supplemented with additional gravity data collected by Stanford University geophysics field courses in 1974 and 1975. The seismic noise and self-potential surveys were conducted to gain information on the geothermal system. Gravity and magnetic data were used mainly for structural interpretation. Since a bipole-dipole resistivity survey conducted by Lawrence Berkeley Laboratory in late 1973 served as a basis for some of the geophysical work reported here, the results of that survey are summarized below following a brief overview of the regional geophysical setting.

Geophysical Setting

Situated within the Basin and Range physiographic province, the Beowawe area displays the characteristic extensional features of ranges bounded by steep normal faults and tilting of the uplifted fault blocks. A center of Cenozoic tectonism and volcanism, the Basin and Range is a province of higher than average heat flow for continental areas. Heat-flow measurements average greater than 2 HFU (heat-flow unit-- 10^{-6} cal/cm²/sec) within this province, in contrast with the continental average of 1.5 HFU. Within this region of above average heat flow, a localized zone of anomalously high heat flow has been defined. Heat-flow values generally about twice the continental mean have been measured within a roughly 40-mile radius of the town of Battle Mountain (see Figure 11). This zone has been designated as the Battle Mountain high by Sass et al. (1971). Within the Battle Mountain high there is a fairly dense, regular distribution of warm-to-hot springs which includes the Beowawe "Geysers."

A striking aeromagnetic lineation passes through the Beowawe area near where the Shoshone Range splits into the Mal Pais and the Argenta Rim. Composed of aligned aeromagnetic highs striking north-northwest, the lineation extends from the Roberts Mountains area 110 km to the south to close to the Oregon border (see Figure 12). Associated with this prominent magnetic feature are on-line, NNW-trending faults; voluminous mid-Miocene (14-17 m.y.) volcanic rocks (including the basaltic andesite in the Beowawe area); and the diabase dike swarms (discussed previously) located in the Cortez and Roberts Mountains to the south of the present mapping area.

This magnetic and associated magmatic trend is thought to delineate a mid-Miocene rift in northern Nevada (Stewart et al., 1975, and Zoback and Thompson, 1978). Modelling of the aeromagnetic data indicates that the surface volcanics are not sufficient to produce the wavelength or amplitude of the observed anomaly; sources extending deep into the crust (to ~15 km, approximately the depth to the Curie Isotherm in this region) are required (Robinson, 1970 and Zoback, 1978). Physically these deep sources are presumed to represent the zone of diabase dike intrusion extending up through the crust and exposed at the surface in the Cortez and Roberts Mountains.

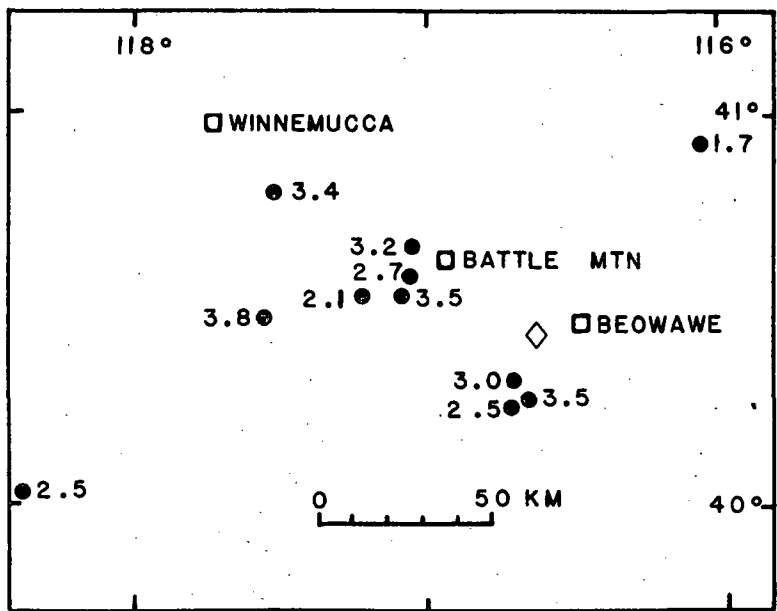


Figure 11. Battle Mountain high (from Sass et al., 1971), heat flow values given in HGU (10^{-6} cal/cm²/sec). Diamond indicates location of Beowawe hot springs.

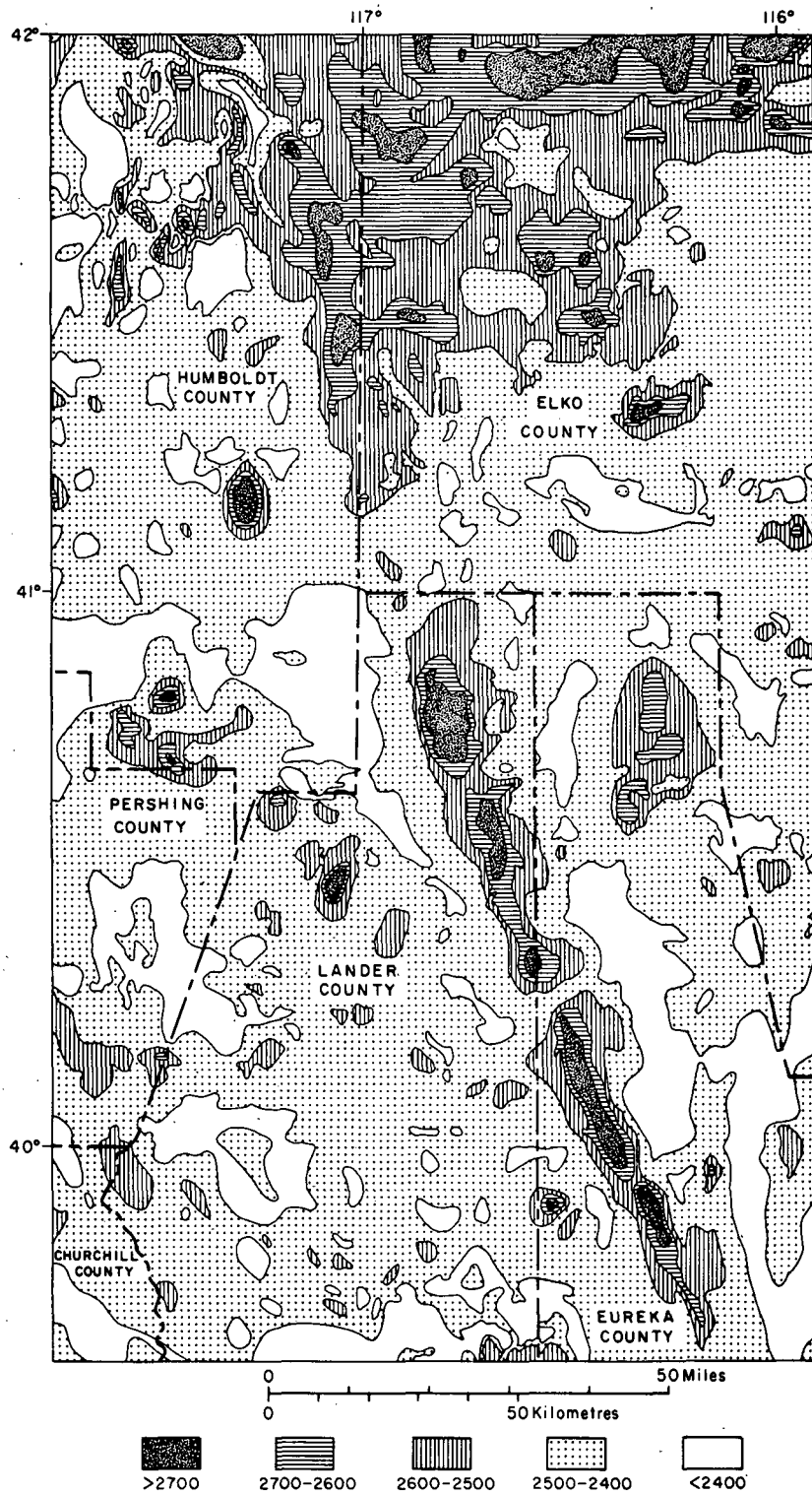


Figure 12. Aeromagnetic map of north-central Nevada, values relative to an arbitrary datum-(from Stewart et al., 1975; used with permission).

The inferred age of emplacement of the magnetic material along the rift responsible for the aeromagnetic anomalies, 15-16.5 m.y.B.P. from the dating of the associated volcanic rocks, corresponds to the inception of Basin and Range faulting in north-central Nevada (Christiansen and Lipman, 1972). The inferred age and high apparent magnetization of the intrusions (Robinson, 1970 and Zoback, 1978) exclude them as possible heat sources for geothermal activity in this region.

Faulting and seismic activity have continued into the present time in the region around Beowawe. Slemmons et al. (1965) report a M=5.1 earthquake (approximate magnitude from the U.S. Coast and Geodetic Survey) that occurred in the Mal Pais region on September 18, 1945. The exact epicenter is not known, but the earthquake was felt only by people in the town of Beowawe, and not in any of the surrounding towns. Richard K Hose (U.S. Geological Survey, 1974, personal communication) ran a 48-hour microearthquake survey near the geysers and detected three small events in that time period.

Bipole-Dipole Resistivity

Geoelectrical prospecting has proven to be one of the most useful geophysical methods for investigating geothermal areas, particularly those systems dominated by hot water. Combined effects of temperature, porosity, and salinity of thermal waters make resistivities within geothermal areas much lower than those of rocks in the surrounding region. High clay content (observed in some geothermal areas) also lowers the resistivity.

Bipole-dipole resistivity studies (also known as the dipole mapping method) have proven useful in outlining geothermal fields in the Taupo volcanic area of New Zealand (see Risk et al., 1970) and more recently in other areas (see Keller et al., 1975, for example). The primary value of a survey of this kind is that it is more sensitive to lateral variations in resistivity than to vertical changes. (See Keller et al., 1975, for a complete discussion of the method.)

Because of its relative insensitivity to variations with depth, in addition to the fact that the source dipole remains fixed, the bipole-dipole method tends to produce results that reflect variations in resistivity in the neighborhood of the receiving dipole rather than at points between the source and the receiver. At the large distances (3-5 km) between the source and the receiver characteristic of these surveys, the method probably samples the electric properties of rocks in the vicinity of the receiver dipole to depths on the order of 1-2 km (Keller et al., 1975).

As a result of joint efforts on the part of U. C. Berkeley and Lawrence Berkeley Laboratories, a bipole-dipole resistivity survey was conducted in the Beowawe region in late 1973 (Wollenberg et al., 1975). Two, one-mile (1.6 km) long source dipoles were used; one located near the middle of Whirlwind Valley 2.4 km north of "The Geysers" and the second located on the dip slope side of the Mal Pais, 4 km southwest of the geysers. The locations of these transmitters and the receiving stations are given, with the results, in Figures 13 and 14.

The results obtained using transmitter 1 (T1) located within Whirlwind Valley (Figure 13) indicate a well-defined apparent resistivity low (less than 20 ohm-meters) centered on the known hot springs and geyser area. A second low is located on the dip slope side of the range, more than 1 mile southwest of the geysers. In addition, a small low was detected in the valley west of the main cross fault. The values obtained using transmitter 2 (T2) (located on the dip slope side of the range) are given in Figure 14 and confirm the existence of an electrically conductive zone corresponding to the present day active hot springs and blowing wells. This second survey also defined a pronounced resistivity high (greater than 100 ohm-meters) located about 1 mile south of the Geysers. It did not, however, detect the two smaller resistivity lows northeast and southwest of the Geysers indicated by the results of T1.

There are several possible explanations for the discrepancy between the two sets of results. In one instance the transmitter was located on highly

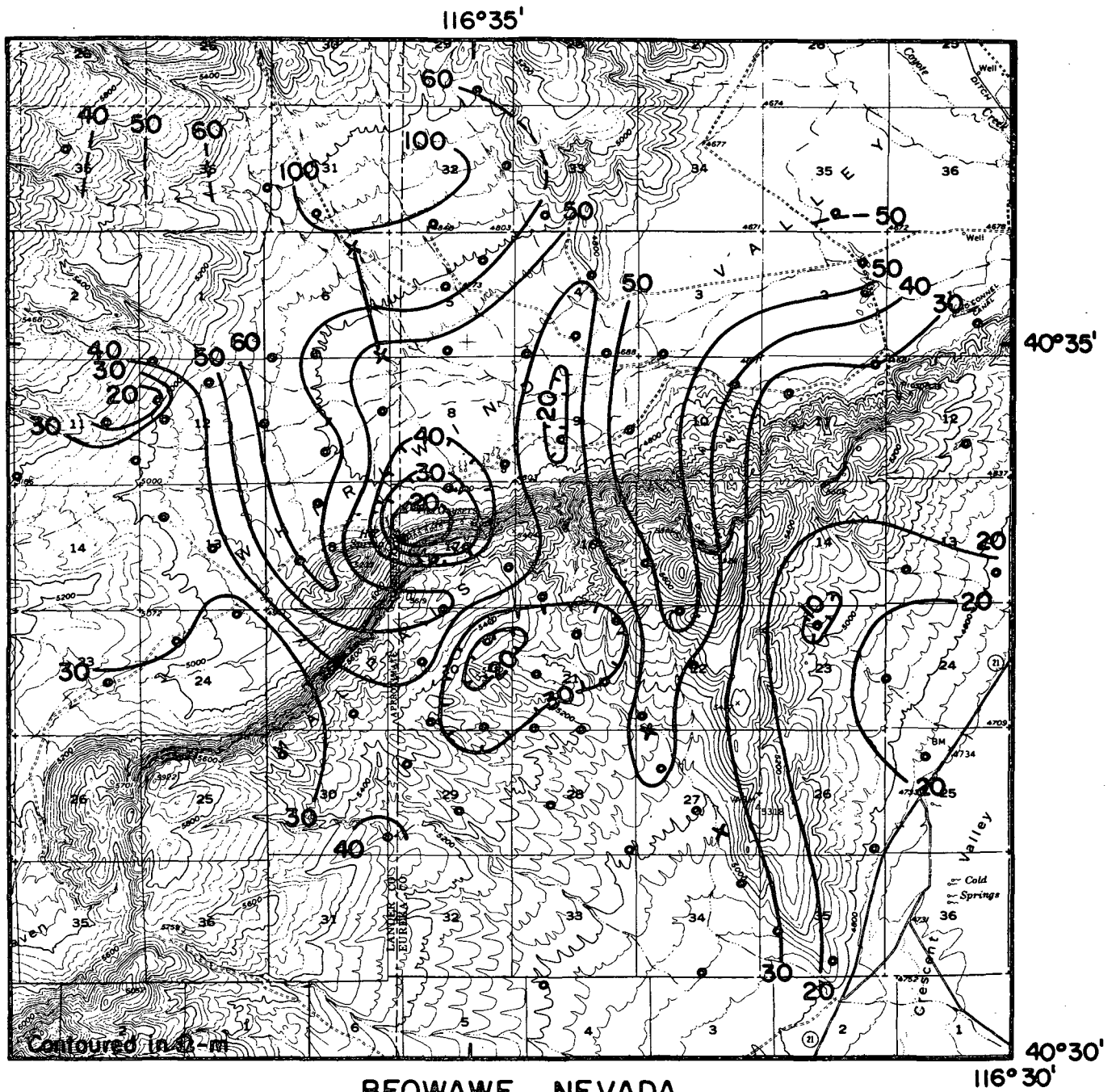


Figure 13. Apparent resistivity contour, Whirlwind Valley area; transmitter located in Whirlwind Valley (from Wollenberg et al., 1975; used with permission).

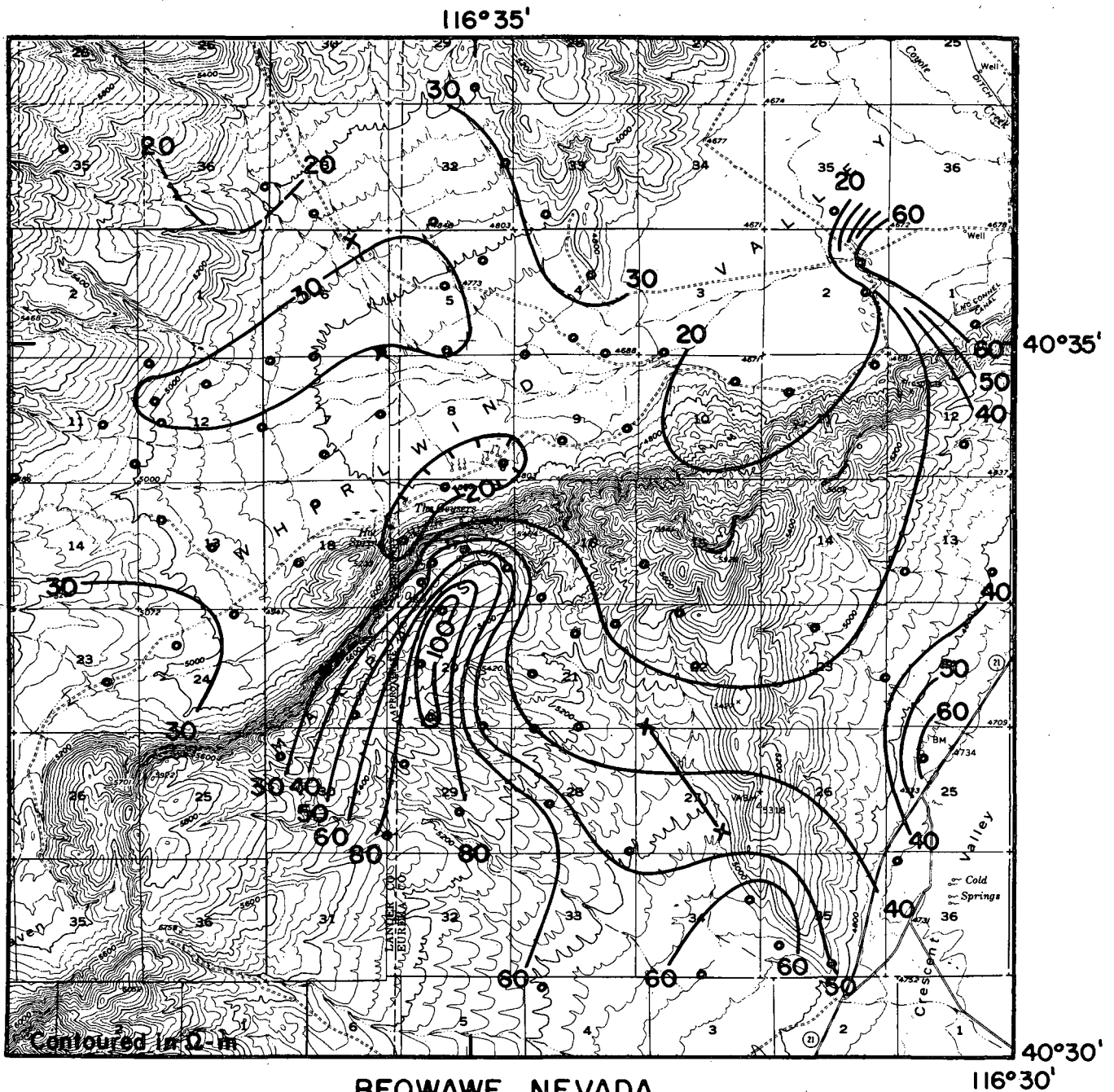


Figure 14. Apparent resistivity contours, Whirlwind Valley area; transmitter located on the dip slope of the Mal Pais ridge (from Wollenberg et al., 1975; used with permission).

resistive, volcanic rock, while in the other, the transmitter was positioned within the valley, known to have a relatively high water table. In both cases the surveys crossed the main range front fault along which the valley fill with its high water table and, in places, geothermal activity is juxtaposed against the volcanic rock; this fault must represent a major discontinuity in electrical properties. It is also possible that the fault scarp will add a complicating topographic effect to the results (H. Beyer, personal communication, 1975). Keller et al. (1975) have computed contour maps of bipole-dipole apparent resistivity for simple transmitter and structural configurations. Their results show that dipping contacts (faults) juxtaposing material of different resistivities complicate the field pattern and can even create false resistivity lows when the transmitter is aligned parallel to the fault strike. Wollenberg et al. (1975) recommended that dipole-dipole traverses (much more sensitive to variations in electrical properties with depth) be run in Whirlwind Valley to substantiate the bipole-dipole anomaly pattern.

The low resistivity in the vicinity of the present day geothermal activity appeared on both surveys and is most likely real. In that this anomaly does not extend outside of the known active area, the survey does not contribute any important new information. The broad low defined by T1 southeast of the geysers and centered on the dip slope side of the Mal Pais is suspect because of its close proximity to the pronounced resistivity high detected in the survey using T2. It is possible that the two results are compatible in that they may reflect a variation in electrical properties with depth; the pronounced high was located close to transmitter 2 and may indicate either the high resistivity of the near-surface volcanic rocks (although such a pattern was not observed elsewhere on the range) or may be related to the steep escarpment in that area. The low was observed from the more distant transmitter located in the valley and may be related to a deeper phenomenon. However, it must be kept in mind that this survey is most sensitive to lateral variations in resistivity, rather than depth-dependent changes.

The small low in the center of the valley northeast of the Geysers is perhaps the most interesting in view of its possible relation to the modern cross valley fault. The region of this anomaly was studied in more detail with other geophysical methods to examine this buried fault trace for possible geothermal potential. It is possible, however, that this low is merely an artifact of the method (as discussed above) since the transmitter dipole (T1) is aligned roughly parallel to the NNW trend of this faulting.

Self Potential

The self-potential (SP) method involves the measurement, at the surface, of electric potentials generated by naturally occurring electric fields in the earth. Two possible sources of SP anomalies, thermoelectric coupling and streaming potentials, are of interest in geothermal exploration. Recent field studies (Zohdy et al., 1973, and Corwin, 1976) have indicated that SP and geothermal activity may be related. Corwin (1976) recently summarized the state-of-the-art knowledge of the SP method and suggested two sources for a geothermally related electric potential field: (1) actual heat of the reservoir (this mechanism only applies when the reservoir lies within a region of contrasting thermoelectrical coupling, a reservoir in a homogeneous half space does not generate an electrical field, Nourbehecht, 1963); (2) subsurface fluid flow resulting in a streaming (electrokinetic) potential due to separation of ions.

Using Nourbehecht's (1963) theoretical formulations and realistic in situ conditions, Corwin (1976) concluded that typical SP anomalies that can be expected directly from a geothermal reservoir due to thermoelectrical coupling are between 5-10 mv, while a very large anomaly would be on the order of several tens of millivolts. These predicted anomalies are much smaller than observed anomalies of 50-100 mv commonly seen in areas of active subsurface flow, particularly over faults along which water is moving (Corwin, 1976).

Several workers have derived analytical expressions for streaming (electrokinetic) potentials (see Corwin, 1975, for a list of them). These expressions depend upon electrical and mechanical properties of the pore fluid, flow rate, and the so called "zeta potential," which is related to the potential between the free ions in the fluid and the ions bound to the surface of the solid. It is difficult to estimate streaming potential values theoretically because of the large variation in both magnitude and sign of the zeta potential in geologic materials. The sign convention for SP anomalies is empirical; early investigations by Poldini (1938, 1939) and recent investigations in Yellowstone (Zohdy et al., 1973) indicate a positive potential (relative to a distant point) associated with upwelling water.

The blowing wells and natural geothermal activity at Beowawe are a direct manifestation of upward migrating water most probably moving along the range front fault(s?). In an attempt to establish the SP signature in a region where large volumes of thermal fluids travel to the surface as well as to investigate the region of localized low resistivity in the valley near the main cross fault, a self potential survey (total length 15 km) was conducted at Beowawe in July, 1974. A Danameter Model 2000 digital VOM meter was used to measure the potential differences in millivolts with an accuracy of ± 1 mv. Contact with the ground was made using non-polarizing electrodes, porous porcelain pots with a copper rod immersed in a saturated solution of copper sulphate.

The location of the self potential survey lines is given in Figure 15. In both surveys the reference point (indicated by a large dot) was located

well outside the region of known geothermal activity. In conducting the survey, one electrode was fixed and the second occupied stations at intervals of 200 feet. The maximum electrode spacing was 1900 feet. New lines were begun at the end point of the previous line and a potential map was constructed with all potentials relative to the distant reference point by adding the final potential difference of each line to all values measured on the next. The reference point was attached to the negative input of the voltmeter to yield potentials relative to that point. The results of these surveys are given in Figure 17.

A 1900 foot test profile was run in the center of Whirlwind Valley (2.5 km from the geothermal activity) to investigate the background noise level. Ideally, a relatively high water table in the valley should provide near-surface homogeneity in the water-saturated alluvium. The location of this profile is shown by the dotted line in Figure 15 and the values are given in Figure 16. The largest potential difference (the reference point being the start of the line) was only 13 mv. The steepest gradient was 24 mv/200 feet in contrast with values of greater than 170 mv/200 feet measured near the base of the sinter terrace in the active hot springs area.

The measured values along the background line fluctuate over short distances from as much as +11 mv to -13 mv with no apparent trend and are most likely reflecting local differences in the temperature, moisture content, and particularly chemistry of the soil. The known alkaline nature of desert soils suggest that potentials due to a variation in soil chemistry may be a real source of background noise in this SP survey. Potentials as large as 5 mv were observed between electrodes only ~10 cm apart in the ground.

Another source of background noise common to all SP surveys are telluric currents. By continual monitoring of self potential in Nevada, Corwin (1976) detected telluric currents with periods between 10 and 40 seconds responsible for SP fluctuations up to 6-8 mv. Corwin also believes that electrode handling and ground contact are common sources of errors in SP surveys; he recommends that holes for the electrodes be dug deep enough to encounter sufficient soil moisture to allow a reasonable contact resistance instead of simply wetting shallow holes as is standardly done in electrical surveys. Corwin's studies suggest that such wetting can lead to SP anomalies as large as 10 mv relative to a dry electrode. The wetting method was used in the current surveys. In view of the observed fluctuations on the background noise line and the net effect of all the above sources of errors in SP surveys, an uncertainty of ± 15 mv should be assigned to the values reported here.

The results of the SP survey of the active hot springs area are given in Figure 17. Also given in Figure 17 are structure contours showing roughly the depth, in feet, from the valley floor to the main range front fault plane. These contours were obtained by projecting the fault from the assumed trace at the top of the terrace under the valley with a constant dip of 65° . (This dip is based on the observed intersection of the Ginn well with the

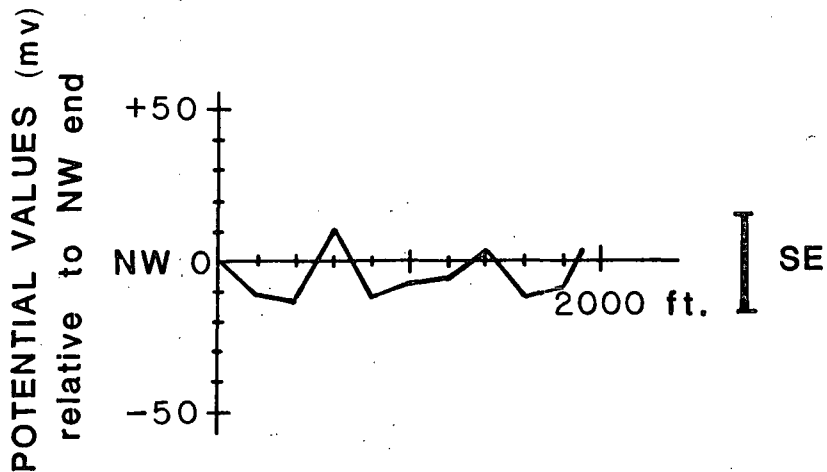


Figure 16. Test profile for background SP noise level. Heavy bar to right indicates ± 15 mv uncertainty. See Figure 15 for location.

48

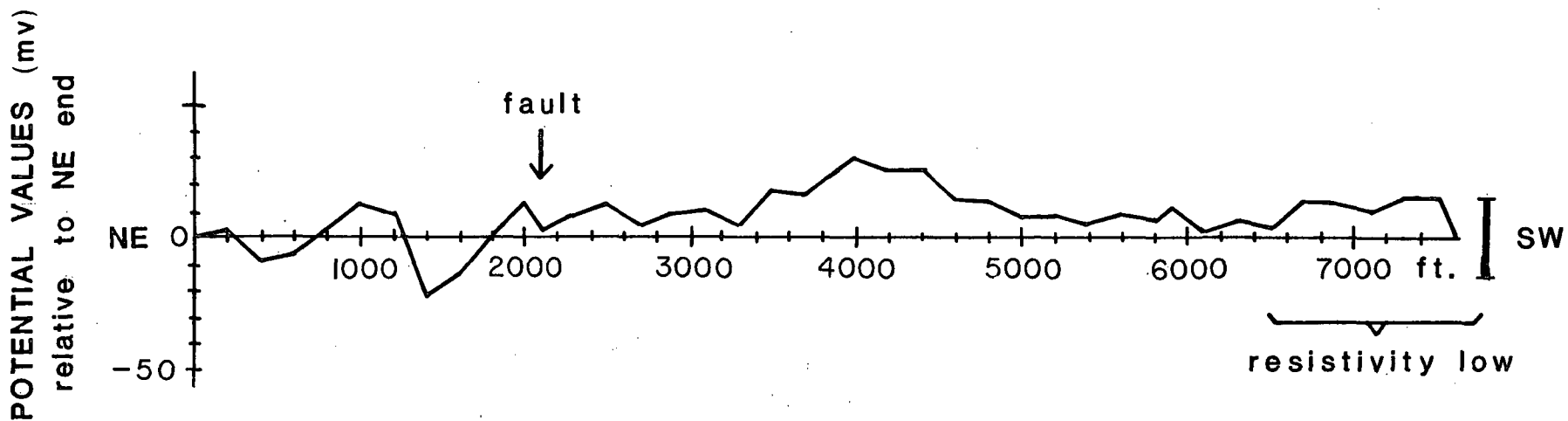


Figure 19. SP values along cross valley profile shown in Figure 18. Heavy bar to right indicates ± 15 mv uncertainty.

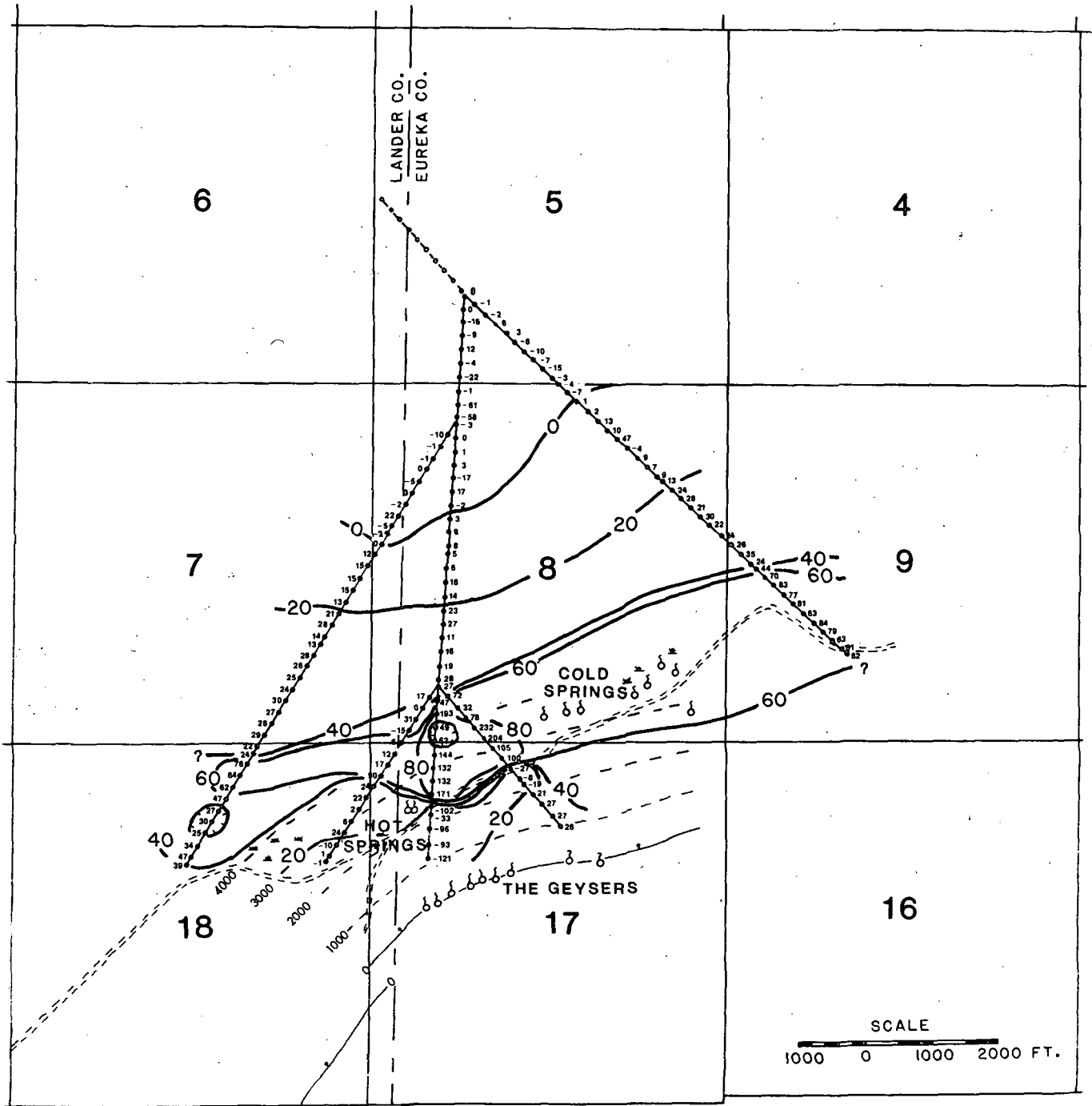


Figure 17. Self potential (SP) contour map in hot springs area, values expressed in mv and are positive unless otherwise indicated. Double dashed lines show location of roads and thin solid and dashed lines give depth (in feet) to the main range front fault. See Figure 15 for location within Whirlwind Valley.

main fault plane.) The survey reveals a complex, but well-established SP anomaly pattern in the active hot springs area. A consistent trend of steadily increasing positive potentials parallel to the range front begins roughly 1 km from the main fault escarpment. The broad, generally positive anomalies associated with the active hot springs area are interpreted as being due to the observed upwelling of large volumes of thermal waters in this region. The character of the anomaly varies from line to line; the outermost profiles (lines A and E) slowly increase then peak nearly 1 km from the sinter terrace, whereas the inner three profiles within the active region record intense fluctuations with gradients as large as 170 mv/200 feet. One possible interpretation of the data is that there is a broad high associated with the general region of upwelling thermal fluids upon which smaller scale variations in the spring area have been superimposed and may reflect a complex pattern of subsurface flow.

The sinter terrace (built up along the main fault escarpment) is evidence that thermal waters reach the surface along that fault. One possible explanation for the hot springs found at the base of the terrace is that some of the hot water rising along the main fault is diverted laterally when it reaches the near-surface water table in the valley (flowing over cold ground water), creating the hot springs located near the base of the terrace. It is possible, however, that the main range front fault is not the only fracture channeling geothermal fluids to the surface. The major SP anomalies encountered in this study are located in a region where the projected depth to the main fault plane is between 3000-4000 feet whereas the second, basinward subsidiary fault, buried under the alluvium is inferred to strike somewhere through this high potential zone possibly coincident with the steep SP gradient shown in Figure 17. It seems, therefore, likely that the SP anomalies observed in the active hot springs area are related to upwelling along the parallel, subsidiary fault(s?). The apparent alignment of the cold springs in section 8 (Eureka County) with the presumed trace of the subsidiary fault indicates that only a limited segment of this fault could be geothermally active, with a NW-trending fault separating the two regions.

In addition to the actual zones of upwelling, there must be considerable lateral near-surface flow in the cavernous sinter region at the base of the terrace. Horizontal flow is also known to create SP anomalies (Poldini, 1938, 1939); however, there is no current theoretical basis for predicting either the character or sign of these anomalies. All the profiles ended before or near the base of the sinter terrace because as it was approached the sinter became so porous that it was virtually impossible to establish adequate ground contact with the electrodes. On lines B, C, and D which came closest to the base of the terrace, the SP values tended to decrease and level off and on line C even became negative. This effect may be due to runoff water from the terrace filtering down through the sinter, consistent with empirical observations of negative anomalies associated with descending water movement.

A cross valley profile (Figure 15) was run to investigate the bipole-dipole resistivity low in section 9, as well as the possibility of fluid movement related to the main NNW cross fault. Figure 18 shows the location

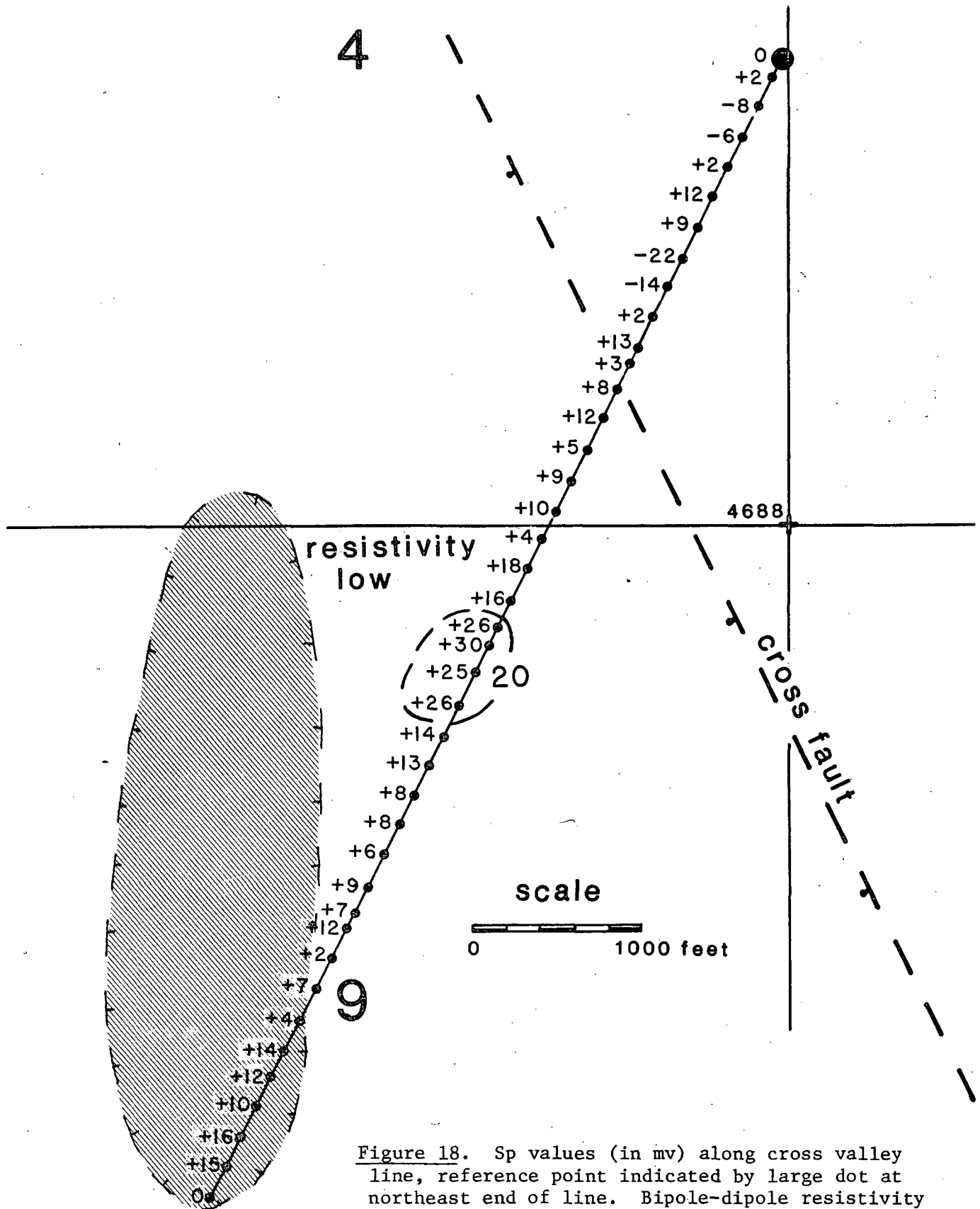


Figure 18. Sp values (in mv) along cross valley line, reference point indicated by large dot at northeast end of line. Bipole-dipole resistivity low (<20 Ω-m) indicated by ruled region. Approximate trace of cross fault is also shown. See Figure 15 for location within Whirlwind Valley.

of the line with respect to the trace of the cross fault and the resistivity low in section 9 and gives the SP values relative to a point on the north side of the valley. The profile is plotted in Figure 19.

In general, the level of values is low and only in places emerges above the noise level. The gradients are relatively small, the maximum observed was only 31 mv/200 feet, in contrast with values as large as 170 mv/200 feet in the active hot springs area. There appears to be a small, relatively steep-sided negative anomaly just northeast of the cross fault; however, this anomaly cannot be considered significant because it is based largely on one point, the -22 mv potential measured at 1300'. Also, there is an indication of a small SP high emerging above the noise level between the fault trace and the resistivity low (see the contoured region on Figure 18); however, it is unlikely that this high is related to the resistivity low because of its localized extent and also because there is no apparent effect on SP values when the profile actually crossed into the low resistivity region on the southwest end of the line. The soil in the area where the high is located is very moist and the ground rather grassy. If significant at all, this localized high may be reflecting fluid movement (most likely cold water) along the subsidiary fault in much the same manner as in the marshy, cold springs area to the southwest in section 8. Extension of the presumed trace of the subsidiary fault through this region would maintain its subparallel alignment with the main range front fault.

In conclusion, the self-potential method appears most effective in detecting water movement along faults. A broad, complex pattern of SP anomalies is associated with the known fault-related upwelling of thermal waters in the geothermal system. The data can be interpreted as revealing a broad high (> +80 mv) presumably reflecting the general upwelling, with superimposed smaller scale fluctuations and steep gradients undoubtedly due to a complicated pattern of near-surface flow, probably both horizontal and vertical, in the active hot springs area. Negative gradients and potentials near the base of the sinter terrace may be due to downward movement of cool runoff from the terrace. The observed anomaly pattern is presumed related to upwelling (of either hot or possibly cold water) along subsidiary fault(s?) paralleling the range front fault because the main fault plane is located at a depth of 3000-4000 feet below the valley floor in the vicinity of the anomaly. The entire anomaly, however, may be the result of lateral flow directed from the upwelling thermal fluids along the main fault plane.

A second profile was run in the valley across the main NNW cross fault and in the vicinity of the bipole-dipole resistivity low with the hope of detecting fault-related upwelling of geothermal waters lacking surface manifestations. No significant anomaly pattern was detected; however, a small localized high was observed which could conceivably be related to upwelling of water along the subsidiary range front fault. If this interpretation is valid, then it would allow extension of the trace of the buried fault more than 1 km to the northeast.

Seismic Noise

Recent surveys of seismic noise conducted in known geothermal areas have indicated that the background noise level in such regions is typically high. (See, for example, Douze and Sorrells, 1972; Luongo and Rapollo, 1973; Clacy, 1968; and Iyer and Hitchcock, 1974.) In a rather complete study at Yellowstone National Park, Iyer and Hitchcock (1974) were able to demonstrate that at least part of the high noise level was associated with subsurface convection of thermal waters typically with frequencies of 2 to 8 Hz, while surface manifestations of the geothermal activity produced higher frequency noise. Luongo and Rapolla (1973), working on volcanic islands in Italy known to be underlain by a magma chamber, identified frequencies less than 10 Hz with the fumarole and hot springs activity while a noise survey conducted by Douze and Sorrells (1972) over a known reservoir in the Imperial Valley, California, similarly noted that frequencies of .5 to 5 Hz dominated the noise above the reservoir.

A large-scale seismic noise survey was conducted in Whirlwind Valley during July 1974. To overcome the effects of wind and cultural activity, all recording was done overnight, resulting in 12-14 hour records for each station. Several hours of a consistently low noise level were observed in the very early morning (generally between 1:00 and 4:00 AM) portion of the records. A decrease in wind activity during this time interval amounted to a 50% or greater decrease in the noise level compared to the beginning of the record (which was usually around 6:00 PM).

Recording was done using three Sprengnether Model MEQ-800 Smoked Drum Recorders and three Geo Space HS-10, Model K Vertical Seismometers with a natural frequency of 2 Hz. Shunt resistance of 1.5K-ohms across the leads of the seismometer provided an essentially flat response to ground velocity between 2 and 50 Hz. The recorder amplifier was filtered to provide an essentially flat spectrum from .5 to 10 Hz. The effective combined peak response of the system was thus limited to the 2 to 10 Hz frequency band. This range was selected primarily on the basis of previous work in other geothermal areas, mentioned above, which indicated that low frequencies (in the range 1 to 10 Hz) are generally associated with subsurface convection of thermal waters.

Amplitudes of representative noise levels were measured by a magnifying glass and a finely ruled (hundredths of an inch) scale. These relative values were then corrected for measured variations in the response of the three seismometers. The recorder amplitudes, normalized to a common db level are given in Figure 20; to convert to ground velocity in $\mu\text{m}/\text{sec}$ all values must simply be multiplied by 2.86×10^3 . The estimated accuracy of the values is ± 2.5 units. In general, the noise level in the hot springs area is relatively high. Local exceptions (stations near the base of the sinter terrace) are probably the result of near-surface geology; the porous, loosely connected, and in places, cavernous sinter is certainly an inefficient transmitter of seismic energy. Values all along the range front outside of about 1 km from the main center of the geothermal activity are roughly equivalent in view of the measuring accuracy.

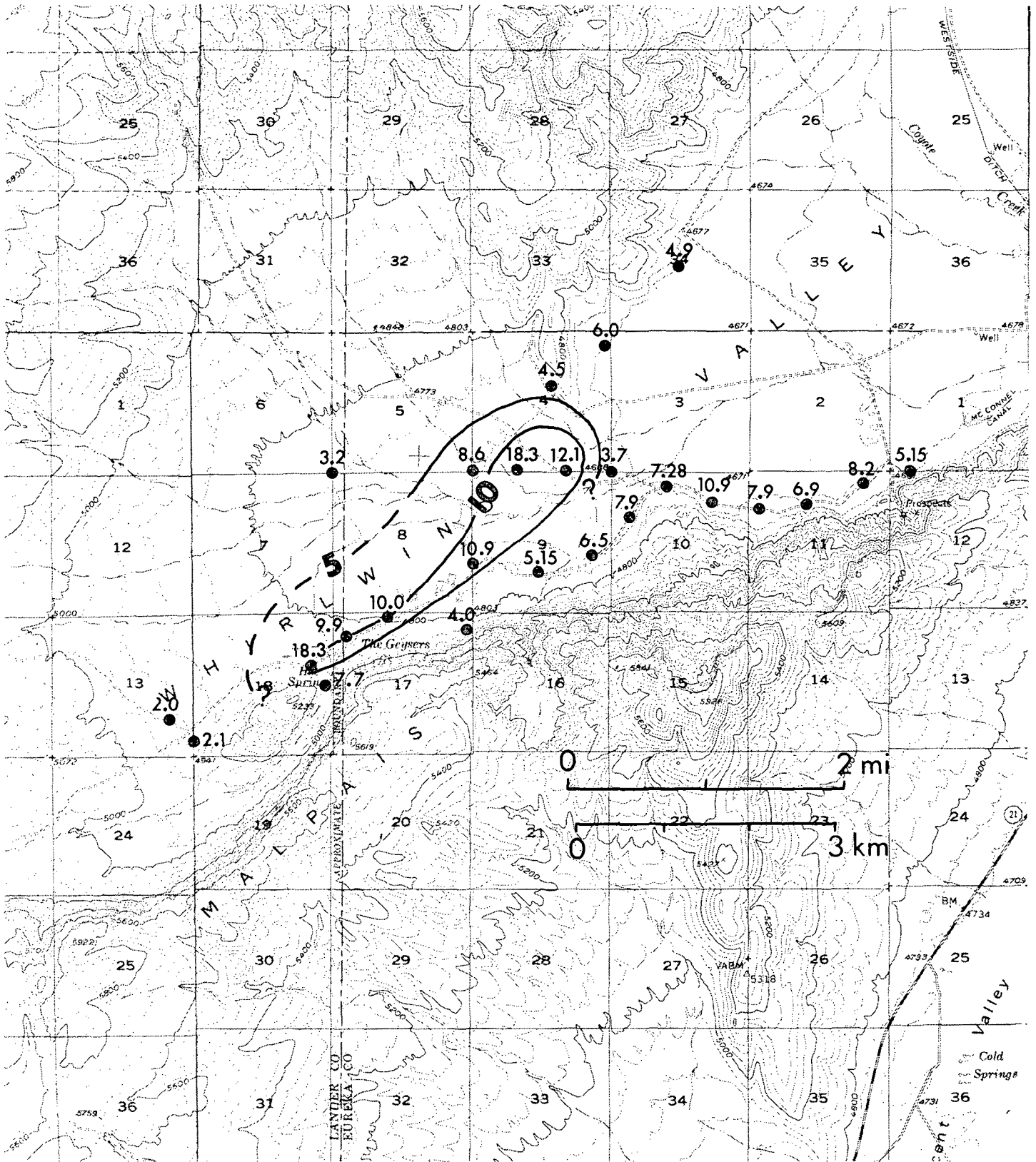


Figure 20. Seismic noise values (in 2-10 Hz range) in Whirlwind Valley. To convert values to ground velocity in $\mu\text{m}/\text{sec}$, multiply by 2.86×10^{-3} .

The most interesting result of the survey is several very high noise values located in the center of the valley west of the main cross fault. This localized zone of high values is well defined by measurements along the section line separating sections 4 and 5 from 8 and 9. The very low value (3.7) measured at the corner of sections 4, 5, 9, and 10 was verified by a second recording on a different night. One possible interpretation of these values is that they define a northeast-southwest trend of high noise values extending out from the presently active hot springs area. The location and subparallel alignment of this trend with the range front suggests the anomaly is related to the subsidiary range front fault inferred to strike through this region. The trace of the concealed subsidiary fault (on the basis of the self-potential data interpretation) is presumed to lie within the 10 unit contour on Figure 20. Thus, both the self-potential and seismic noise data suggest a more northeasterly trend (relative to the main fault that bounds the range) for this buried fault.

If this northeast-trending zone is, in fact, fault-related as the self potential and seismic noise data suggest, then the source of the noise anomaly may also be subsurface fluid movement along the fault as inferred for the self-potential data. As was discussed in the interpretation of the SP results, it is unknown what portions, if any, of this subsidiary fault are geothermally active. Near the Geysers, hot springs indicate upwelling of hot water along the postulated fault, whereas northeast of the Geysers cold springs are aligned along it. Farther northeast, there are no springs and either hot or cold water could conceivably be upwelling in that region.

In conclusion, the results of the seismic noise survey indicate a high noise level associated with the known geothermal area where water is discharging at the surface. A northeastward extension of the high noise values in the geyser area is in accord with self-potential data thought to indicate the extension of a concealed fault. Such an anomaly, aligned nearly parallel with the axis of the valley, would be the least susceptible to error resulting from amplification effects due to varying thickness of valley fill. In this case the noise anomaly may be related to subsurface fluid flow along the subsidiary range front fault.

Gravity Data

Gravity values were measured at various points within Whirlwind Valley to investigate the active geothermal area and to gain structural information on the subsurface form of the valley. The data were collected with a La Coste Romberg gravimeter and tied to Mabey's (1964) regional survey of Eureka County. Simple Bouguer anomalies (using a correction of 0.06 mgal/ft) are shown in Figure 21.

Qualitatively the available data indicate a fairly uniform, thin alluvial veneer in the broad southwestern end of Whirlwind Valley; whereas in the northeastern end of the valley the data suggest that the fill thickens both eastward and southward as the Mal Pais Ridge is approached. The thin alluvial cover in the southwestern end of Whirlwind Valley is attributed largely to filling of the basin by the late Miocene(?) basalt flows exposed in sections 14 and 23 (Lander County) and encountered in the Ginn well.

In general, the available gravity data in the east end of Whirlwind Valley confirm an asymmetric, tilted block structure inferred for the valley from geologic and drill hole evidence (Figure 22). Projecting the dip slope surface of Argenta Rim under Whirlwind Valley to the faults bounding the Mal Pais in the vicinity of the Geysers, one can predict a total vertical offset of 1700-2150 feet (520-650 m) along the range front faults and a maximum thickness of valley fill (basinward of the subsidiary fault) of 1000-1400 feet (305-425 m). Offsets on the two main range front faults shown in Figure 22 are based upon the drill hole data discussed in a previous section. The discrepancy between the observed and computed vertical displacements suggest additional small faults within the basin as indicated with queries on Figure 22.

The computed gravity anomaly for the valley model (with a constant density contrast) along with observed values along the profile are also given in Figure 22. The observed values were not terrain corrected; the corrections would tend to increase all the values with values closest to the range increased the most. The maximum terrain correction in this region would probably be less than 1 mgal. As shown in Figure 22, the maximum calculated anomaly (for $\Delta\rho = -0.4 \text{ g/cm}^3$) is -4 mgals with the largest lows predicted basinward of the subsidiary fault. Unfortunately, the available gravity data (collected largely at sites of known elevation) is insufficient to detail the subsurface form of the valley.

An additional complicating factor in interpretation of valley structure is the extent of the late Miocene(?) basalt flows within the basin. With a drainage configuration similar to the present the basalt would have flowed generally eastward, down the valley. A possible natural barrier to the flows would be the NNW-trending cross faulting (east side up) in the vicinity of the landslide. Net vertical offset on this faulting was estimated at 120 m; measured thickness of the young basalt in the Ginn well was approximately 110 m. Thus, the young basalt was probably restricted to the west end of the valley and also probably basinward of the subsidiary range front fault (total offset ~215 m) depending on when that offset occurred.

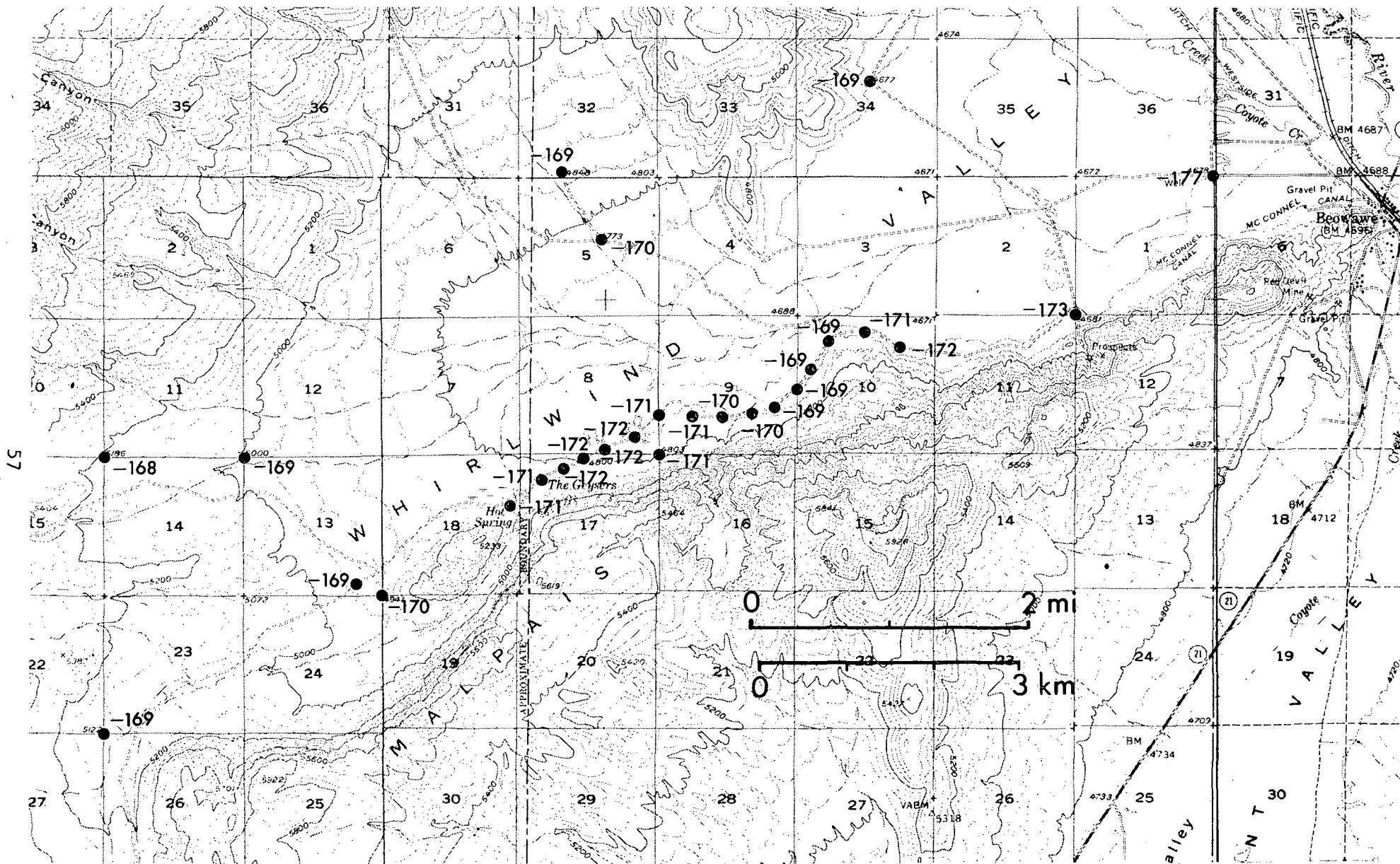


Figure 21. Simple Bouguer gravity values in Whirlwind Valley rounded to the nearest mgal. Gravity values tied to Mabeys' (1964) regional survey.

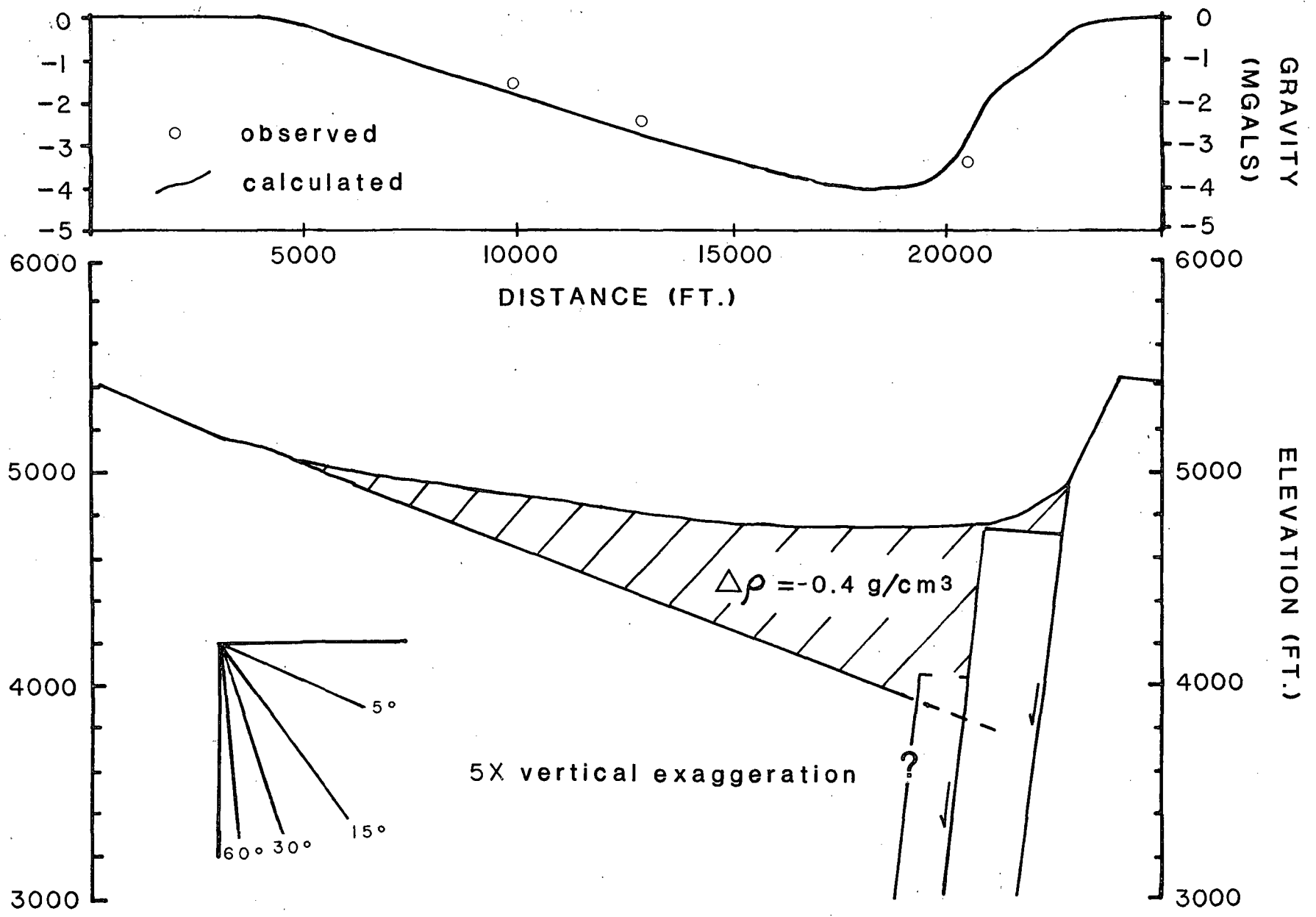


Figure 22. Structural model of Whirlwind Valley shown in cross-section. Computed gravity due to valley fill shown as solid line; available observed gravity data indicated by circles.

A detailed gravity profile was run along the road paralleling the range front to investigate the active geothermal area and structure related to the cross-faulting trend. The values do not support the observation of densification of sediments in the Imperial Valley geothermal region due to silica filling of pores reported by Biehler and Combs (1972). The overall trend of the data indicate lower values near the geysers and a gradual increase eastward, as a profile taken parallel to the range front with the values projected reveals (Figure 23a). One possible explanation is an eastward decrease in fill thickness on the subsidiary block due to cross faulting. A second possibility is a density contrast between the thick section of basaltic andesite inferred to have filled a NNW-trending graben and the Paleozoic siliceous rocks which make up the east side of the graben (Figure 23b). Density measurements and a second gravity profile run along the front of the Argenta Rim (Zoback, 1978) verify that the basaltic andesite is less dense than the Paleozoic quartzites and cherts, with a density contrast of about -0.1 g/cm^3 .

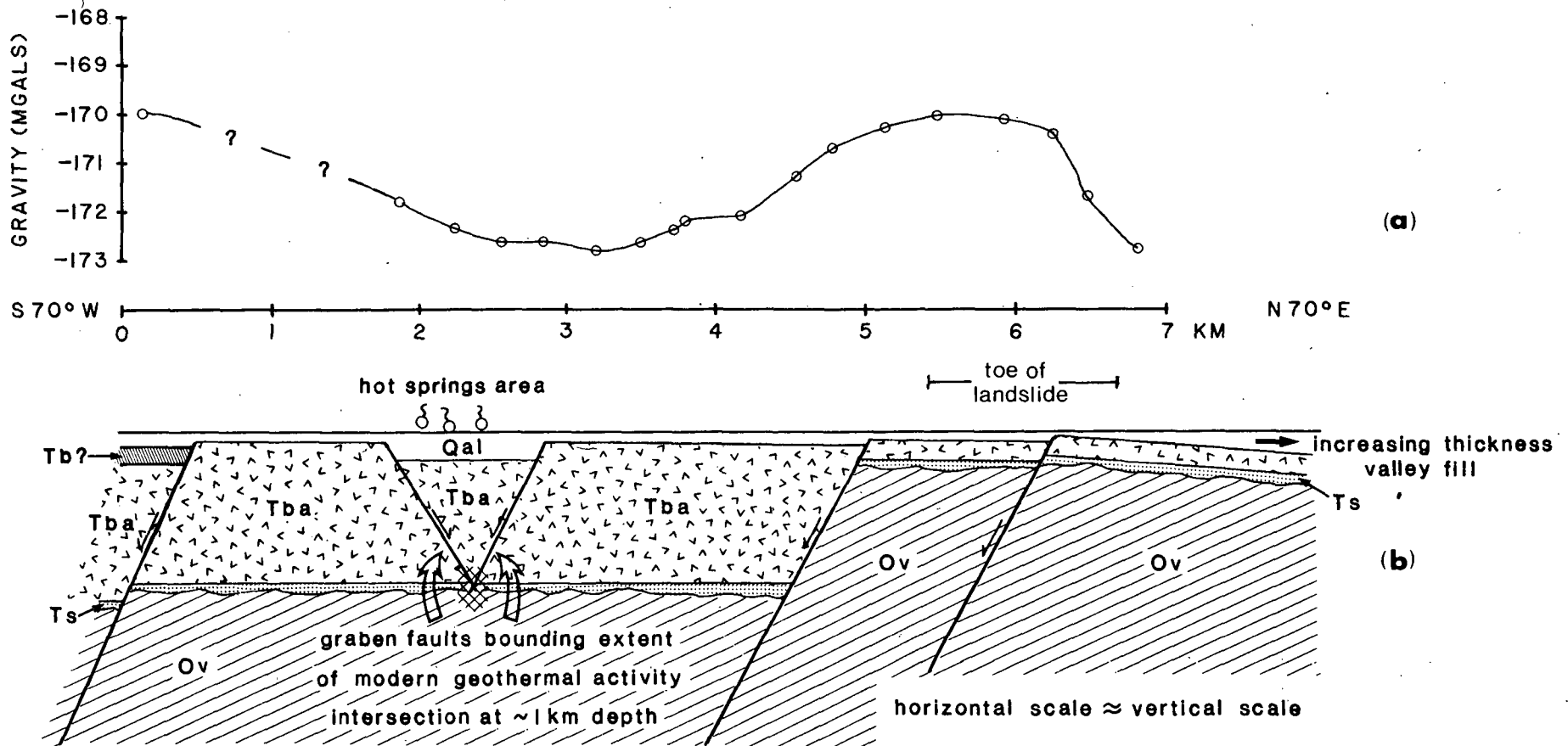


Figure 23. (a) Observed gravity (simple Bouguer) values along a profile parallel to the range front. (b) Interpreted geologic section along profile line. Valley fill thickness shown somewhat exaggerated. See geologic map (Plate I) for explanation of symbols.

Magnetic Investigations

Aeromagnetic coverage for the Beowawe area is provided by surveys flown at an elevation of 9000 feet above sea level by the U.S. Geological Survey. The total field map of the region (with an arbitrary datum subtracted out) is shown superimposed on the topographic map in Figure 24. The prominent NNW grain on the west edge of the map is due to an approximately two-dimensional source centered over the north end of the Shoshone Range, west of the Mal Pais Ridge. This high is part of the linear zone of NNW-trending aeromagnetic highs that extends from Eureka, Nevada, almost to the Oregon border (see Figure 12). As mentioned in the geophysical setting, these highs have been interpreted as reflecting an approximately 5 km wide zone of diabase dike intrusion which extends up through the crust with associated surficial volcanics (see Zoback, 1978, for a more complete discussion). The diabase dikes are inferred to represent feeders for the mid-Miocene basaltic andesite both in the Beowawe area and regionally.

Qualitatively, several features are obvious from the aeromagnetic data for the Mal Pais Ridge area: (1) pronounced effects due to the topographic relief of lava flows, particularly associated with the major NNW-trending cross faulting, and (2) a broad low on the northeastern end of the range which appears to correspond to the thin section of flows (~100 m thick) exposed there. The shape and sign of the anomaly suggest unusual magnetization directions.

A paleomagnetic investigation of the lavas in the Beowawe area was undertaken in part to aid in the interpretation of the aeromagnetic data. Oriented hand samples (generally two to four samples per flow) were collected in the field. In the laboratory, two cores were drilled, oriented, and measured from each sample. Further details of the investigation have been presented elsewhere (Zoback, 1978) and only the results are summarized here. The mid-Miocene basaltic andesite flows were sampled in three localities in the range; in addition, the late Miocene(?) flows exposed in the western end of Whirlwind Valley were also sampled (sample localities are indicated on Figure 25).

Flow mean natural remanent magnetization (NRM) intensities, and directions after cleaning are given in Table 2. Also given are the induced intensities (based on susceptibility measurements and a regional field value of 54500 gammas, 1965 IGRF value) and Q, the Koenigsberger ratio (the ratio of remanent intensity to induced intensity). Stereo-plots of the magnetization directions after cleaning (remanent directions) for the sites sampled are given in Figure 26. Inferred relative stratigraphic positions of the sections sampled in the range are indicated numerically with BW1 being stratigraphically lowest.

The mid-Miocene basaltic andesite flows sampled in the range at sites BW1 and BW2 plot far from the expected mid-Miocene pole position and appear to have erupted rapidly during a transition of the earth's magnetic field. Since the inferred stratigraphically highest flows (at BW3) appear normally magnetized (although scattered); it is likely that a large portion of the basaltic andesite flows erupted during a reverse-to-normal polarity transition.

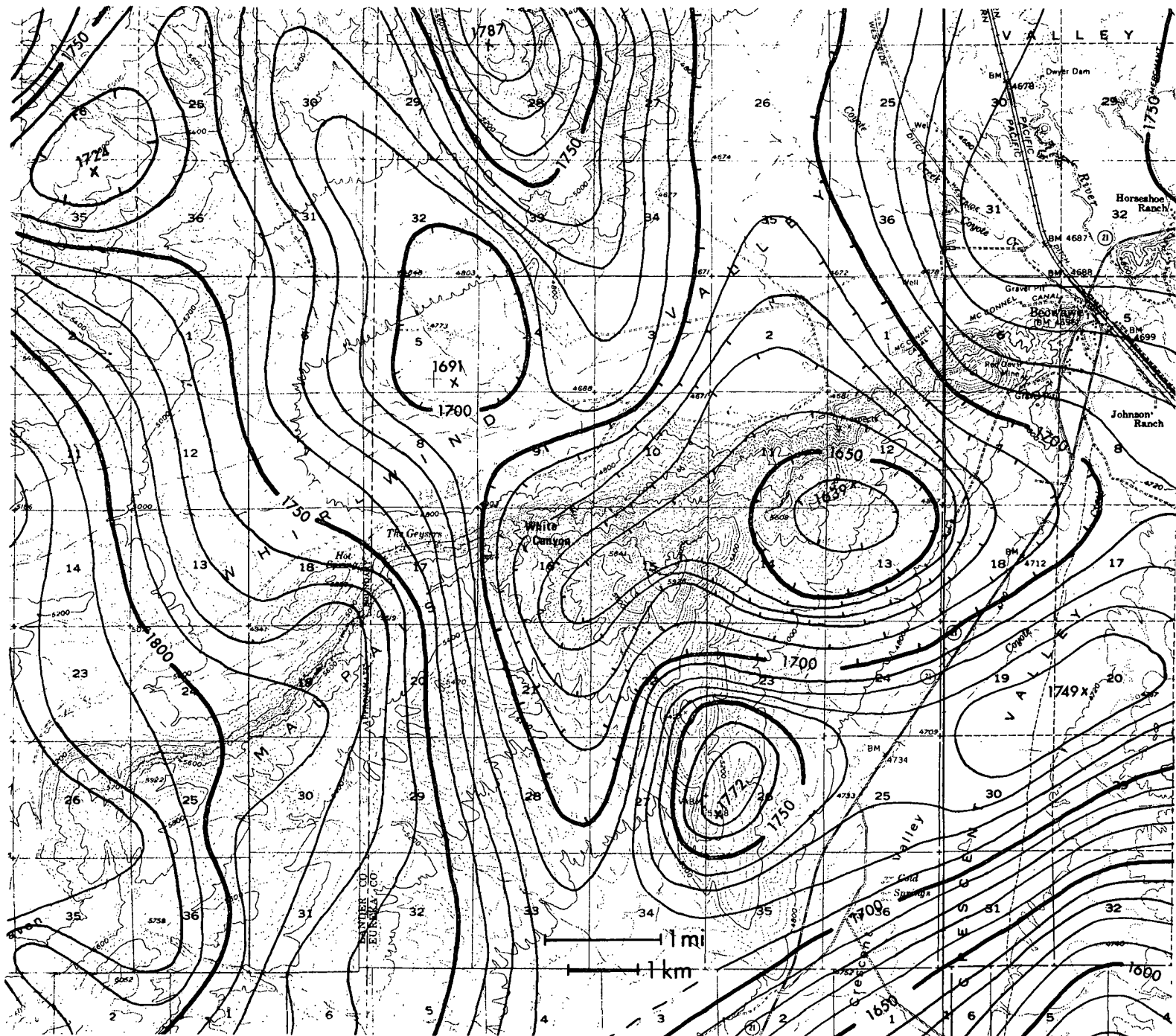


FIGURE 3 AEROMAGNETIC MAP OF MALPAIS AREA, CONTOUR INTERVAL 10 GAMMAS RELATIVE TO ARBITRARY DATUM (FROM ZOBACK, 1979, STANFORD UNIVERSITY SCHOOL OF EARTH SCIENCES)

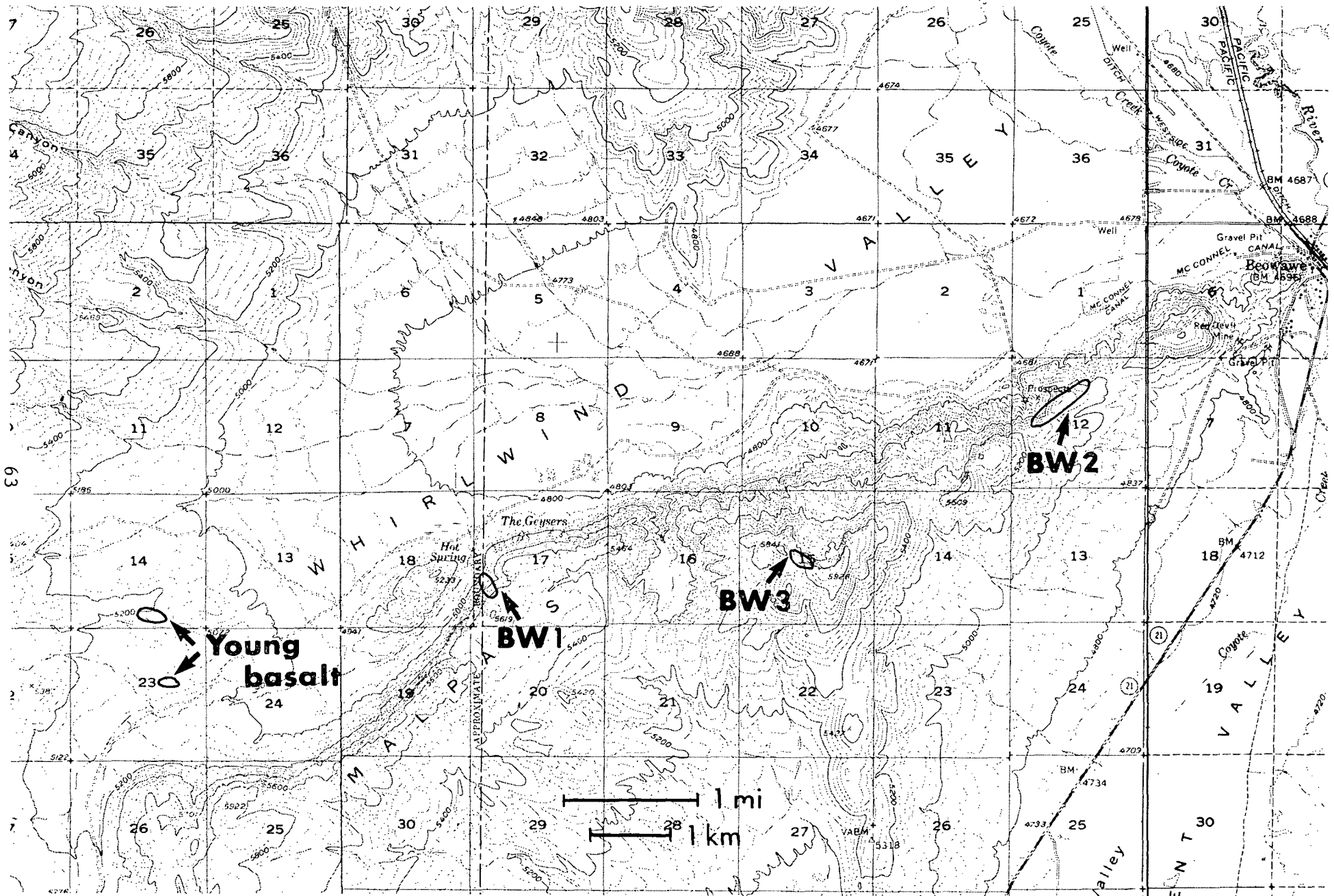


Figure 25. Paleomagnetic sampling sites referred to in text. Site names correspond to those used in Table 2 and Figure 26.

TABLE 2

Paleomagnetic Data: Beowawe Volcanic Rocks

Location ¹	Rock type & magnetization ²	Number of flows	Mean I	Mean D	α_{95}	J NRM	J IND	Q
Beowawe (BW1)	Tba I (transition)	6	-65.8°	127.9°	6.3°	4.32×10^{-4}	2.80×10^{-4}	1.57
Beowawe (BW2)	Tba II (transition)	4	-28.7°	162.4°	11.6°	1.08×10^{-3}	3.10×10^{-4}	3.57
Beowawe (BW3)	Tba III (normal)	3	+59.3°	23.6°	50.8°	7.55×10^{-3}	7.54×10^{-4}	10.3
Beowawe (valley flows)	Tb (reverse)	3	-59.1°	165.5°	9.8°	1.55×10^{-3}	2.47×10^{-4}	10.9

¹Numbers following location names refer to localities shown in Figure 25.

²Tba - mid-Miocene basaltic andesite flows
Tb - late Miocene(?) basalt flows

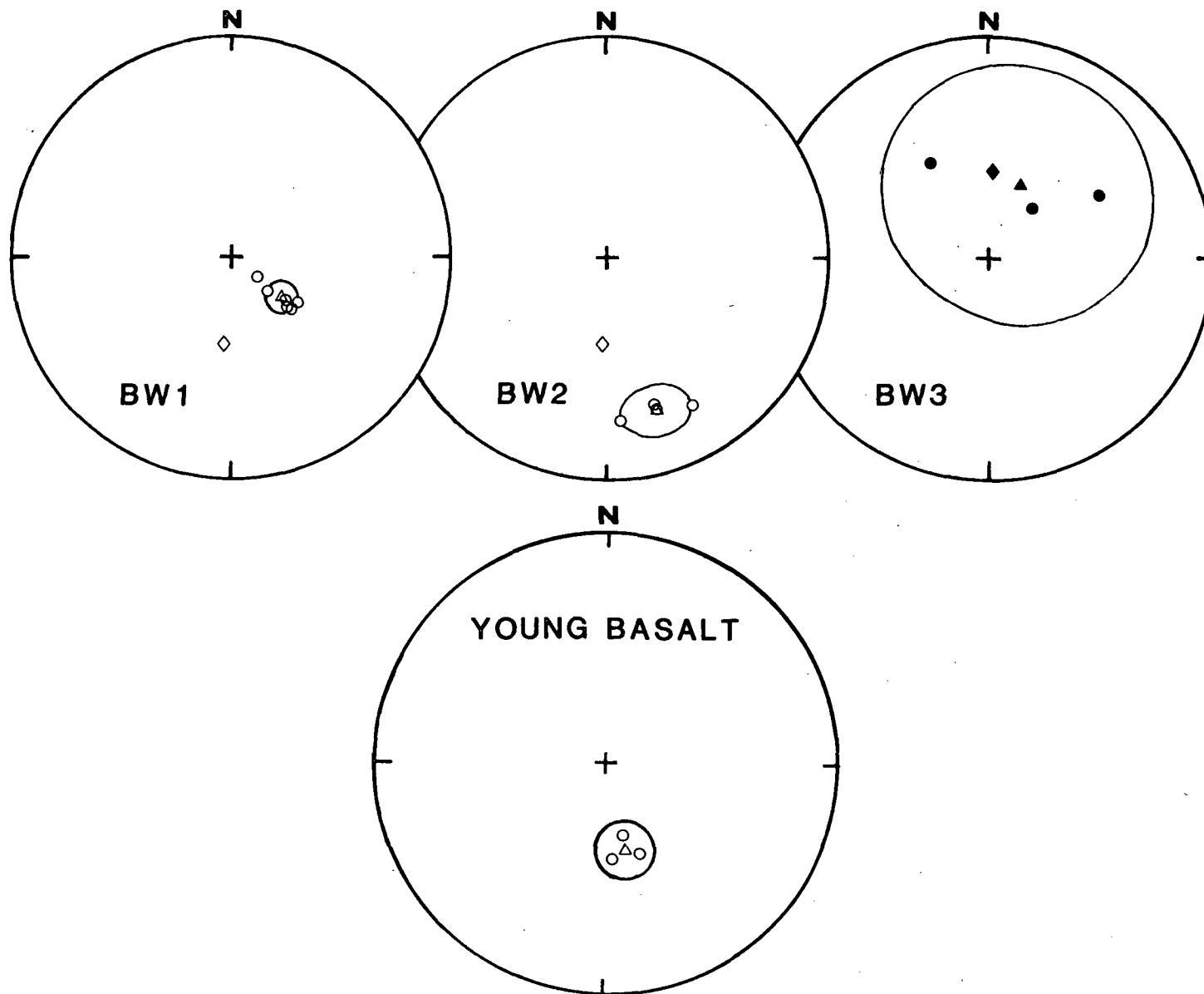


Figure 26. Natural remanent magnetization directions after partial demagnetization. Open symbols refer to points on upper hemisphere; closed symbols correspond to symbols on lower hemisphere. Mean directions indicated by triangles with appropriate α_{95} . Diamonds mark mid-Miocene axial dipole field directions.

Since only the upper 300 m of the approximately 1 km thick basaltic andesite section is exposed, possibly reversely magnetized flows near the base were not sampled. However, such an interpretation is consistent with a regional picture of SSE-propagation of the mid-Miocene rifting event associated with the basaltic andesite eruption (Zoback, 1978). Since polarity transitions are thought to last only about 5000 years (Cox et al., 1975) the bulk of the flows may have erupted in a geologically very short period of time.

The flows sampled on the northeastern end of the range (BW2) have shallow, negative inclinations directed approximately to the south (Figure 26). Mean Q for this section of flows was 3.57; thus, both the remanent and induced magnetization would be expected to contribute to the aeromagnetic anomaly in this region. The structurally and stratigraphically higher and apparently normally magnetized flows near the top of the main landslide (BW3) further complicate the anomaly pattern over the northeast end of the range. In addition, the large aeromagnetic low begins near the eastern edge of the inferred NNW-trending graben containing the thick section of basaltic andesite, suggesting that the negative anomaly may, in part, be an edge effect of that graben.

Preliminary three-dimensional modeling of the observed anomaly using a uniformly magnetized slab corresponding to the exposed flows suggested a near horizontal magnetization vector pointing north with an intensity of about 3×10^{-3} emu/cm³. Such a magnetization was not sampled in either BW2 or BW3 and suggests that the observed anomaly is the result of a complex superposition of topographic effects (including the graben edge effect) and a combination of induced and various remanent magnetizations.

The lack of any distinct anomaly associated with the thick section of flows in the inferred mid-Miocene graben west of White Canyon despite measured transitional magnetizations at BW1 may be due to several effects. The width of the graben (probably about 10 km although major faulting on the western side of the graben is not exposed) compared to its thickness (about 1 km) suggests an associated anomaly composed mainly of edge effects. As indicated above the edge effect due to the eastern edge of the graben probably contributes to the low centered over the northeastern end of the range. Also, since only the upper 300 m of the section was sampled, it is impossible to predict the total magnetization; the net effect of the thick pile of transitionally(?) magnetized flows may be that the remanent directions nearly cancel one another resulting in a low apparent magnetization, possibly with induced effects dominating. Finally, the anomaly pattern in the vicinity of the known thick sections of flows in the graben may be completely dominated by the main, deep source (diabase dikes) to the west. Realistically, all the effects may be in part responsible for the apparent lack of an anomaly associated with the thick section of flows in the graben.

The paleomagnetic data for the late Miocene(?) basalts (Table I and Figure 26) in the western end of Whirlwind Valley indicate high Q's and reverse polarity close to the axial dipole field. The NRM data support structural and stratigraphic evidence that these flows are a different age (presumably younger) than the basaltic andesite in the range.

Geophysical Summary

The active hot springs area at Beowawe is characterized by: low apparent resistivity, a positive self-potential (SP) anomaly, and high seismic noise levels. The region of low apparent resistivity ($<20\Omega\text{m}$ as determined from bipole-dipole surveys) is restricted to the active geothermal area; however, the seismic noise and SP anomalies appear to extend eastward (basinward of and subparallel to the main range front fault) outside of the currently active area. A separate small resistivity low area detected by only one of the transmitters may be related to the same source as the eastward extensions of the SP and seismic noise anomalies.

The bipole-dipole data revealed a complex resistivity structure in the Mal Pais Ridge/Whirlwind Valley with results from two transmitters (one located in the valley and the other on the dip slope of the Mal Pais) largely in disagreement. The only anomaly duplicated in both transmitter surveys was the anomaly in the vicinity of the geysers. A small low in the valley northeast of the geysers detected by the valley transmitter may also be real. It roughly coincides with a region of high seismic noise values and a SP anomaly which parallels the range front. This resistivity low is also approximately on-line with the interpreted major NNW-trending graben fault, a fault which juxtaposes the thick (~ 1 km) section of basaltic andesite and interbedded sediments to the west against Paleozoic quartzites, cherts and shales on the east. An abrupt resistivity contrast along this fault may be the cause of the anomaly.

The self-potential (SP) method appeared most effective in detecting water movement along faults. A complex pattern of SP anomalies was found associated with the known, fault-related upwelling of thermal waters in the geothermal system. The data can be interpreted as revealing a broad high ($>+80$ mv) presumably reflecting the general upwelling, with superimposed high frequency fluctuations and steep gradients undoubtedly due to a complicated pattern of near-surface flow, probably both horizontal and vertical, in the active hot springs area. Negative gradients and potentials near the base of the sinter terrace may be due to a downward movement of cool runoff water from the terrace. The observed anomaly pattern is presumably related to upwelling along a subsidiary fault parallel to the range front fault because the main fault plane is located at a depth of 3000-4000 (.9-1.2 km) feet below the valley floor in the vicinity of the anomaly. This interpretation is further substantiated by the eastward extension of the broad high well outside the active area into a region where there is no observed upwelling along the main range-front fault. Since the anomaly appears to extend through a region of cold springs presumed to be aligned along the subsidiary fault; cool-water discharge (possibly Artesian due to the nearby head on the terrace) may also contribute to the anomaly.

Although plagued by uncertain amplification effects due to varying thicknesses of valley fill, the seismic noise survey did record high noise values in the vicinity of the active hot springs and blowing wells. The high noise values appear to extend northeastward outside of the modern geothermal area. A subparallel alignment to the main range-front fault and an overall

coincidence with trends in the self-potential data appear to indicate that the noise anomaly may be related to fluid movement along the subsidiary range-front fault. Since the noise anomaly is well defined by points along the axis of the valley, it is probably not due to amplification effects.

Both the SP and seismic noise data suggest a more northeasterly trend for the subsidiary fault relative to the main range-front fault east of the geysers. This more northeasterly trend is similar to the strike of the range southwest of the geysers. The one low resistivity value on which the bipole-dipole anomaly was largely based lies very near the buried trace of the subsidiary range-front fault.

Although coverage was sparse, the gravity data indicate a thin, fairly uniform alluvial veneer in the broad southwestern end of Whirlwind Valley whereas, in the northeastern end of the valley the data suggest that the fill thickens both eastward and southward as the Mal Pais Ridge is approached. The thin alluvial cover in the southwestern end of Whirlwind Valley is attributed largely to filling of the basin by late Miocene(?) basalt flows. The available gravity data are compatible with an asymmetric tilted block structure inferred for the valley from geologic and drill hole evidence. The data are insufficient to further detail the subsurface structure of the valley or identify the buried trace of the subsidiary range-front fault.

Gravity values in the active hot springs area are low relative to the surrounding region. These low values may be due to the highly porous, low density opaline sinter apron on the valley floor or alternately may be part of a broad low associated with the thick accumulation of basaltic andesite having a -0.1 g/cm^3 density contrast with the Paleozoic quartzites.

The aeromagnetic anomaly pattern in the Beowawe area results from the juxtaposition of several different effects: a deep-seated, approximately two-dimensional source to the west; complex geometric and topographic effects of the flows; and a combination of induced magnetization with remanent magnetizations of unusual directions. Flows on the Mal Pais Ridge appear to have erupted during a reverse-to-normal polarity transition although probably only the uppermost part of the transition was recorded in the exposed rocks. The dark and very vesicular flows capping the range are interpreted as being the same age as the underlying flows, based consistent remanent magnetizations. Flows in the southwestern end of Whirlwind Valley (late Miocene(?) basalt) are distinct, with good reverse remanent magnetizations.

CONCLUSIONS AND RECOMMENDATIONS

In a regional context, the Beowawe/Mal Pais Ridge area is located within a zone of anomalously high heat flow within the Basin and Range province, itself a region of above normal heat flow. The geothermal system at Beowawe is believed to be hot-water-dominated and is one of only 15 such systems in the entire U.S. with subsurface temperatures in excess of 200°C (Renner et al., 1975). As with the majority of geothermal systems in the Basin and Range province, the modern activity at Beowawe is situated along one of the major range-bounding normal faults attesting to the role of fault-controlled permeability in the system.

Details and results of geologic and geophysical investigations have been summarized earlier. In this section these results are integrated into a synthesis of available data on the nature of the modern geothermal system. Economic considerations and recommendations for further work are also discussed.

Nature of the Geothermal System and Possible Reservoirs

The modern geothermal system at Beowawe is controlled by silica-rich hot water migrating upwards along the main range front fault and probably also along a parallel, subsidiary fault located approximately one kilometer basinward. At shallow levels (probably near the ground water table) some of the geothermal water is diverted laterally, feeding hot springs near the base of the main escarpment while the remainder of the fluid partially flashes to steam and escapes primarily from the top of the sinter terrace (Figure 27). A best estimate of the age of the modern system based on the volume of siliceous sinter deposited is ~200,000 yrs with an uncertainty of ~50%.

Modern activity is restricted to a narrow (~1.5 km wide) NW-trending graben which crosses the main NE-trending range front fault where that fault bends roughly 30° eastward. Complex geometry of intersecting fault trends and predicted strike-slip in addition to dip-slip offsets (see section on regional structural analysis) in the vicinity of this bend may be responsible for localization of the modern activity. Geologic evidence, however, suggests that in the past, hydrothermal fluids moved along a considerable portion of the range front fault east of the currently active area. The most prominent indications of past activity are a large chalcedony-carbonate vein located at the mouth of White Canyon and a travertine deposit (~3 m long) along the fault splay in section 12, Eureka County. The quicksilver deposits in section 6 (Eureka County) may also be related (in a late Cenozoic time frame) although the only age control is post-Paleozoic. These scattered occurrences suggest shifting centers of activity in the region over a time period much greater than the age of the modern activity.

Geochemical studies of the hydrothermal waters at Beowawe yield SiO₂ temperatures of 226°C and Na/K/Ca temperatures of 242°C, in fairly good agreement with the highest reported temperatures (212°C) encountered in shallow drilling (Renner et al., 1972). Temperatures in the shallow wells

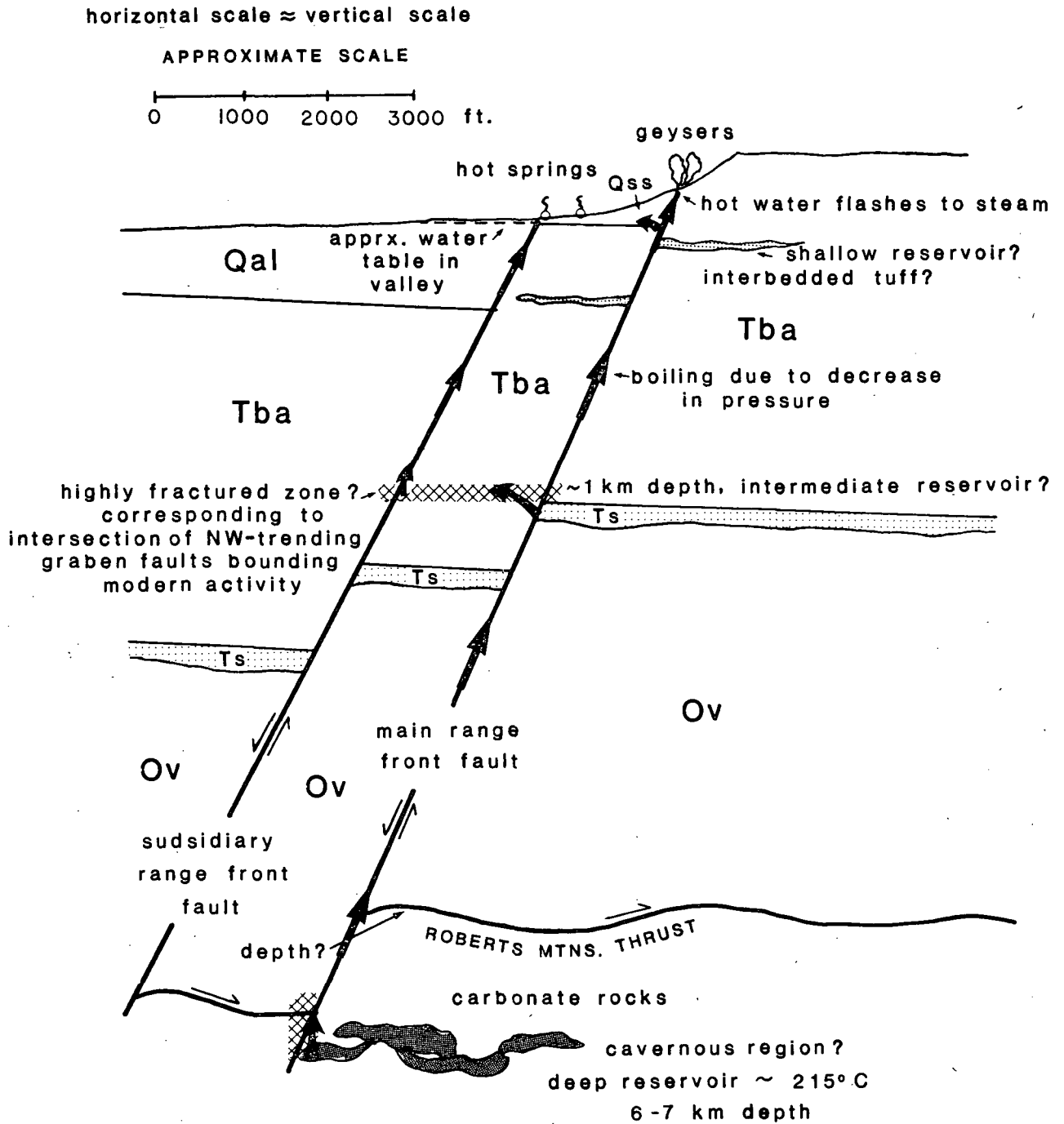


Figure 27. Schematic cross-sectional view of the geothermal convective system at Beowawe along a line perpendicular to the range front. Heavy arrows mark inferred path of hydrothermal upwelling.

(~700 feet, 200 m) in the active hot springs area are only slightly lower than temperatures recorded in the deepest wells (~2.9 km) along the main range front fault, suggesting that water is moving upward rapidly enough to prevent a large heat loss. The deepest well is located roughly 2.5 km southwest of the active hot springs. There are no surface manifestations of this flow along the fault between the well and the springs implying significant lateral diversion of geothermal waters at some level above 2.9 km.

Highly permeable zones or storage regions are probably located at several levels under the Mal Pais Ridge/Whirlwind Valley area. A shallow reservoir directly feeding the sinter terrace was probably the source for production in the 1960's from depths of approximately 200-250 m. This reservoir may be located in interbedded tuffaceous units within the basaltic andesite section (mentioned in the geologic log summaries of both deep wells) in the uplifted range block. This shallow reservoir may have developed as a result of gradual clogging (by silica deposition) of fractures that communicated with the surface. Unable to escape, the rising thermal waters were diverted and collected in porous rock thus creating the reservoir.

Since in the Ginn well located 2.5 km southwest of the Geysers only the main range front fault was found to be actively connected with a deep source of hot water; an additional highly permeable zone, tapped by both the main and the subsidiary range front faults, may exist at intermediate levels under the hot springs area. (Alternately, in the vicinity of the geysers the subsidiary range front fault may also be actively connected with a deep "reservoir.") Conceivably such a permeable region may be related to the intersection, at depth, of the two NW-trending faults bounding the graben in which the modern activity is localized. Intersection of these faults with each other at the main range front fault (at approximately 1 km depth) may have created a highly fractured zone connecting the main and the subsidiary range front fault, allowing significant upwelling to be diverted to the subsidiary fault. This upwelling is probably the source of the ~+80 mv self-potential anomaly which appears to be associated with the subsidiary range front fault.

Data on the geochemistry of the geothermal system at Beowawe (Reed, 1977) indicates water of sodium bicarbonate type and suggests reaction with carbonate rocks (as opposed to sodium chloride type water noted in many geothermal systems taken to indicate reaction with siliceous rocks). Hence, the ultimate deep "reservoir" or hot water source for the geothermal system at Beowawe probably occurs within carbonate rocks of the lower plate of the Roberts Mountains thrust. Estimates on thicknesses of the siliceous upper plate of the thrust vary widely. Based on exposures of upper plate rocks in the northern Shoshone Range 15 km to the southwest, Gilluly and Gates (1965) estimated a composite thickness for the upper plate of 12,000 to 30,000 feet (3.7 to 9.1 km). Internal thrusting and slicing within the sequence has caused local repetition and thinning. Lower plate carbonate rocks are exposed in windows in the thrust in the three major ranges to the south of Beowawe. The minimum thickness of upper plate rocks in the Beowawe area based on drill hole data is 1.53-km.

Heat-flow data can also be used to constrain the depth of circulation. The mean conductive heat flow in three wells located 25 to 30 km southwest of the geysers is 3.0 HFU (2.5, 3.0, 3.5 HFU; Sass et al., 1971). The average temperature gradient in upper plate rocks is $\sim 30^{\circ}\text{C}/\text{km}$. Assuming the heat source for the system is merely conductive heat loss from the rock, then rocks at reservoir temperatures ($\sim 210\text{--}220^{\circ}$) would be located at approximately 7 km depth. Earthquake hypocenters in Nevada are commonly in the 5–10 km depth range indicating brittle fracturing of rock within proposed reservoir depths; thus, range front faults could conceivably provide communication to the surface for the deep reservoirs.

In summary, the geothermal system at Beowawe is apparently characterized by permeable zones at several different levels: a deep zone probably located within cavernous carbonate rocks of the lower plate of the Roberts Mountains thrust, an intermediate depth, fractured zone created by complex fault intersections tapped by both the main and the subsidiary range front fault, and a shallow reservoir presumably within the basaltic andesite section which primarily feeds hydrothermal activity on the sinter terrace. Meteoric water is probably heated by conductively by rocks at roughly 7 km depth in fractures and solution cavities within the autochthonous carbonate rocks. Intersection of the main range front fault with this deep source of hot water (between ~ 3 and 7 km depth) provides a channeling for rapid upward migration of the geothermal water. Structural controls have apparently resulted in significant northeastward lateral diversion (at least 2.5 km) of water rising along the main range-front fault at some level above 2.9 km depth.

Presently thermal waters reach the surface along a short (~ 1.5 km long) segment of the main and subsidiary range front faults bounded by two NW-trending faults. These NW-trending faults have created a graben into which the modern activity is localized. Near the surface these NW-trending faults are not geothermally active and, in fact, separate regions of hydrothermal upwelling from cold springs to the east along the subsidiary range front fault. However, intersection of the two NW-trending faults at depth (~ 1 km) with each other at the main range-front fault may have created a highly fractured zone connecting both the main and the subsidiary range front fault. A shallow reservoir (at approximately 200 m) within the basaltic andesite section in the uplifted range block was probably the source for exploration and minor production in the 1960's.

The ultimate target for geothermal production at Beowawe is probably tapping of a highly permeable part of the fault zone at relatively shallow depths using the fault as a conduit to deeper sources. If, because of large solution cavities, the carbonate rocks prove to be significantly more permeable than the fault, then production from these rocks might be economically more feasible. The carbonate rocks are located at the shallowest level on the main uplifted block forming the range. Relative vertical offset (~ 1 km) uplifting the northeast end of the range in mid-Miocene time and creating the graben into which the basaltic andesite accumulated has resulted in the shallowest structural levels in the northeast end of the range; however, lack of any modern surface manifestations of hydrothermal activity in that region suggest that the rocks there are isolated (possibly by the fault offset) from the modern reservoir.

Economic Considerations

Production statistics quoted by Koenig (1970) for one of the shallow (~200 m) wells of the 1960's, 50,000 pounds per hour of steam and 1,400,000 pounds of hot water, represent, in his words, a significant commercial discovery. The estimated age of the modern system (~200,000 years) and the extensive surficial activity suggest that total reservoir resources may be sufficient to sustain commercial production.

Since there is no geologic evidence for a local magma chamber under the region, it is reasonable to assume that the heat source for the system is related to the same phenomenon that is supplying the high heat flow to the entire Battle Mountain high. With such a broad and extensive source, a possible decline in total heat of the system is certainly not an economic factor. Thus, sufficient reservoir permeability and recharge are the main economic factors to be evaluated. The high water table in the valley and filtration of cool ground water into shallow wells (Koenig, 1970) indicates that abundant meteoric water is available; however, with present information it is not possible to estimate if cold water recharge would be sufficient to support production from the deep reservoir.

Reservoir permeability is probably the single most important factor pertaining to full-scale commercial production. Presuming the deep reservoir is in lower plate carbonate rocks (possibly within cavernous regions in the carbonate section), sufficient porosity is most likely available to provide surface area for heating of the meteoric water. In addition, such cavernous zones imply a high permeability. Intersection of a cavernous region by the range-front fault apparently provides communication to the surface for the thermal waters. Thus, production possibly could come from shallow, highly permeable regions along the range front fault rather than the deep region where the water is actually being heated. The relative permeabilities hence would control the depth of production.

Recommendations for Further Work

The Beowawe area is an excellent example of a natural hot-water dominated geothermal system that can and should be thoroughly investigated before any large-scale production completely alters the natural system.

If a large reservoir underlies the Mal Pais Ridge/Whirlwind Valley area, it would be useful to attempt to determine its extent electrically by mapping the deep resistivity structure. A previously conducted bipole-dipole study at Beowawe (Wollenberg, 1975) produced ambiguous results which probably largely reflected near-surface lateral resistivity structure. Perhaps a technique more sensitive to vertical variations in resistivity (such as dipole-dipole sounding) could better delineate a deep zone of hot water under Whirlwind Valley.

The zone of high seismic noise values in the center of the valley near the end of the landslide (along the boundary between sections E4 and E9) should be further investigated in light of its possible alignment with the buried trace of the subsidiary range front fault. This data and the extension of the self-potential anomaly along this fault east of the active hot springs through a region of cold springs and beyond may be indicating lateral flow of thermal water along this fault at depth.

Seismic reflection profiling (such as Vibroseis or some other source) in Whirlwind Valley could be useful in elucidating the structure and possibly identifying reservoirs. The postulated, nearly horizontal fractured zone corresponding to the intersection at depth (~ 1 km) of the two NW-trending graben faults bounding the modern activity might be detectable. In addition, large, deep cavernous regions filled with hot water might also be detectable. A well-maintained gravel road which parallels the range front and runs through the active hot springs area would be the obvious place for an initial survey. This road crosses nearly orthogonally the presumed trace of the major NNW-trending mid-Miocene graben fault located east of the hot springs; hence, information on the offset of this fault and its possible role in isolating the modern reservoir might also be obtained.

In a broader context there are several key problems whose study could shed some light on the overall tectonic setting of the Beowawe geothermal activity including:

- 1) Age of basalt flows in the southwest end of Whirlwind Valley--By nature of their apparent localization in Whirlwind Valley, these basalt flows place crucial constraints on the timing of the formation of one of the prominent ENE-trending valleys characterizing this part of north-central Nevada.

- 2) Pattern of horizontal displacements within the region--Through either a detailed microearthquake study or possibly an investigation of fault movements utilizing grooves and slickensides (although most scarps are highly eroded), fault offsets on the intersecting faults of widely varying trends could be predicted and a pattern of regional strain established.

3) Heat source for the Battle Mountain high--Using seismic and possibly deep electrical work, the lower crust and uppermost mantle in this region of Nevada should be investigated in light of recently proposed thermal models for the Battle Mountain high by Lachenbruch and Sass (1978).

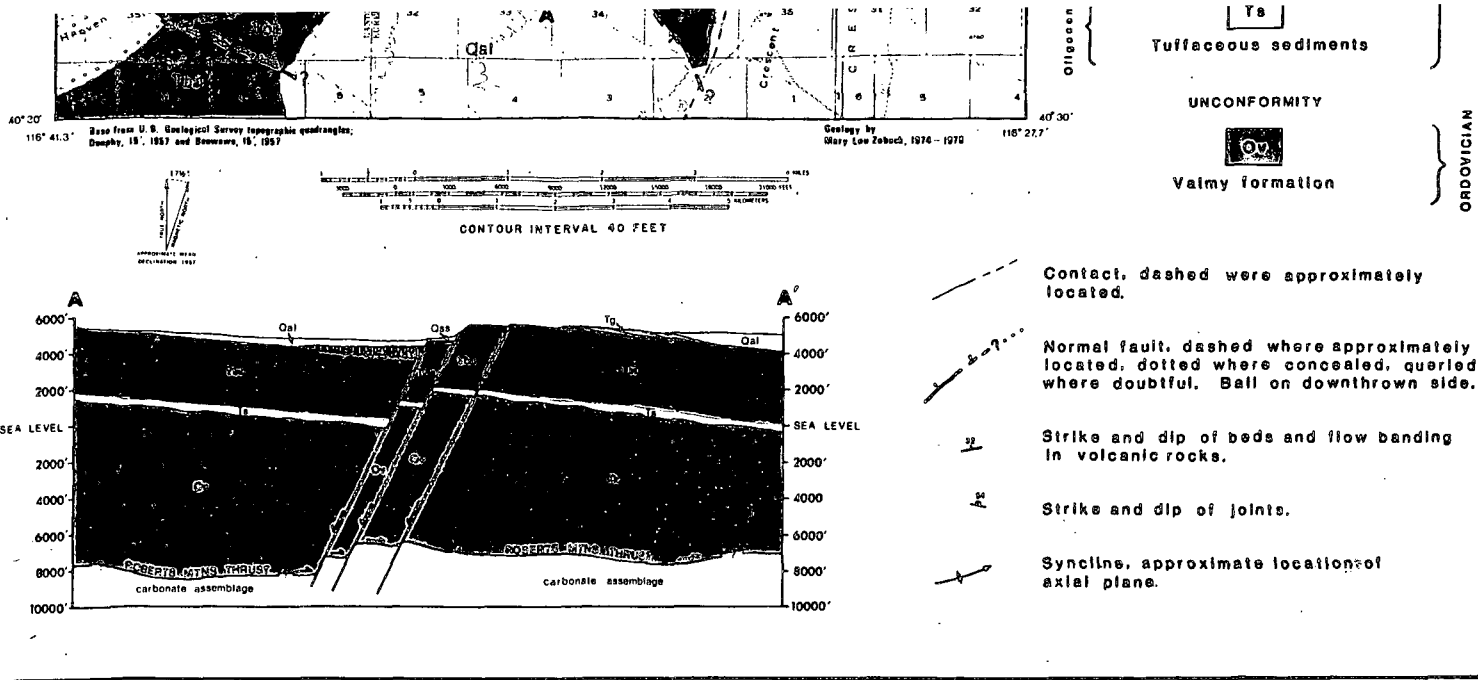
REFERENCES

- Banwell, G.J., and MacDonald, W.J.P., 1965, Resistivity surveying in New Zealand thermal areas: Proc. 8th Commonwealth Mining and Metall. Congress, Australia and New Zealand, v. 7, Paper 213.
- Biehler, S. and Combs, J., 1972, Correlation of gravity and geothermal anomalies in the Imperial Valley, Southern California: Geol. Soc. Amer. Abs. with Programs, v. 4, 128.
- Christiansen, R.L. and Lipman, P.W., 1972, Cenozoic volcanism and plate-tectonic evolution of the western United States. II. Late Cenozoic: Roy. Soc. London Phil. Trans., v. 271, 249-284.
- Clacy, G.R.J., 1968, Geothermal ground noise amplitude and frequency spectra in the New Zealand volcanic region: Jour. Geophys. Res., v. 73, 5377-5384.
- Corwin, R.F., 1976, Self-potential exploration for geothermal reservoirs: Proc. Second U.N. Symp. on the Development and Use of Geothermal Resources, San Francisco, Calif., U.S. Govt. Printing Office, Washington, D.C., v. 2, 937-945.
- Cox, A.V., Hillhouse, J. and Fuller, M., 1975, Paleomagnetic records of polarity transitions, excursions, and secular variation: Rev. of Geophys. and Space Physics: v. 13, 185-189.
- Douze, E.J., and Sorrells, G.G., 1972, Geothermal ground noise surveys: Geophys., v. 37, 813-824.
- Evans, A.S. , 1869, In Whirlwind Valley: The Overland Monthly, v. 2, 111-115.
- Garside, L.J., 1974, Geothermal exploration and development in Nevada through 1973: Nevada Bureau of Mines and Geology, Report 21, 12 p.
- Gilluly, J., and Gates, O., 1965, Tectonic and igneous geology of the Northern Shoshone Range: U.S. Geol. Surv. Prof. Paper 465, 153 p.
- Gilluly, J., and Masursky, H.A., 1965, Geology of the Cortez quadrangle, Nevada: U.S. Geol. Surv. Bull. 1175, 117 p.
- Hague, A. and Emmons, S.F., 1877, Descriptive geology: U.S. Geol. Explor. 40th Parallel, v. 2, p. 618.
- Hatherton, T., MacDonald, W.J.P., and Thompson, G.E.K., 1966, Geophysical methods in geothermal prospecting in New Zealand: Bull. Volcanol., v. 29, 485-498.
- Hose, R.K., and Taylor, B., 1974, Geothermal systems of northern Nevada: U.S. Geol. Surv. Open File Report #74-271.

- Hyndman, D.W., 1972, Petrology of igneous and metamorphic rocks: McGraw-Hill, New York, p. 171.
- Iyer, H.M., and Hitchcock, T., 1974, Seismic noise measurements in Yellowstone National Park, *Geophys.*: v. 39, 389-400.
- Keller, G.V., Furgerson, R., Lee, C.Y., Harthill, N., and Jacobson, J.J., 1975, The dipole mapping method: *Geophys.*, v. 40, 451-472.
- Ketner, K., 1965, "Economic Geology", in Tectonic and Igneous Geology of the Northern Shoshone Range, Nevada, (eds. J. Gilluly and O. Gates), U.S. Geol. Surv. Prof. Paper 465, 153 p.
- Koenig, J.B., 1970, Geothermal exploration in the Western United States: *Geothermics Spec. Issue 2*, v. 2, part 1, 1-13.
- Lachenbruch, A.H. and Sass, J.H., 1978, Models of an extending lithosphere and heat flow in the Basin and Range province, in Cenozoic Tectonics and Regional Geophysics of the Western Cordillera, *Geol. Soc. Amer. Memoir 152*, in press.
- Luongo, G. and Rapolla, A., 1973, Seismic noise in Lipari and Vulcano Islands, Southern Tyrrhenian Sea, Italy: *Geothermics*, v. 2, 29-31.
- Mabey, D.R., 1964, Gravity map of Eureka County and adjoining areas, Nevada: U.S. Geol. Surv. Geophys. Inv. Map GP-415.
- McKee, E.H., 1971, Tertiary igneous chronology of the Great Basin of the western United States - implications for tectonic models: *Geol. Soc. Amer. Bull.*, v. 82, 3497-3502.
- McKee, E.H., and Silberman, M.L., 1970, Geochronology of Tertiary igneous rocks in central Nevada: *Geol. Soc. Amer. Bull.*, v. 81, 2317-2327.
- Muffler, L.J.P., 1964, Geology of the Frenchie Creek quadrangle, north-central Nevada: U.S. Geol. Surv. Bull. 1179, 99 p.
- Murphy, M.A., McKee, E.H., Winterer, E.L., Matti, J.C., and Dunham, J.B., 1978, Preliminary geologic map of the Roberts Creek Mountain Quadrangle: U.S. Geol. Surv. Open File Map.
- Noble, D.C., 1972, Some observations on the Cenozoic volcano-tectonic evolution of the Great Basin, western U.S.: *Earth and Planet. Sci. Lett.*, v. 17, 142-150.
- Nolan, T.B., and Anderson, G.H., 1934, The geyser area near Beowawe, Eureka County, Nevada: *Amer. Jour. Sci.*, 5th ser., v. 27, 215-229.
- Nourbehecht, B., 1963, Irreversible thermodynamic effects in homogeneous media and their applications in certain geoelectric problems (Ph.D. Thesis): Cambridge, Massachusetts Institute of Technology, 121 p.

- Poldini, E., 1938, Geophysical exploration by spontaneous polarization methods: Mining Mag., London, v. 59, 278-282, 347-352.
- Poldini, E., 1939, Geophysical exploration by spontaneous polarization methods: Mining Mag., London, v. 60, 22-27, 90-94.
- Reed, M.J., 1977, Geochemical comparison of deep geothermal waters in North America: Geol. Soc. Amer. Abs. with Programs, v. 9, 1138.
- Renner, J.L., White, D.E., and Williams, D.L., 1975, Hydrothermal convection systems, in Assessment of Geothermal Resources of the United States - 1975 (eds. D.E. White and D.L. Williams), U.S. Geol. Surv. Circ. 72b, 5-57.
- Rinehart, J.S., 1968, Geyser activity near Beowawe, Eureka County, Nevada: Jour. Geophys. Res., v. 73, 7703-7706.
- Risk, G.F., MacDonald, W.J.P., and Dawson, G.B., 1970, D.C. resistivity surveys of the Broadlands geothermal region, New Zealand: Geothermics Spec. Issue 2, v. 2, 287-294.
- Roberts, R.J., 1951, Geologic map of the Antler Peak quadrangle, Nevada: U.S. Geol. Surv. Geol. Quad. Map GQ-10, scale 1:62,500.
- Roberts, R.J., Montgomery, K.M., and Lehner, R.E., 1967, Geology and mineral resources of Eureka County, Nevada: Nevada Bureau of Mines, v. 64, 152 p.
- Robinson, E.S., 1970, Relations between geologic structure and aeromagnetic anomalies in central Nevada: Geol. Soc. Amer. Bull., v. 81, 2045-2060.
- Sass, J.H., Lachenbruch, A.H., Monroe, R.J., Greene, G., Moses, T.H., Jr., 1971, Heat flow in the western United States: Jour. Geophys. Res., v. 76, 6376-6413.
- Slemmons, D.B., Jones, A.F., and Gimlett, J.I., 1965, Catalog of Nevada earthquakes: Bull. Seism. Soc. Amer., v. 55, 537-583.
- Stewart, J.H., and Carlson, J.E., 1974, Preliminary geologic map of Nevada: U.S. Geol. Surv. Misc. Field Studies, Map MF-609.
- Stewart, J.H., Walker, G.W., and Kleinhampl, F.J., 1975, Oregon-Nevada lineament: Geology, v. 3, 265-268.
- Stewart, J.H., McKee, E.H., and Stager, H.K., 1977, Geology and mineral deposits of Lander County, Nevada: Nev. Bureau of Mines and Geology, Bull. 88, 106 p.
- Studdt, F.E., and Thompson, G.E., 1969, Geothermal heat flow in the North Island of New Zealand: N.Z. Jour. Geol. and Geophys., v. 12, 673-683.

- U.S. Geol. Survey, 1967, Open File Aeromagnetic Maps in north-central Nevada #12, Beowawe and Carlin quadrangles.
- U.S. Geol. Survey, 1968, Open File Aeromagnetic Maps in north-central Nevada #11, Battle Mountain and Dunphy quadrangles.
- White, D.E., 1967, Mercury and base metal deposits with associated thermal and mineral waters: in Geochemistry of Hydrothermal Ore Deposits, (ed. H.L. Barnes), Holt, Rinehart, and Winston, New York, 575-631.
- White, D.E., 1968, Hydrology, activity, and heat flow of the Steamboat Springs thermal system, Washoe County, Nevada: U.S. Geol. Surv. Prof. Paper 458-C, 109 p.
- White, D.E., 1970, Geochemistry applied to the discovery, evaluation, and exploitation of geothermal energy resources: Geothermics, Spec. Issue 2, v. 1, 58-80.
- White, D.E., 1974, Characteristics of geothermal resources: in Geothermal Energy, (ed. P. Kruger and C. Otte), Stanford University Press, Stanford, Calif., 69-94.
- Wollenberg, H.A., Asaro, F., Bowman, H., McEvelly, T., Morrison, F. and Witherspoon, P., 1975, Geothermal energy resource assessment, Energy and Environment Divison, Lawrence Berkeley Lab, Univ. of Calif., UCID-3762, 92 p.
- Zoback, M.L., 1978, Mid-Miocene rifting in north-central Nevada: a detailed study of late Cenozoic deformation in the northern Basin and Range (Ph.D. Thesis), Stanford Univ., Stanford, CA 247 p.
- Zoback, M.L. and Thompson, G.A., 1978, Basin and range rifting in northern Nevada: clues from a mid-Miocene rift and its subsequent offsets: Geology, v. 6, 111-116.
- Zohdy, A.A.R., Anderson, L.A., and Muffler, L.J.P., 1973, Resistivity, self potential, and induced polarization surveys of a vapor-dominated geothermal system: Geophys., v. 38, 1130-1140.



GEOLOGIC MAP AND SECTION OF THE BEOWAWE GEOTHERMAL AREA, LANDER AND EUREKA CO., NEVADA

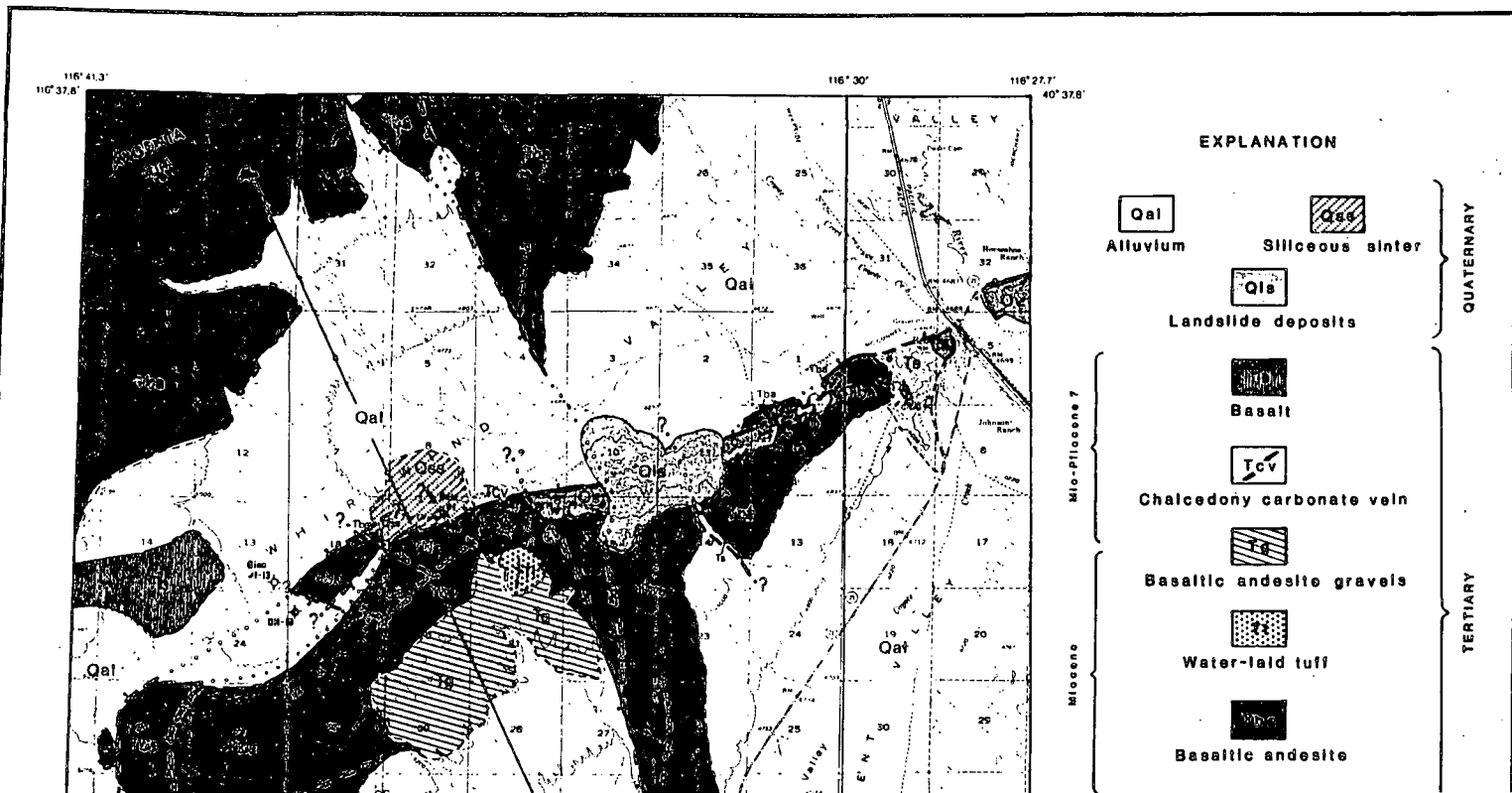
By
Mary Lou C. Zoback

UNIVERSITY OF UTAH
RESEARCH INSTITUTE
EARTH SCIENCE LAB.

SCHOOL OF EARTH SCIENCES
STANFORD UNIVERSITY

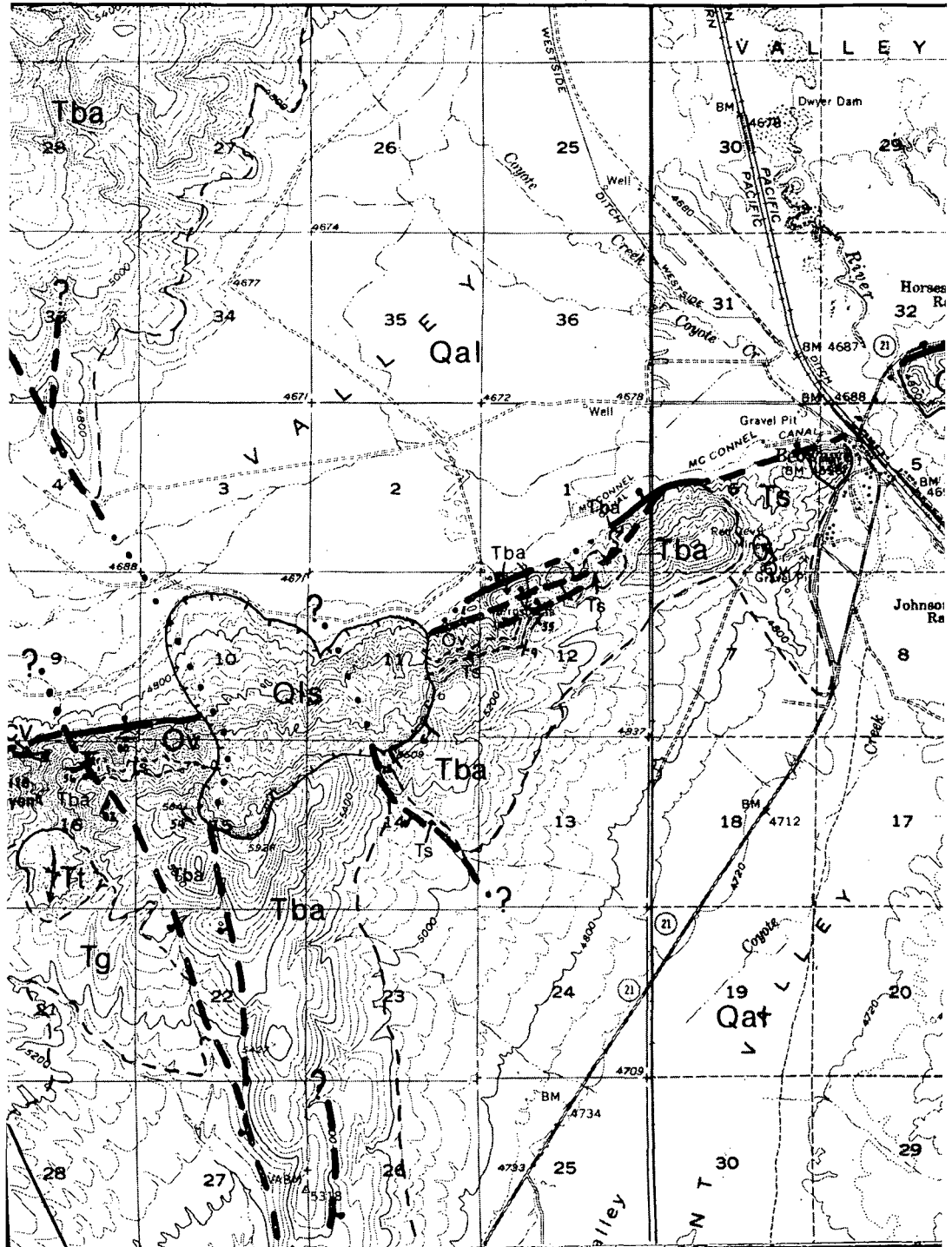
STANFORD UNIVERSITY PUBLICATIONS
GEOLOGICAL SCIENCES

VOLUME XVI
PLATE 2



STANFORD UNIVERSITY PUBLICATIONS
GEOLOGICAL SCIENCES

116° 30'



SCHOOL OF EARTH SCIENCES
STANFORD UNIVERSITY

116° 41.3'
116° 37.8'

